THE TUMOR MICROENVIRONMENT AS THERAPEUTIC TARGET IN PEDIATRIC ACUTE LEUKEMIA

HET TUMOR MICROMILIEU ALS THERAPEUTISCH DOELWIT VOOR ACUTE LYMFATISCHE KINDERLEUKEMIE

Bob de Rooij

THE TUMOR MICROENVIRONMENT AS THERAPEUTIC TARGET IN PEDIATRIC ACUTE LEUKEMIA

HET TUMOR MICROMILIEU ALS THERAPEUTISCH DOELWIT VOOR ACUTE LYMFATISCHE KINDERLEUKEMIE

Proefschrift

ter verkrijging van de graad van doctor aan de
Erasmus Universiteit Rotterdam
op gezag van de rector magnificus
Prof.dr. H.A.P. Pols
en volgens besluit van het College voor Promoties.
De openbare verdediging zal plaatsvinden op
woensdag 7 juni 2017 om 9:30

Bob de Rooij
geboren te Woerden

Erasmus University Rotterdam

The work described in this thesis was performed at the Department of Pediatric Oncology/Hematology of the Erasmus MC-Sophia Children's Hospital, Rotterdam, the Netherlands. This work was funded by the Dutch Cancer Society and KiKa.

ISBN 978-94-6182-792-0

Layout, cover and printing: Off Page, Amsterdam

PROMOTIECOMMISSIE

Promotor

Prof.dr. M.L. den Boer

Overige leden

Prof.dr. R. Fodde
Prof.dr. J.C. Clevers
Prof.dr. C.M. Zwaan

Copromotor

Dr. J.M. Boer

TABLE OF CONTENTS

Chapter 1	General introduction	7
Chapter 2	B-cell precursor acute lymphoblastic leukemia cells use tunneling nanotubes to orchestrate their microenvironment	21
Chapter 3	Disrupting tunneling nanotube signaling in the leukemic niche using actin inhibitors	57
Chapter 4	Tunneling nanotubes facilitate autophagosome transfer in the leukemic niche	79
Chapter 5	Acute lymphoblastic leukemia cells create a leukemic niche without affecting the CXCR4/CXCL12 axis	93
Chapter 6	General discussion and summary	115
Chapter 7	Nederlandse samenvatting voor niet ingewijden	131
Chapter 8	About the author	143
	List of publications	144
	PhD Portfolio	145
	Dankwoord	147

Chapter 1

GENERAL INTRODUCTION

CANCER

All life on Earth is thought to share a common ancestor that lived roughly 3.5 billion years ago[1-3]. As simple life forms evolved, cooperation between unicellular organisms paved the way for more complex multicellular organisms. This process is elegantly visualized by culturing groups of the bacterium *Pseudomonas Fluorescens*. Individual bacteria spontaneously mutate to acquire a cell-cell glue, producing multicellular mats that are more effective in collecting oxygen[4]. These unicellular organisms promote their own evolutionary success by cooperating as a multicellular organism. In a similar manner, the approximate 4 x 10^{13} cells in our body also work together and prioritize the fitness of the organism above the prosperity of individual cells[5]. However, cooperation between cells is sometimes disrupted. In the example of *Pseudomonas Fluorescens*, 'cheating' bacteria arise that take advantage of the increased oxygen without contributing to the multicellular mats, eventually sending these groups of cells into their demise[6]. Cells in the human body can also develop characteristics that allow them to prosper at the expense of the entire organism. When these malignant cells behave according to several hallmarks, they are thought to be cancerous. Cancer cells induce proliferative signaling, evade growth suppressors, resist cell death, replicate uncontrollably, induce angiogenesis, and actively invade tissues[7]. Cancer can arise from virtually any tissue in the human body and is among the leading causes of morbidity worldwide[8]. Moreover, the number of new cancer cases is expected to rise by 70% in the coming decades[8].

HEMATOPOIESIS AND THE BONE MARROW NICHE

All cells in the human body are connected to the blood system: a dynamic network of arteries and veins which transports two major types of blood cells. Red blood cells, or erythrocytes, transport O_2 and CO_2 bound to hemoglobin, while white blood cells (WBCs), or leukocytes, protect against infectious agents. Blood cells descent from a single cell type, the hematopoietic stem cell (HSC), which is maintained and regulated by the bone marrow (BM) microenvironment[9-11]. HSCs create progenitor cells devoted to producing specific lineages of mature blood cells[12]. Common myeloid progenitors produce myeloid cells (myeloid means resembling BM) and common lymphoid progenitors give rise to B cells and T cells. Combined, the blood system provides nutrients and oxygen, removes waste products and protects the entire body from pathogens. While all blood cells have a limited life span, HSCs are capable of self-renewal and producing additional HSCs. These characteristics are driven by chemical and physical interactions from the microenvironment in which HSCs reside[9,13]. The BM niche is rich in stem cell factor, stromal cell-derived factor 1 (CXCL12), transforming growth factor beta-1, angiopoietin 1, thrombopoietin and platelet factor 4; while endothelial cells, megakaryocytes and mesenchymal stromal cells (MSCs) provide crucial cell-cell interactions that sustain HSCs[9,14]. Together these signals facilitate the hierarchy between HSCs and all other blood cells. HSCs are maintained to replenish the blood system, while mature blood cells undergo apoptosis upon completion of their task.

LEUKEMIA

Leukemia is a type of cancer that originates from the BM and disturbs the balance between blood cells. It is caused by WBCs that are transformed and proliferate uncontrollably. If left untreated, leukemia leads to severe symptoms and death. Leukemias are classified based on their phenotype. Acute leukemia is caused by a rapid increase of immature WBCs while chronic leukemia can take years to progress. Further subdivision is performed based on the origin of the malignant cell, which is either of the lymphoid or myeloid lineage. This thesis focuses on acute lymphoblastic leukemia (ALL), which is the most frequent cause of death from cancer among children[15]. More specifically, we focus on ALL that arises from B cell precursors (BCP-ALL), the most common form of ALL[16]. BCP-ALL cells are genetically altered compared to their healthy counterparts, often by changes in chromosome number and chromosome translocations[15]. Chromosome translocations produce recombined gene loci that alter the expression of oncogenes and induce chimeric fusion genes with transforming properties[17,18]. They are recognized as driving events in childhood leukemia and consequently, BCP-ALL are classified by their chromosomal rearrangement[19]. BCR-ABL1, ETV6-RUNX1, TCF3-PBX1, and MLL-rearranged leukemia account for more than one-third of the BCP-ALL cases[20]. Furthermore, 25% of cases show hyperdiploidy (> 50 chromosomes per leukemic cell)[20]. Finally, BCP-ALL with neither of the previous aberrations are classified as B-Other. Part of the B-Other leukemias have been observed by gene expression arrays to induce transcriptionally related programs to BCR-ABL1$^+$ cells and are therefore called BCR-ABL1-like leukemia[21].

TREATMENT

Cytogenetically classifying leukemia predicts patient outcome and chemotherapy resistance[20,22]. This has been used to optimize treatment protocols, which has improved survival from 10% in the 1960's to approximately 90% survival in the 21st century[15]. Other types of childhood cancer follow this trend although survival is on average 80%[23]. Improvements in treatment have brought about that 1 out of every 1000 twenty-year-olds is a survivor of childhood cancer[24]. Due to a lack of treatment specificity almost two third of survivors suffer from a chronic condition, and in 28% late effects are life-threatening[25]. Cardiac damage, severe pulmonary damage, fibrosis to the gastrointestinal tract, hepatitis and cirrhosis, kidney and bladder damage, skeletal damage, muscle atrophy, hyper and hypothyroidism, obesity, short stature, gonadal failure, damage to the central nervous system affecting cognitive abilities, cataracts, hearing loss, damaged teeth and gums; all are off-target effects of chemo and radiotherapy .[24-40] Moreover, childhood cancer survivors are at more than 19-fold increased risk for developing another malignancy, caused in part by cancer therapy[25,40]. This underlines the importance of finding novel therapeutic options that specifically and effectively kill leukemic cells.

THE LEUKEMIC NICHE

To pinpoint new therapeutic targets, it is key to elucidate which cells drive leukemia and how these cells are transformed. Cancer cells resemble stem cells, as they share the ability to self-renew and are mostly driven by the same molecular pathways[41]. Simultaneous to the discovery of HSCs, it was observed that only low frequencies of leukemic cells could form colonies both *in vitro* and *in vivo*[42-45]. These findings pointed to the existence of leukemia stem cells (LSCs), also called leukemia propagating cells, which existence has been demonstrated for the first time in acute myeloid leukemia[46]. LSCs disrupt normal HSC niches[47] and are unresponsive to the intrinsic and extrinsic cues that keep HSCs in check[48]. The disrupted, so called *leukemic*, niche is essential in initiating and facilitating leukemogenesis[49-53]. Current treatment is aimed at the bulk of leukemic cells, but arguably a more successful strategy would be to target the LSC. LSCs have increased resistance to chemotherapeutic agents and are protected from elimination by immune responses by the leukemic niche[54-59]. Therefore, disrupting the interaction between leukemic cells and their microenvironment offers a promising new therapeutic strategy. However, it is largely unclear how crosstalk occurs within the leukemic niche, and how this drives leukemic cell survival and chemotherapy resistance.

INTERCELLULAR COMMUNICATION

Communication between cells governs their behavior in favor of the organisms' benefit. This importance of cell-cell communication is underlined by the broad amount of signaling mechanisms that have evolved in human cells (Figure 1). Signaling between nearby cells is facilitated by ligand-receptor interactions and through electrical signals exchanged via specialized structures called gap junctions. Cells that communicate over (long) distances use cytokines, vesicles, hormones or even dissolved gases like nitric oxide that spread via the blood system. However, current knowledge on intercellular signaling is lacking in its ability to explain interactions in the leukemic niche. In 2004, cytoskeletal structures called tunneling nanotubes (TNTs), or membrane nanotubes, were discovered to facilitate signaling between eukaryotic cells[60-62]. TNTs protrude from the cell membrane and are driven by the polymerization of monomeric actin into filamentous actin[61,62] (Figure 1 and 2). They can reach lengths of multiple cell diameters and facilitate intercellular signaling of diverse cargo, including organelles, pathogens, calcium fluxes, membrane bound proteins and death signals[61,63-66]. TNTs have been observed in numerous cell types, like cancer cells, complex tissues and organisms[61,62,65,67-71]. Their pathophysiological importance has been demonstrated by studies showing the spread of prions and HIV-1 particles via TNTs[62,72]. However, their presence and importance in the leukemic niche have not yet been addressed. The broad array of signal molecules that may be exchanged between leukemic cells and the BM microenvironment via TNTs make these structures prime candidates for investigation.

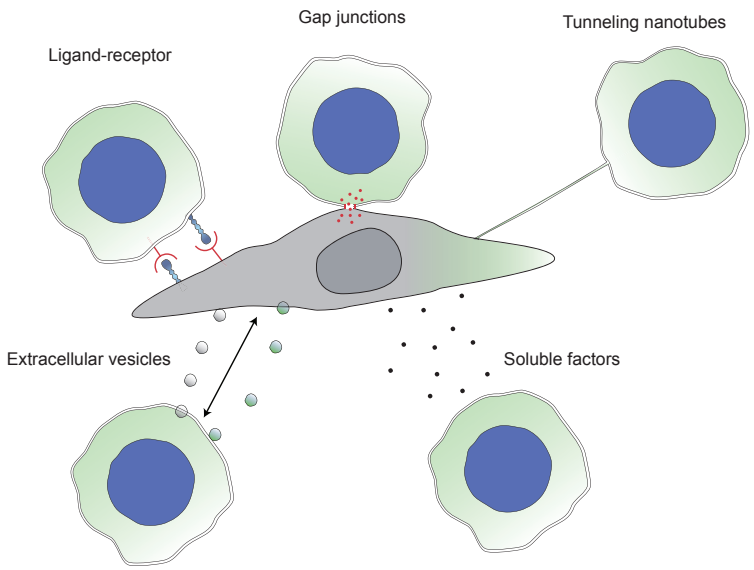

Figure 1. Intercellular communication mechanisms. Illustration summarizing how leukemic cells (green cells) might communicate with MSCs (grey cell). Cells express ligands on the plasma membrane which are detected by specialized receptors on the target cell, gap junctions exchange electrical signals, tunneling nanotubes connect nearby cells through an extension of the plasma membrane, extracellular vesicles are secreted and exchanged between distant cells, and multiple soluble factors are spread through the blood system.

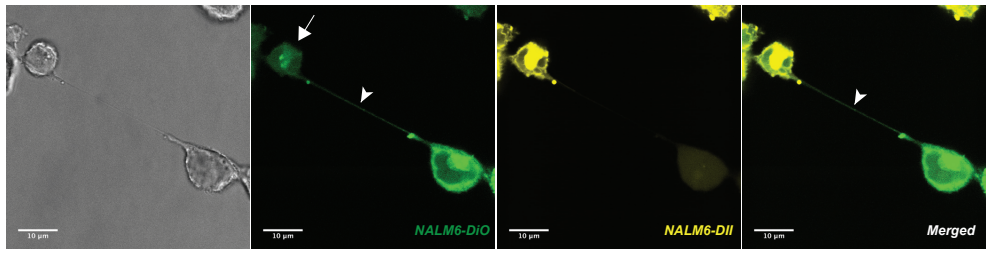

Figure 2. Tunneling nanotube formation between leukemic cells. Confocal images showing TNT formation (white arrowhead) between two BCP-ALL cells (NALM6; DiI, yellow; DiO, green) after co-culture for 24 hours. White arrow indicates transfer of lipophilic structures to recipient cell.

LEUKEMIC CELL MIGRATION

One of the hallmarks of cancer cells is their ability to invade tissues[7]. In ALL, the BM is taken over by leukemic blasts that overgrow healthy cell types[73]. Much effort is put into finding targets that disrupt the migration of leukemic cells to clear these cells from the bone marrow. Migration of ALL cells toward the BM microenvironment is thought to be similar to that of HSCs. HSCs are attracted by CXCL12, a chemoattractant actively produced by MSCs in the BM.[74-76] ALL cells, like HSCs, have high expression of the CXCL12 receptor CXCR4[76]. Disturbance of the CXCR4/CXCL12 axis, by treatment with cytokines or CXCR4 antagonists, mobilizes HSCs to the peripheral blood[77] and reduces ALL engraftment in animal models[57,78]. However, in mice suffering from ALL, CXCR4/CXCL12 inhibition does not reduce the leukemic cell number in the BM[78,79]. This suggests that ALL cells use additional mechanisms to retain a protective microenvironment. Leukemic cells protected from chemotherapeutic treatment cause minimal residual disease, one of the most important predictors of patient outcome[80-82]. Discovering how ALL cells create a leukemic niche is crucial to develop more specific and effective ways to eliminate (residual) leukemic cells.

OUTLINE THESIS

Studies addressing the behavior of cancer cells and their similarities to stem cells have given new insights into improving treatment. HSCs are driven and maintained largely by their microenvironment and therefore it is likely that LSCs are also dependent on their niche. In the work described in this thesis, we aimed to identify novel mechanisms used by leukemic cells to create a leukemic niche.

In **Chapter 2** we describe the discovery of TNT signaling between BCP-ALL cells and MSCs, a crucial and abundant cell type in the BM. Confocal microscopy revealed high resolution images of TNTs connecting ALL cells and MSCs derived from patients. Signaling via TNTs was visualized by detecting the transfer of a lipophilic dye in ALL-MSC co-cultures. Finally, TNT signaling was inhibited to investigate its effect on the secretion of pro-survival factors and leukemic cell viability and drug resistance.

Currently, TNT signaling cannot be inhibited in patients. Since TNTs are cytoskeletal structures, we explored the effect of a large panel of actin and tubulin inhibitors for their potency in disrupting TNT signaling in **Chapter 3**. Until now, only actin polymerization has been shown to play a role in TNT signaling. In this chapter we investigated whether tubulin and actin nucleation and disassembly play similar roles. In addition, cytoskeletal inhibitors were screened for their effects on the viability of primary leukemic and healthy blood cells.

Chapter 4 investigated which structures are transported from ALL cells toward MSCs by detecting the transfer of ectopically expressed fluorescent marker proteins using flow cytometry.

Migration and invasion of the BM microenvironment by BCP-ALL cells is the focus of **Chapter 5.** We modelled the leukemic niche using primary ALL-MSC co-cultures and used this to compare migration of healthy and leukemic cells. Importantly, we validated these experiments using serum derived from bone marrow aspirates of leukemia patients and healthy controls. These experiments show that the leukemic niche specifically attracts malignant cells independent of CXCR4/CXCL12 signaling and identify potential targets for leukemic niche disruption.

Finally, **Chapter 6** discusses the impact of the findings in this thesis and offers perspectives for follow-up research.

REFERENCES

1. Theobald DL. A formal test of the theory of universal common ancestry. *Nature*. 2010;465(7295):219-222.
2. Ohtomo Y, Kakegawa T, Ishida A, Nagase T, Rosing MT. Evidence for biogenic graphite in early Archaean Isua metasedimentary rocks. 2014;7(1):25-28.
3. Noffke N, Christian D, Wacey D, Hazen RM. Microbially induced sedimentary structures recording an ancient ecosystem in the ca. 3.48 billion-year-old Dresser Formation, Pilbara, Western Australia. *Astrobiology*. 2013;13(12):1103-1124.
4. Spiers AJ, Kahn SG, Bohannon J, Travisano M, Rainey PB. Adaptive divergence in experimental populations of Pseudomonas fluorescens. I. Genetic and phenotypic bases of wrinkly spreader fitness. *Genetics*. 2002;161(1):33-46.
5. Bianconi E, Piovesan A, Facchin F, et al. An estimation of the number of cells in the human body. *Ann Hum Biol*. 2013;40(6):463-471.
6. Hammerschmidt K, Rose CJ, Kerr B, Rainey PB. Life cycles, fitness decoupling and the evolution of multicellularity. 2014;515(7525):75-79.
7. Hanahan D, Weinberg RA. Hallmarks of cancer: the next generation. *Cell*. 2011;144(5):646-674.
8. Stewart B, Wild CP. World Cancer Report: WHO; 2014.
9. Morrison SJ, Scadden DT. The bone marrow niche for haematopoietic stem cells. *Nature*. 2014;505(7483):327-334.
10. Main JM, Prehn RT. Successful skin homografts after the administration of high dosage X radiation and homologous bone marrow. *J Natl Cancer Inst*. 1955;15(4):1023-1029.
11. Till JE, Mc CE. A direct measurement of the radiation sensitivity of normal mouse bone marrow cells. *Radiat Res*. 1961;14:213-222.
12. Orkin SH, Zon LI. Hematopoiesis: an evolving paradigm for stem cell biology. *Cell*. 2008;132(4):631-644.
13. Schofield R. The relationship between the spleen colony-forming cell and the haemopoietic stem cell. *Blood Cells*. 1978;4(1-2):7-25.
14. Schepers K, Campbell TB, Passegue E. Normal and leukemic stem cell niches: insights and therapeutic opportunities. *Cell Stem Cell*. 2015;16(3):254-267.
15. Hunger SP, Mullighan CG. Acute Lymphoblastic Leukemia in Children. *N Engl J Med*. 2015;373(16):1541-1552.
16. Pui CH, Robison LL, Look AT. Acute lymphoblastic leukaemia. *Lancet*. 2008;371(9617):1030-1043.
17. Rabbitts TH. Chromosomal translocations in human cancer. *Nature*. 1994;372(6502):143-149.
18. Look AT. Oncogenic transcription factors in the human acute leukemias. *Science*. 1997;278(5340):1059-1064.
19. Rowley JD. The critical role of chromosome translocations in human leukemias. *Annu Rev Genet*. 1998;32:495-519.
20. Meijerink JP, den Boer ML, Pieters R. New genetic abnormalities and treatment response in acute lymphoblastic leukemia. *Semin Hematol*. 2009;46(1):16-23.
21. Den Boer ML, van Slegtenhorst M, De Menezes RX, et al. A subtype of childhood acute lymphoblastic leukaemia with poor treatment outcome: a genome-wide classification study. *Lancet Oncol*. 2009;10(2):125-134.
22. Pui CH, Carroll WL, Meshinchi S, Arceci RJ. Biology, risk stratification, and therapy of pediatric acute leukemias: an update. *J Clin Oncol*. 2011;29(5):551-565.
23. Howlader N NA, Krapcho M, et al. SEER Cancer Statistics Review, 1975-2011. Vol. 2014: SEER; 2014.
24. Oeffinger KC, Mertens AC, Hudson MM, et al. Health care of young adult survivors of childhood cancer: a report from the Childhood Cancer Survivor Study. *Ann Fam Med*. 2004;2(1):61-70.
25. Dickerman JD. The late effects of childhood cancer therapy. *Pediatrics*. 2007;119(3):554-568.
26. Kremer LC, Caron HN. Anthracycline cardiotoxicity in children. *N Engl J Med*. 2004;351(2):120-121.
27. Bowers DC, Liu Y, Leisenring W, et al. Late-occurring stroke among long-term survivors of childhood leukemia and brain tumors: a report from the Childhood Cancer Survivor Study. *J Clin Oncol*. 2006;24(33):5277-5282.
28. Weiner DJ, Maity A, Carlson CA, Ginsberg JP. Pulmonary function abnormalities in children treated with whole lung irradiation. *Pediatr Blood Cancer*. 2006;46(2):222-227.
29. Emami B, Lyman J, Brown A, et al. Tolerance of normal tissue to therapeutic irradiation. *Int J Radiat Oncol Biol Phys*. 1991;21(1):109-122.
30. Bessho F, Kinumaki H, Yokota S, Hayashi Y, Kobayashi M, Kamoshita S. Liver function studies in children with acute lymphocytic leukemia after cessation of therapy. *Med Pediatr Oncol*. 1994;23(2):111-115.
31. McIntosh S, Davidson DL, O'Brien RT, Pearson HA. Methotrexate hepatotoxicity in children with leukemia. *J Pediatr*. 1977;90(6):1019-1021.
32. Smith GR, Thomas PR, Ritchey M, Norkool P. Long-term renal function in patients with irradiated bilateral Wilms tumor. National Wilms' Tumor Study Group. *Am J Clin Oncol*. 1998;21(1):58-63.
33. McCune JS, Friedman DL, Schuetze S, Blough D, Magbulos M, Hawkins DS. Influence of age upon Ifosfamide-induced nephrotoxicity. *Pediatr Blood Cancer*. 2004;42(5):427-432.
34. Rehman Q, Lane NE. Effect of glucocorticoids on bone density. *Med Pediatr Oncol*. 2003;41(3):212-216.
35. Kaste SC, Rai SN, Fleming K, et al. Changes in bone mineral density in survivors of childhood acute lymphoblastic leukemia. *Pediatr Blood Cancer*. 2006;46(1):77-87.
36. Fletcher BD. Effects of pediatric cancer therapy on the musculoskeletal system. *Pediatr Radiol*. 1997;27(8):623-636.
37. Chow EJ, Friedman DL, Yasui Y, et al. Decreased adult height in survivors of childhood acute lymphoblastic leukemia: a report from the Childhood Cancer Survivor Study. *J Pediatr*. 2007;150(4):370-375, 375 e371.
38. Effinger KE, Migliorati CA, Hudson MM, et al. Oral and dental late effects in survivors of childhood cancer: a Children's Oncology Group report. *Support Care Cancer*. 2014;22(7):2009-2019.
39. Alberth M, Kovalecz G, Nemes J, Math J, Kiss C, Marton IJ. Oral health of long-term childhood cancer survivors. *Pediatr Blood Cancer*. 2004;43(1):88-90.
40. Argani P, Lae M, Ballard ET, et al. Translocation carcinomas of the kidney after chemotherapy in childhood. *J Clin Oncol*. 2006;24(10):1529-1534.
41. Passegue E, Jamieson CH, Ailles LE, Weissman IL. Normal and leukemic hematopoiesis: are leukemias a stem cell disorder or a reacquisition of stem cell characteristics? *Proc Natl Acad Sci U S A*. 2003;100 Suppl 1:11842-11849.
42. Park CH, Bergsagel DE, McCulloch EA. Mouse myeloma tumor stem cells: a primary cell culture assay. *J Natl Cancer Inst*. 1971;46(2):411-422.

43. Bruce WR, Van Der Gaag H. A Quantitative Assay for the Number of Murine Lymphoma Cells Capable of Proliferation in Vivo. *Nature*. 1963;199:79-80.

44. Sabbath KD, Ball ED, Larcom P, Davis RB, Griffin JD. Heterogeneity of clonogenic cells in acute myeloblastic leukemia. *J Clin Invest*. 1985;75(2):746-753.

45. Griffin JD, Lowenberg B. Clonogenic cells in acute myeloblastic leukemia. *Blood*. 1986;68(6):1185-1195.

46. Bonnet D, Dick JE. Human acute myeloid leukemia is organized as a hierarchy that originates from a primitive hematopoietic cell. *Nat Med*. 1997;3(7):730-737.

47. Colmone A, Amorim M, Pontier AL, Wang S, Jablonski E, Sipkins DA. Leukemic cells create bone marrow niches that disrupt the behavior of normal hematopoietic progenitor cells. *Science*. 2008;322(5909):1861-1865.

48. Huntly BJ, Gilliland DG. Leukaemia stem cells and the evolution of cancer-stem-cell research. *Nat Rev Cancer*. 2005;5(4):311-321.

49. Flynn CM, Kaufman DS. Donor cell leukemia: insight into cancer stem cells and the stem cell niche. *Blood*. 2007;109(7):2688-2692.

50. Raaijmakers MH, Mukherjee S, Guo S, et al. Bone progenitor dysfunction induces myelodysplasia and secondary leukaemia. *Nature*. 2010;464(7290):852-857.

51. Walkley CR, Olsen GH, Dworkin S, et al. A microenvironment-induced myeloproliferative syndrome caused by retinoic acid receptor gamma deficiency. *Cell*. 2007;129(6):1097-1110.

52. Walkley CR, Shea JM, Sims NA, Purton LE, Orkin SH. Rb regulates interactions between hematopoietic stem cells and their bone marrow microenvironment. *Cell*. 2007;129(6):1081-1095.

53. Yilmaz OH, Valdez R, Theisen BK, et al. Pten dependence distinguishes haematopoietic stem cells from leukaemia-initiating cells. *Nature*. 2006;441(7092):475-482.

54. Jin L, Hope KJ, Zhai Q, Smadja-Joffe F, Dick JE. Targeting of CD44 eradicates human acute myeloid leukemic stem cells. *Nat Med*. 2006;12(10):1167-1174.

55. Matsunaga T, Takemoto N, Sato T, et al. Interaction between leukemic-cell VLA-4 and stromal fibronectin is a decisive factor for minimal residual disease of acute myelogenous leukemia. *Nat Med*. 2003;9(9):1158-1165.

56. Nervi B, Ramirez P, Rettig MP, et al. Chemosensitization of acute myeloid leukemia (AML) following mobilization by the CXCR4 antagonist AMD3100. *Blood*. 2009;113(24):6206-6214.

57. Sipkins DA, Wei X, Wu JW, et al. In vivo imaging of specialized bone marrow endothelial microdomains for tumour engraftment. *Nature*. 2005;435(7044):969-973.

58. Tavor S, Petit I, Porozov S, et al. CXCR4 regulates migration and development of human acute myelogenous leukemia stem cells in transplanted NOD/SCID mice. *Cancer Res*. 2004;64(8):2817-2824.

59. Zeng Z, Shi YX, Samudio IJ, et al. Targeting the leukemia microenvironment by CXCR4 inhibition overcomes resistance to kinase inhibitors and chemotherapy in AML. *Blood*. 2009;113(24):6215-6224.

60. Onfelt B, Nedvetzki S, Yanagi K, Davis DM. Cutting edge: Membrane nanotubes connect immune cells. *J Immunol*. 2004;173(3):1511-1513.

61. Rustom A, Saffrich R, Markovic I, Walther P, Gerdes HH. Nanotubular highways for intercellular organelle transport. *Science*. 2004;303(5660):1007-1010.

62. Sowinski S, Jolly C, Berninghausen O, et al. Membrane nanotubes physically connect T cells over long distances presenting a novel route for HIV-1 transmission. *Nat Cell Biol*. 2008;10(2):211-219.

63. Watkins SC, Salter RD. Functional connectivity between immune cells mediated by tunneling nanotubules. *Immunity*. 2005;23(3):309-318.

64. Arkwright PD, Luchetti F, Tour J, et al. Fas stimulation of T lymphocytes promotes rapid intercellular exchange of death signals via membrane nanotubes. *Cell Res*. 2010;20(1):72-88.

65. Pasquier J, Galas L, Boulange-Lecomte C, et al. Different modalities of intercellular membrane exchanges mediate cell-to-cell p-glycoprotein transfers in MCF-7 breast cancer cells. *J Biol Chem*. 2012;287(10):7374-7387.

66. Rainy N, Chetrit D, Rouger V, et al. H-Ras transfers from B to T cells via tunneling nanotubes. *Cell Death Dis*. 2013;4:e726.

67. Chinnery HR, Pearlman E, McMenamin PG. Cutting edge: Membrane nanotubes in vivo: a feature of MHC class II+ cells in the mouse cornea. *J Immunol*. 2008;180(9):5779-5783.

68. Marzo L, Gousset K, Zurzolo C. Multifaceted roles of tunneling nanotubes in intercellular communication. *Front Physiol*. 2012;3:72.

69. Seyed-Razavi Y, Hickey MJ, Kuffova L, McMenamin PG, Chinnery HR. Membrane nanotubes in myeloid cells in the adult mouse cornea represent a novel mode of immune cell interaction. *Immunol Cell Biol*. 2013;91(1):89-95.

70. Pasquier J, Guerrouahen BS, Al Thawadi H, et al. Preferential transfer of mitochondria from endothelial to cancer cells through tunneling nanotubes modulates chemoresistance. *J Transl Med*. 2013;11:94.

71. Lou E, Fujisawa S, Morozov A, et al. Tunneling nanotubes provide a unique conduit for intercellular transfer of cellular contents in human malignant pleural mesothelioma. *PLoS One*. 2012;7(3):e33093.

72. Gousset K, Schiff E, Langevin C, et al. Prions hijack tunnelling nanotubes for intercellular spread. *Nat Cell Biol*. 2009;11(3):328-336.

73. Ibbott JW, Whitelaw DM, Thomas JW. The significant percentage of blast cells in the bone marrow in the diagnosis of acute leukaemia. *Can Med Assoc J*. 1960;82:358-361.

74. Aiuti A, Webb IJ, Bleul C, Springer T, Gutierrez-Ramos JC. The chemokine SDF-1 is a chemoattractant for human CD34+ hematopoietic progenitor cells and provides a new mechanism to explain the mobilization of CD34+ progenitors to peripheral blood. *J Exp Med*. 1997;185(1):111-120.

75. Peled A, Petit I, Kollet O, et al. Dependence of human stem cell engraftment and repopulation of NOD/SCID mice on CXCR4. *Science*. 1999;283(5403):845-848.

76. van den Berk LC, van der Veer A, Willemse ME, et al. Disturbed CXCR4/CXCL12 axis in paediatric precursor B-cell acute lymphoblastic leukaemia. *Br J Haematol*. 2014;166(2):240-249.

77. Flomenberg N, Devine SM, Dipersio JF, et al. The use of AMD3100 plus G-CSF for autologous hematopoietic progenitor cell mobilization is superior to G-CSF alone. *Blood*. 2005;106(5):1867-1874.

78. Juarez J, Dela Pena A, Baraz R, et al. CXCR4 antagonists mobilize childhood acute lymphoblastic leukemia cells into the peripheral blood and inhibit engraftment. *Leukemia*. 2007;21(6):1249-1257.

79. Parameswaran R, Yu M, Lim M, Groffen J, Heisterkamp N. Combination of drug therapy in acute lymphoblastic leukemia with a CXCR4 antagonist. *Leukemia*. 2011;25(8):1314-1323.

80. Coustan-Smith E, Gajjar A, Hijiya N, et al. Clinical significance of minimal residual disease in childhood acute lymphoblastic leukemia after first relapse. *Leukemia*. 2004;18(3):499-504.

81. Campana D. Minimal residual disease in acute lymphoblastic leukemia. *Semin Hematol*. 2009;46(1):100-106.

82. van Dongen JJ, van der Velden VH, Bruggemann M, Orfao A. Minimal residual disease diagnostics in acute lymphoblastic leukemia: need for sensitive, fast, and standardized technologies. *Blood*. 2015;125(26):3996-4009.

Chapter 2

B-CELL PRECURSOR ACUTE LYMPHOBLASTIC LEUKEMIA CELLS USE TUNNELING NANOTUBES TO ORCHESTRATE THEIR MICROENVIRONMENT

Roel Polak*, Bob de Rooij*, Rob Pieters & Monique L. den Boer

* authors contributed equally

Blood. 2015;126(21):2404-2414.

ABSTRACT

Acute lymphoblastic leukemia (ALL) cells reside in the bone marrow microenvironment which nurtures and protects cells from chemotherapeutic drugs. The disruption of cell-cell communication within the leukemic niche may offer an important new therapeutic strategy. Tunneling nanotubes (TNTs) have been described as a novel mode of intercellular communication, but their presence and importance in the leukemic niche are currently unknown. Here, we show for the first time that primary B-cell precursor ALL cells use TNTs to signal to primary mesenchymal stromal cells (MSCs). This signaling results in secretion of pro-survival cytokines, such as IP10/CXCL10, IL8 and MCP-1/CCL2. A combination of TNT disrupting conditions allows us to analyze the functional importance of TNTs in an *ex vivo* model. Our results indicate that TNT signaling is important for the viability of patient-derived B-cell precursor ALL cells and induces stroma-mediated prednisolone resistance. Disruption of TNTs significantly inhibits these leukemogenic processes and re-sensitizes B-cell precursor ALL cells to prednisolone. Our findings establish TNTs as a novel communication mechanism by which ALL cells modulate their bone marrow microenvironment. The identification of TNT signaling in ALL-MSC communication gives insight into the pathobiology of ALL and opens new avenues to develop more effective therapies that interfere with the leukemic niche.

KEY POINTS

Primary BCP-ALL cells use tunneling nanotubes to signal to mesenchymal stromal cells and thereby trigger cytokine secretion.

Inhibiting tunneling nanotube signaling is a promising approach to induce apoptosis and sensitize BCP-ALL cells towards prednisolone.

INTRODUCTION

Acute lymphoblastic leukemia (ALL) cells reside in the local microenvironment of the bone marrow and are able to disrupt normal hematopoietic stem cell niches[1]. The disrupted, so called leukemic, niche is essential in initiating and facilitating leukemogenesis[2-6]. In addition, the leukemic niche protects leukemic cells from elimination by immune responses and chemotherapeutic agents, and can facilitate the development of drug resistance of leukemic cells[7-10]. Therefore, the disruption of the ALL-leukemic niche interaction offers a promising new therapeutic strategy[11-16]. However, it is still largely unclear how crosstalk occurs within the leukemic niche, and how this drives leukemic cell survival and chemotherapy resistance.

Recently, tunneling nanotubes (TNTs), or membrane nanotubes, have been described as a novel mode of communication between eukaryotic cells[17-21]. TNTs are thin membrane protrusions consisting of F-actin, that connect cells and facilitate the transport of several types of cargo, including organelles, pathogens, calcium fluxes, death signals, and membrane bound proteins[19,20,22-24]. These intercellular membrane conduits have been observed in several cell types, like cancer cells, complex tissues and organisms[20,21,24-29]. The pathophysiological importance of TNTs has become evident by studies showing that prions and HIV-1 particles use TNTs to promote disease spread[21,30]. However, the presence of TNTs within the leukemic niche and hence their role in communication between leukemic cells and the bone marrow microenvironment has not yet been addressed. Here, we study the role of TNT signaling in communication between primary B-cell precursor ALL (BCP-ALL) cells and MSCs and the contribution of TNT signaling to mesenchymal-mediated survival and resistance to the chemotherapeutic drug prednisolone.

METHODS

Cell lines

BCP-ALL cell lines, NALM6 (B-Other) and REH (TEL-AML1), were obtained from DSMZ (Braunschweig, Germany). Only low cell passages were used, and the identity of cell lines was routinely verified by DNA fingerprinting. Immortalized hTERT-MSCs were a kind gift from Prof. Dr. D. Campana, St. Jude Children's Hospital, Memphis, TN, USA.

Primary patient-derived material

Bone marrow aspirates were obtained from children with newly diagnosed BCP-ALL prior to treatment. Mononuclear leukemic cells were collected and processed as previously described[31]. All samples used in this study contained ≥97% leukemic blasts (supplemental Figure 7). Mesenchymal stromal cells (MSCs) were isolated from bone-marrow aspirates obtained from newly diagnosed BCP-ALL patients (before treatment) and healthy controls. MSCs were processed as described previously[32]. Primary MSCs were characterized using positive (CD44/ CD90/ CD105/ CD54/ CD73/ CD146/ CD166/ STRO-1) and negative surface markers (CD19/ CD45/ CD34) (supplemental Figure 6). Multilineage

potential of MSCs was confirmed for adipocyte (Oil Red O staining), osteocyte (Alizarin Red S staining), and chondrocyte (Col2a/ Thionine/ Alcian Blue staining) differentiation.

Dye transfer experiments

Cells were stained with 1,1'-dioctadecyl-3,3,3'3'-tetramethylindocarbocyanine perchlorate (DiI; yellow), 3,3'-dioctadecyloxacarbocyanine (DiO; green), 1,1'-dioctadecyl-3,3,3'3'-tetramethylindodicarbocyanine perchlorate (DiD; red), or Calcein red-orange AM (all from Life Technologies) according to the manufacturer's protocol. Target populations were analyzed before and after co-culture with flow cytometry (BD Bioscience, San Jose, CA, USA) or confocal microscopy (see below).

Confocal laser scanning microscopy

For high resolution images, differentially stained cells were cultured on a glass slide coated with 10 µg/mL fibronectin (Sigma) at 37 °C and 5% CO_2. Cells were fixated as previously described[33]. Confocal images were acquired with sequential scanning of different channels at a resolution of 1024 x 1024 pixels in the x ˣ y plane and 0.15 µm steps in z-direction (Leica SP5). For time-lapse confocal imaging, cultures were maintained at 37°C on a heated stage at 5% CO_2 and images were acquired with sequential scanning of different channels at a resolution of 512 x 512 pixels in the x ˣ y plane and 0.5 µm steps in z-direction. 3D image stacks were acquired by optical sectioning using the LAS software provided with the instrument. The system was equipped with a 63× plan-apochromat oil 1.4 NA DIC objective. The pinhole diameter was set to 1 airy unit (95.5 µm). DiO and DiI were excited with a 488-nm Argon laser and a 561-nm Diode-Pumped Solid-State laser, respectively. Phalloidin-FITC (Sigma) was excited with the 488-nm Argon laser. Image processing was done with Fiji software[34].

TNT inhibition

TNTs were inhibited using actin inhibition by latrunculin B (125 – 500 nM; Sigma) or cytochalasin D (250 nM – 1 µM; Sigma)[20], by mechanical disruption via gentle shaking of cell cultures (250 rpm)[21,35], or by physical separation of leukemic cells (cultured in a 3.0 µm pore-sized insert) and MSCs (cultured in the bottom compartment of a transwell system; Corning, NY, USA)[21,36].

Cell viability assays

Primary patient cells (1 x 10^6 cells) were co-cultured with or without primary MSCs (5 x 10^4) for five days in a 24-well plate at 37 °C and 5% CO_2. The percentage of viable leukemic cells was determined by staining with Brilliant Violet 421 anti-human CD19 or CD45 antibody (Biolegend), FITC Annexin V (Biolegend), and Propidium Iodide (PI; Sigma), after which the percentage of $AnnexinV^{neg}/PI^{neg}/CD19^{pos}/CD45^{pos}$ cells within the MSC negative fraction (see Figure 6A for gating strategy) was determined by flow cytometry (BD Biosciences). In supplemental Figure 10, viable leukemic cells were counted (PI^{neg}/$CD19^{pos}$) using a MACSQuant analyzer (Miltenyi Biotec, Gladbach, Germany).

Multiplexed fluorescent bead-based immunoassay (Luminex)

Primary leukemic cells and leukemic cell lines were co-cultured with primary MSCs with or without TNT inhibition (shaking or transwell condition) for indicated time points at 37 °C and 5% CO_2. Next, the supernatant was collected and cell viability of leukemic cells was assessed as described above. The concentration of 64 cytokines/chemokines in supernatants of ALL-MSC co-cultures was analyzed using a fluorescent bead-based immunoassay (Luminex Human Cytokine/Chemokine Panel I and II; Merck Millipore) according to the manufacturer's protocol.

Statistical analysis

Student's t-test was used as a statistical test and a Student's paired t-test was used when applicable (indicated in figure legends). Bar graphs represent the mean of biological replicates. Error bars show as standard error of the mean (SEM).

RESULTS

BCP-ALL cells use TNTs to effectively signal to MSCs

TNT formation within the hematopoietic niche was studied by confocal microscopy and flow cytometry. TNTs are thin membrane tethers and can be visualized using lipophilic carbocyanine dyes[20,21]. These dyes stain lipophilic structures in the entire cell, and exhibit very low cell toxicity, while passive transfer of these dyes is negligible. Therefore, these dyes are widely used in live cell tracking experiments[1,37]. Interestingly, it has been shown that organelles and membrane components stained by these dyes can be actively transported via TNTs[20]. Therefore, these dyes were used to visualize intercellular communication via TNTs within the leukemic niche.

Differential staining of NALM6 BCP-ALL cells (stained with DiI-yellow) and mesenchymal stromal cells (hTERT-MSCs; stained with DiO-green) revealed that TNTs were formed within 3 hours of co-culture (Figure 1A, supplemental Figure 1M-P). 3D reconstruction of these images shows that nanotubular structures *between cells* do not connect with the substratum (i.e. the fibronectin-coated glass slide; see supplemental Video 1A-B and supplemental Video 2). As expected, staining with Phalloidin-FITC shows the presence of F-Actin filaments in these nanotubular structures (see supplemental Figure 1Q-R). Importantly, bidirectional transfer of lipophilic dyes was observed, indicating active crosstalk within the leukemic niche (Figure 1A). Besides formation of TNTs between leukemic cells and MSCs, TNT networks and transfer of lipophilic dye was also observed in mono-cultures of BCP-ALL cells and MSCs (supplemental Figure 1A-L and supplemental Figure 2).

In order to quantify active crosstalk via TNTs we used flow cytometrical analysis of dye transfer from labeled donor cells to unlabeled recipient cells. CD19-positive BCP-ALL cell lines (NALM6 and REH) were stained with lipophilic dye DiI and co-cultured with unstained CD19-negative hTERT-MSCs (supplemental Figure 3A-C for gating strategy). After 6 hours of culture, more than 50% of the MSCs were positive for DiI. This number increased to >85% after 24 hours, highlighting the efficient dye transfer from leukemic cells to MSCs (Figure 1B and supplemental Figure 3D). In reciprocal experiments we also observed dye transfer from MSCs to BCP-ALL cells, but the magnitude of dye transfer was strikingly less than from ALL cells towards MSCs (175-fold, p-value ≤ 0.001) (Figure 1C-D).

Transfer of lipophilic dyes can be mediated by several processes including TNT signaling and signaling via extracellular vesicles (ECV). To evaluate the contribution of TNT signaling to the observed lipophilic dye transfer between leukemic cells and MSCs, we inhibited TNTs using three independent experimental setups: 1) reducing TNT formation through actin inhibition[20], 2) mechanical disruption of TNT connections through gentle shaking of cell cultures[21,35], and 3) prevention of TNT formation by physically separating leukemic cells (cultured in a 3.0 µm pore-sized insert) and MSCs (cultured in the bottom compartment of a transwell system)[21,36].

For inhibition of the polymerized F-actin of which TNTs are composed[20], we used two classes of F-actin polymerization inhibitors: cytochalasin D and latrunculin B. In addition to F-actin elements, TNTs need prolonged cell contact to signal efficiently. Gentle shaking of ALL-MSC co-cultures reduces the lifespan of TNTs, while direct contact between

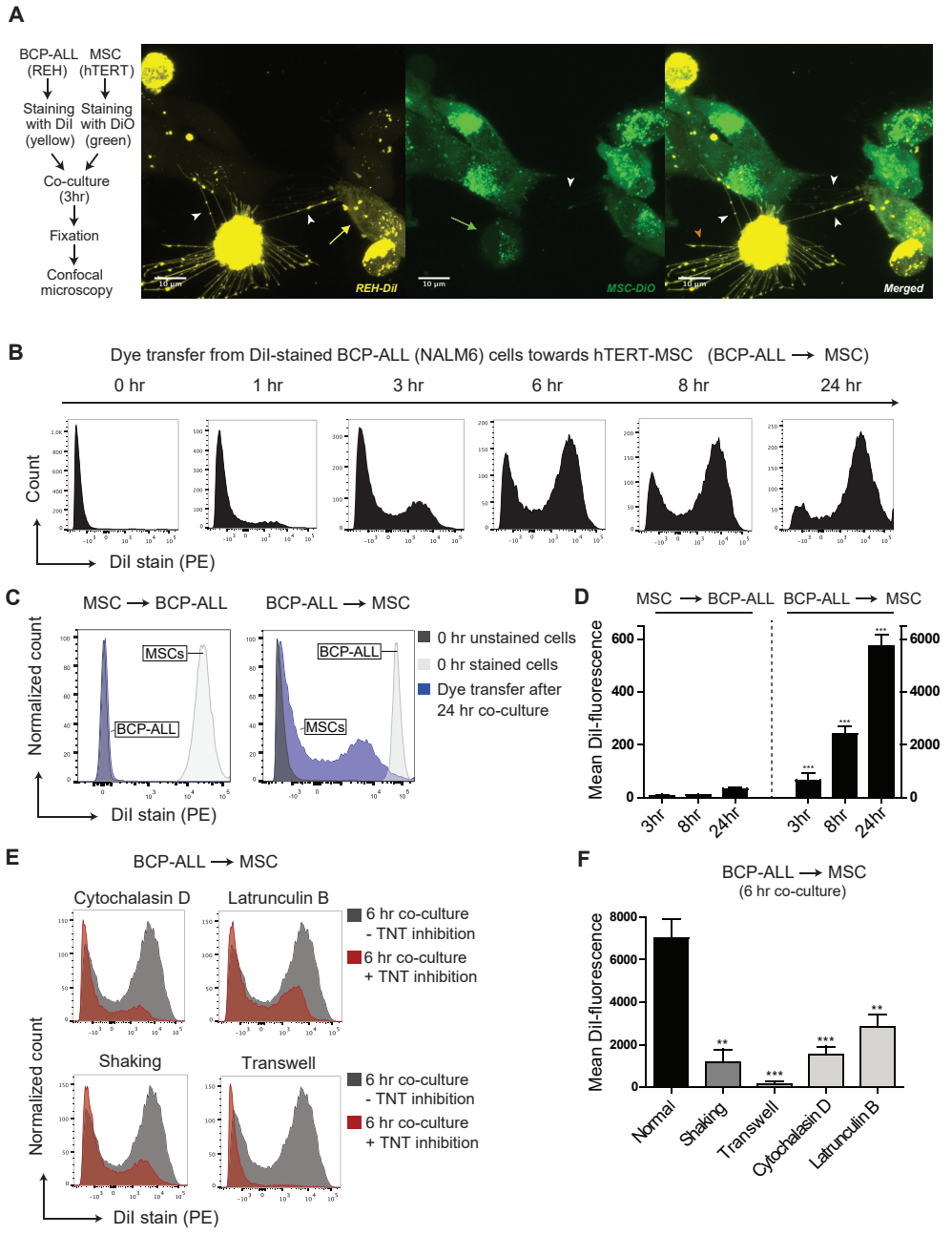

Figure 1. TNT signaling between BCP-ALL cells and MSCs. (A) Representative confocal images (Z-stack) showing TNT networks (white arrowheads) between BCP-ALL cell line REH (DiI, yellow) and hTERT-immortalized MSCs (DiO, green) after co-culture for 3 hours. Bidirectional exchange of lipophilic dye via TNTs was observed (green arrow for MSC to ALL, yellow arrow for ALL to MSC). Leukemic cells also formed TNT-like structures towards the fibronectin-coated substratum (orange arrowhead). (B) Graph showing quantification of dye transfer from DiI-stained NALM6 cells towards unstained hTERT-MSCs (cultured in 4:1 ratio) in time. Figure shows representative experiment (n = 3). (C) Graph showing quantification of dye transfer after 24 hours of co-culture (cultured in 1:1 ratio). Left panel shows dye transfer from DiI-stained hTERT-MSCs towards unstained NALM6 cells. Right panel shows the reciprocal experiment (also performed in a 1:1 ratio). White and grey histograms represent staining intensity at the start of each experiment. (D) Quantification of dye transfer in time of experiment as exemplified in (C), performed with two different BCP-ALL cell lines (REH and NALM6). Dye transfer from MSCs towards ALL was compared to dye transfer from ALL towards MSCs (n = 4; two-tailed t-test, unpaired). (E) Graph showing quantification of dye transfer from DiI-stained NALM6 cells towards unstained hTERT-MSCs with (red histograms) or without (grey histograms) TNT inhibition. Cells were co-cultured in 4:1 ratio for 6 hours. Three independent TNT inhibiting conditions were used: actin inhibition by cytochalasin D or latrunculin B, physical disruption by gentle shaking, or culture in a 3.0 µm transwell system. (F) Quantification of dye transfer experiment exemplified in (E), performed with two different BCP-ALL cell lines (REH and NALM6) (n = 4; one-tailed t-test, unpaired). Data are means ± SEM; ** p ≤ 0.01, *** p ≤ 0.001. See also supplemental Figures 1 and 3, and supplemental Videos 1A-B and 2.

BCP-ALL cells and MSCs is still possible. However, it is well established in literature that flow-derived shear forces (gentle shaking) induce integrin-mediated signaling[38,39]. Therefore, we also physically separate ALL cells and MSCs using a transwell system, to exclude the effects of increased integrin signaling. We used a 3.0 µm transwell system to investigate the contribution of extracellular vesicle signaling to lipophilic dye transfer. In this transwell system leukemic cells are physically separated from MSCs, while exchange of extracellular vesicles (30-1000 nm) is still possible.

Cytochalasin D and latrunculin B both caused a dose-dependent reduction of dye transfer after 6 hours of co-culture ($p \leq 0.01$; Figure 1E-F and supplemental Figure 3E-F). Due to the short half-time of these actin inhibitors[40,41], TNT formation was restored within 24 hours (supplemental Figure 3E-F). Disruption of TNT structures by gentle shaking reduced dye transfer by more than 5-fold ($p \leq 0.01$; Figure 1E-F and supplemental Figure 3G). Importantly, dye transfer from BCP-ALL cell lines to MSCs was nearly absent in transwell experiments ($p \leq 0.001$), which indicates that dye transfer occurs mainly via TNTs and not via extracellular vesicles (Figure 1E-F and supplemental Figure 3H).

The TNT forming capacity was also evaluated in an *ex vivo* niche model using leukemic cells and MSCs that were both freshly obtained from patients with newly diagnosed BCP-ALL (Figure 2A, supplemental Figure 4A-J, supplemental Figure 5A-D, supplemental Figure 6 and supplemental Figure 7). *Ex vivo* co-cultures revealed that TNTs rapidly (< 3 hours) form between primary BCP-ALL cells and primary MSCs, and efficiently transfer lipophilic dye (Figure 2B, supplemental Figure 4G-J, supplemental Figure 5). The source of MSC did not affect the efficacy of TNT signaling. Dye transfer was similarly efficient from ALL cells towards 10 different primary MSCs (n = 5 healthy and n = 5 leukemic primary patient-derived MSCs; Figure 2C-D and supplemental Figure 8A-C).

The dynamics of TNT formation between BCP-ALL cells and MSCs were investigated using time-lapse confocal microscopy. Leukemic cells initiated formation of TNTs and transferred lipophilic dye towards MSCs within minutes (Figure 3A; supplemental Videos 3 and 4A). Leukemic cells were able to form multiple TNTs and signal to several MSCs simultaneously (Figure 3B; and supplemental Videos 3 and 4A-B). TNTs formed between MSCs and leukemic cells were stable for multiple hours and could reach several cell diameters in length (Figure 3C, supplemental Videos 3 and 4A). After 10 hours, the majority of MSCs became DiI-positive (supplemental Videos 3 and 4B), as confirmed by flow cytometry (Figure 1B).

TNTs are important players in signaling from BCP-ALL cells to MSCs

The above-mentioned findings suggest that TNT signaling is a highly effective communication mechanism between ALL cells and MSCs. This was further illustrated by comparing TNT signaling to other intercellular communication mechanisms, including gap junctions, integrins and ECV (Figure 4A). Dye transfer from leukemic cells towards MSCs was minimal using a 3.0 µm transwell system, in which ECV signaling is possible (> 500 fold lower compared to normal co-culture after 24 hours; $p \leq 0.001$; Figure 4B-C). Transfer experiments with the gap junction-specific dye Calcein revealed that signaling from leukemic cells towards primary MSCs via gap junctions is highly ineffective compared to signaling via TNTs (> 90 fold lower after 24 hours; $p \leq 0.001$; Figure 4D-E). Integrin signaling has been implicated in the induction of TNTs[42], raising the question whether TNTs function autonomously or in an integrin-dependent manner. To inhibit integrin signaling between BCP-ALL cells and MSCs, we used RGDS-peptides, reported to prevent the binding of integrins to membranes[43]. RGDS negatively affected

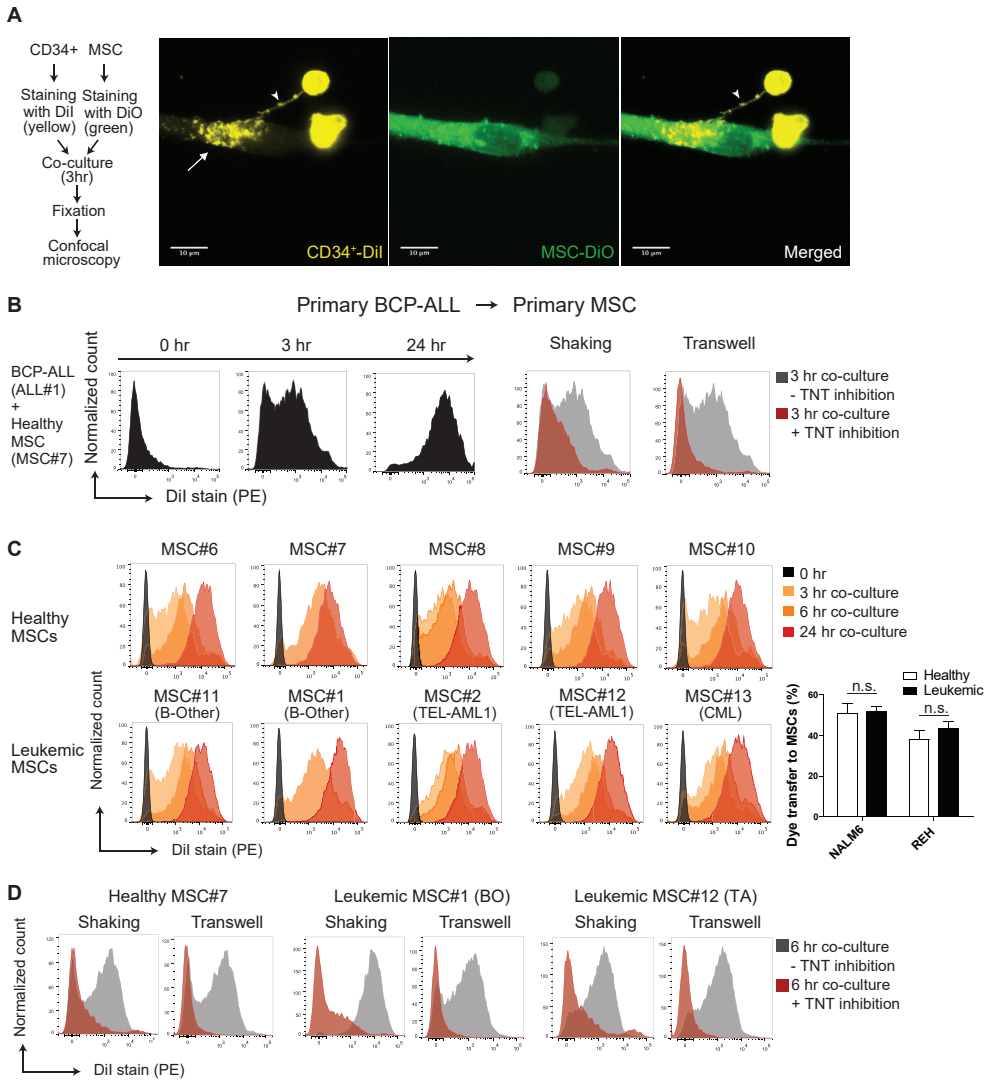

Figure 2. Primary BCP-ALL cells signal to MSCs via TNTs. (A) Representative confocal images (Z-stack) showing TNT formation (white arrowhead) between a primary CD34-positive cell (DiI, yellow) and a hTERT-immortalized MSC (DiO, green) after co-culture for 3 hours. White arrow indicates transfer of dye to recipient cell. (B) Graphs showing quantification of dye transfer in co-cultures of BCP-ALL patient cells with primary MSCs (cultured in 4:1 ratio). Inhibition of TNTs was performed by gentle shaking of co-cultures, or co-culture in a 3.0 µm transwell system (red histograms). (C) Graphs showing quantification of dye transfer from DiI-stained NALM6 cells towards 10 different unstained primary MSCs (cultured in 4:1 ratio) obtained from leukemia patients (n = 5) and healthy controls (n = 5). (D) Graphs showing quantification of dye transfer from DiI-stained NALM6 cells towards 3 different primary MSCs with (red histograms) or without (grey histograms) TNT inhibition. See also supplemental Figures 4-8.

the efficiency of lipophilic dye transfer via TNTs whereas the transfer in the presence of negative control peptides (GRADSP) remained unaffected (Figure 4F). The reduction in lipophilic dye transfer was limited to a maximum of 30% ($p \leq 0.01$). Taken together, these data reveal that TNT signaling acts independently of other important intercellular communication mechanisms, i.e. signaling via extracellular vesicles, gap junctions, and integrins.

BCP-ALL cells use TNTs to drive cytokine release within the microenvironment

The question remains how TNT signaling from leukemic cells affect their microenvironment. Since cytokines and chemokines can greatly affect the survival of leukemic cells[44,45], we considered that the microenvironment responds to TNT signaling by secreting supportive soluble factors. Therefore we investigated the secreted levels of 64 known cytokines/chemokines in co-cultures of primary leukemic cells of two BCP-ALL patients with different sources of primary MSCs. Co-culture of these cells induced the secretion of several cytokines. The cytokine signature produced within co-cultures suggested that this secretion was leukemia-driven and independent of the MSC source (Figure 5). IP10/CXCL10 levels increased more than 1000-fold when patient ALL#7 cells were co-cultured with MSCs, but were undetectable in co-cultures from patient ALL#9 cells (Figure 5A and 5E). Likewise, MDC/CCL22 and TARC/CCL17, both undetectable in patient ALL#7 co-cultures, were induced 6-18 fold when patient ALL#9 cells were co-cultured with MSCs (Figure 5C-D and 5G-H). Interleukin-8 (IL8) levels were induced (2-7 fold) by primary ALL cells from both patients (Figure 5B and 5F). Cytokines that were induced less than 2 fold in co-culture are shown in supplemental Figure 9. Only a limited number of cytokines/chemokines were found to be significantly upregulated in patients' ALL-MSC co-cultures compared to mono-cultures of both cell types. Also in a proliferative setting (using the BCP-ALL cell line NALM6), a limited number of known cytokines were upregulated in co-culture with two different primary MSCs: IL8 and VEGF levels were on average induced 2 and 3 fold respectively (n=3, $p \leq 0.01$, Supplemental Figure 9E-H). These MSC-independent and leukemia-consistent cytokine signatures suggest that leukemic cells, and not MSCs, are responsible for the active modulation of the tumor microenvironment.

Induction of the observed cytokines was dependent on TNT signaling, as TNT inhibition significantly lowered the secreted levels of these factors (Figure 5A-H, Supplemental Figure 9E-H). However, TNT inhibition only partly reversed the induction of cytokine levels in ALL-MSC co-cultures, suggesting that, next to TNT signaling, other intercellular signaling routes contribute to the induction of these secretomes.

TNT signaling is important for the survival of primary BCP-ALL cells

Several studies have shown the importance of the microenvironment for the survival of malignant cells, but without elucidating how[46]. In order to study the effect of TNT signaling on leukemic cell viability, we used *ex vivo* co-cultures of primary BCP-ALL cells

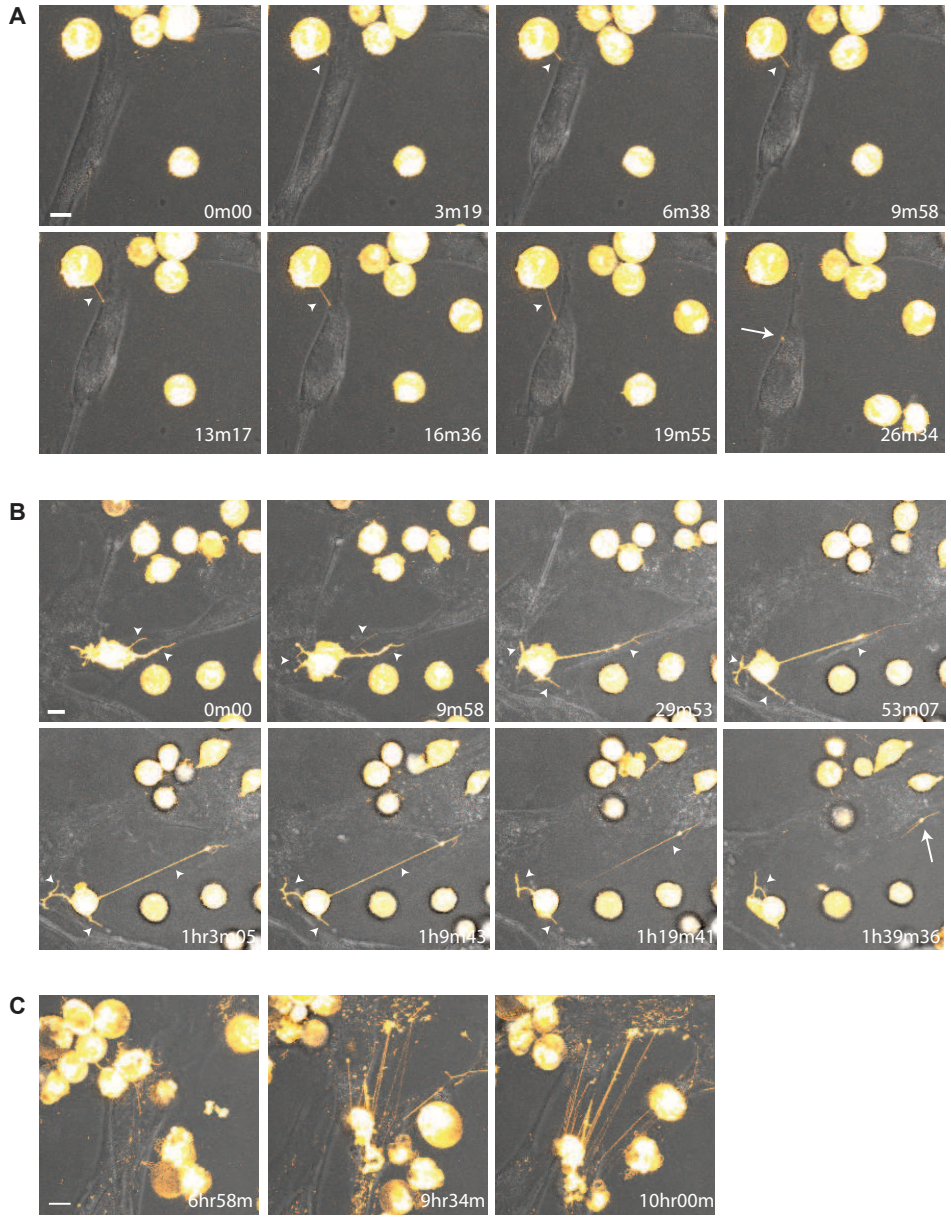

Figure 3. Dynamic nature of TNT formation between BCP-ALL cells and MSCs. (A-C) Time-lapse confocal images (3D image stacks) showing TNT formation (white arrowhead) between NALM6 cells (DiI, yellow) and primary MSCs at multiple time points. White arrow indicates transfer of dye to recipient cell. Time indicated in the right lower corner is the duration from start of the experiment. Orange Hot look-up table (LUT) and transmission overlays were used to illustrate dye transfer towards MSCs. Scale bars represent 10 µm. (A and C) Depicted images are close-ups of the upper left corner of supplemental Video 3. (B) Depicted images are close-ups of supplemental Video 4A. Data is representative of three independent experiments. See also supplemental Figure 5 and supplemental Videos 3 and 4A-B.

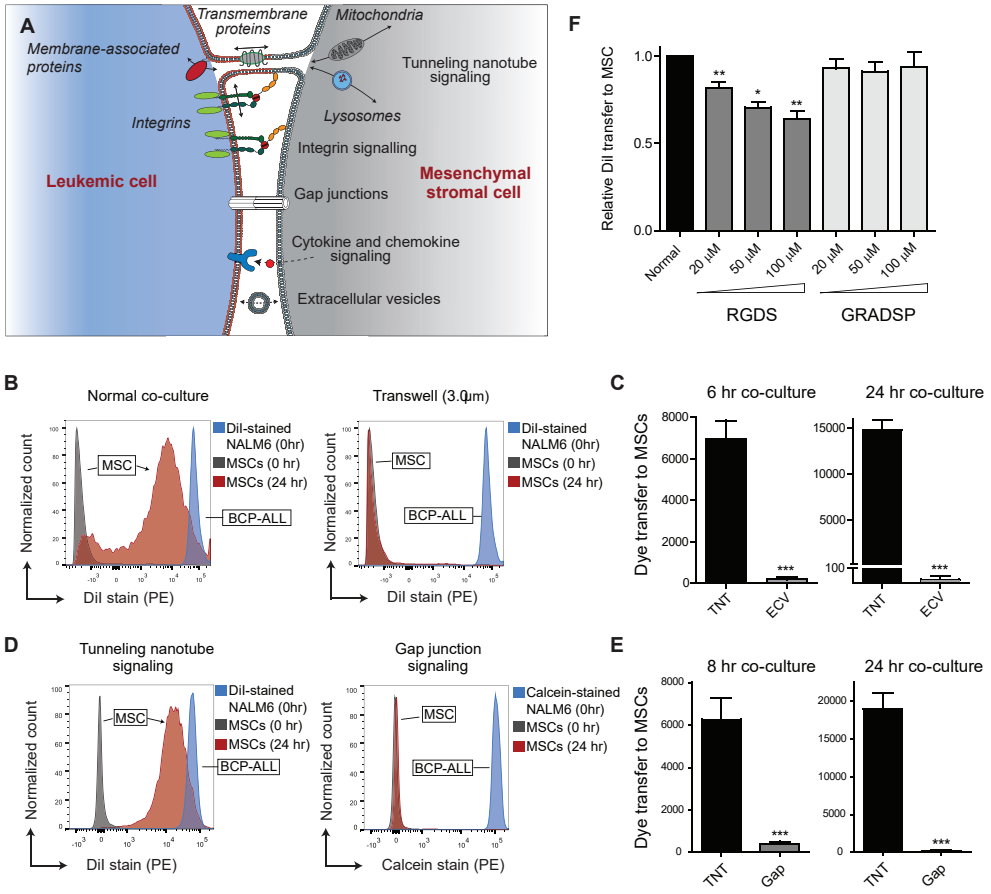

Figure 4. TNTs are important players in signaling from BCP-ALL cells to MSCs. (A) Model of crosstalk between leukemic cells and MSCs in the hematopoietic niche. (B) Graphs showing quantification of dye transfer from DiI-stained NALM6 cells towards unstained hTERT-MSCs. Blue and grey histograms represent staining intensity at the start of each experiment. Red histogram represents signaling efficiency via TNTs (normal co-culture; left panel) and via extracellular vesicles (ECV) (3.0 µm transwell; right panel). (C) Bar graphs of experiment shown in (B) after 6 hours (left panel) and 24 hours (right panel) of co-culture (n = 4; two-tailed t-test, unpaired). (D) Graphs showing quantification of dye transfer from BCP-ALL cell line NALM6, stained with either DiI or calcein, towards primary MSCs after 24 hours of co-culture. Blue and grey histograms represent staining intensity at the start of each experiment. Red histogram shows signaling efficiency via TNTs (left panel) and via gap junctions (right panel). (E) Bar graphs of experiment shown in (D) after 8 hours (n = 6; left panel) and 24 hours (n = 4; right panel) of co-culture (two-tailed t-test, unpaired). (F) Bar graphs representing dye transfer from DiI-stained REH cells towards unstained primary MSCs with and without integrin blocking. Integrin signaling was blocked by addition of RGDS peptide, and compared to addition of the integrin non-binding peptide GRADSP (n = 5; one-tailed t-test, paired). Data are means ± SEM; * $p \leq 0.05$, ** $p \leq 0.01$, *** $p \leq 0.001$.

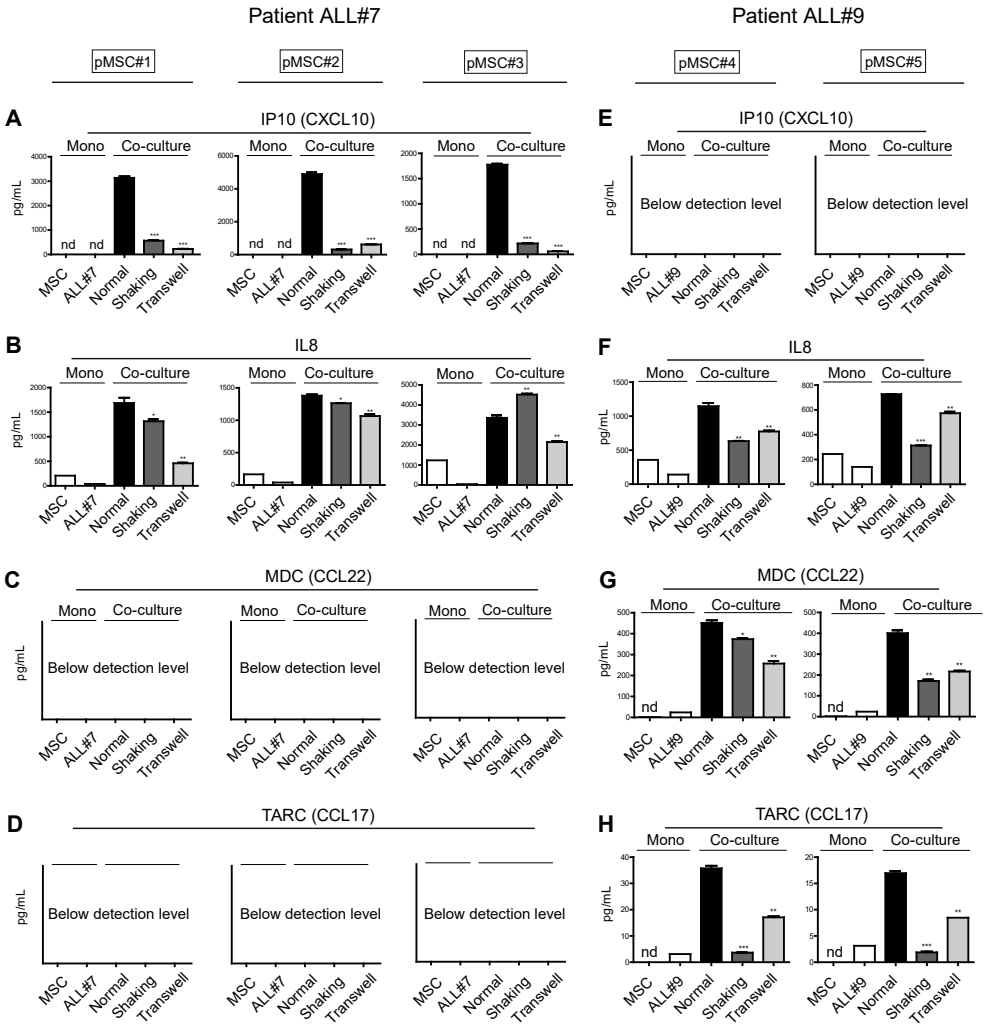

Figure 5. BCP-ALL cells use TNTs to drive cytokine release within the microenvironment. (A) IP10/CXCL10 supernatant levels in co-culture of primary leukemic patient ALL#7 cells with primary MSC#1 (left panel), MSC#2 (middle panel), or MSC#3 (right panel). TNT signaling was inhibited by gentle shaking or culture in a transwell system (one-tailed t-test, unpaired). (B) Same as (A) for IL8 levels. (C) Same as (A) for MDC (CCL22) levels. (D) Same as (A) for TARC (CCL17) levels. (E) IP10/CXCL10 supernatant levels in co-culture of primary leukemic patient ALL#9 cells with primary MSC#4 (left panel), or MSC#5 (right panel). (F) Same as (E) for IL8 levels. (G) Same as (E) for MDC (CCL22) levels. (H) Same as (E) for TARC (CCL17) levels. Data are means ± SEM; * $p \leq 0.05$, ** $p \leq 0.01$. nd = not detectable (below detection level). See also supplemental Figure 9.

and primary MSCs (see table S1 for BCP-ALL subtype information, Figure 6A for gating strategy). Primary BCP-ALL cell survival significantly increased in 5-day co-cultures with primary MSCs compared to mono-cultures. When TNT formation was prevented by shaking of co-cultures or by transwell conditions, this increase significantly reduced 3.5- and 3.6-fold, respectively ($n = 7$, $p \leq 0.001$; Figure 6B-D). The effect of TNT inhibition was consistent across leukemic cells from multiple cytogenetic BCP-ALL subgroups (TEL-AML1, BCR-ABL1-like, and B-Other).

Inhibition of TNTs sensitizes BCP-ALL cells to prednisolone

We investigated whether inhibition of TNT signaling also affects the response of leukemic cells to chemotherapeutic drugs. BCP-ALL patient cells were treated with the ALL spearhead drug prednisolone for 5 days. Prednisolone was less effective in inducing apoptosis of primary BCP-ALL cells in the presence of primary MSCs compared to mono-cultures of primary BCP-ALL cells (70% vs 5% reduced viability; $p \geq 0.001$; Figure 7A), underlining the importance of MSCs in the induction of prednisolone resistance (Figure 7A). The protective effect of MSCs was significantly reduced by 2-3 fold ($n = 4$, $p \leq 0.001$; Figure 7A) when TNT signaling was inhibited. TNT inhibition alone was not sufficient to abrogate all microenvironment-induced drug resistance. In shaking and transwell conditions, which allow signaling via integrins, soluble factors or ECVs, microenvironment-induced resistance to prednisolone was still present ($p \geq 0.01$). Since *ex vivo* cultured leukemic patient cells lose their propensity to proliferate, we also addressed the effect of TNT signaling on drug resistance in a proliferative setting using the BCP-ALL cell line NALM6. Similar to primary BCP-ALL cells, co-culture with MSCs induced prednisolone resistance of NALM6 cells (Figure 7B). Inhibition of TNT formation by shaking of co-cultures or transwell conditions significantly reduced this effect 4.5- and 8.5- fold, respectively ($p \leq 0.01$; Figure 7B and supplemental Figure 10A-B). These data show that inhibition of TNT signaling in co-cultures sensitizes BCP-ALL cells to the anti-leukemic effects of prednisolone in both a primary non-proliferative and a proliferative setting.

DISCUSSION

The presented study identifies TNT formation as a novel regulator of interaction between BCP-ALL cells and their bone marrow niche, which facilitates signaling from leukemic cells towards MSCs and affects the release of cytokines and chemokines in the microenvironment. Disruption of TNTs inhibits this release, decreases the survival benefit that MSCs provide to primary BCP-ALL cells, and sensitizes BCP-ALL cells to the important anti-leukemic drug prednisolone (supplemental Figure 11).

Relapse of leukemia is caused by a small number of leukemic cells that are able to withstand chemotherapy and can cause the complete reconstitution of the tumor. Leukemogenic mouse models show the importance of signaling between leukemic cells and their bone marrow microenvironment and emphasize the pathophysiological relevance of cytokines within the leukemic niche[1,47-49]. However, a major shortcoming in our knowledge about the leukemic niche is the lack of insight into the functional mechanism mediating crosstalk between leukemic cells and their local niche. Our data adds significant insight into this process and provides an opportunity to inhibit the leukemic

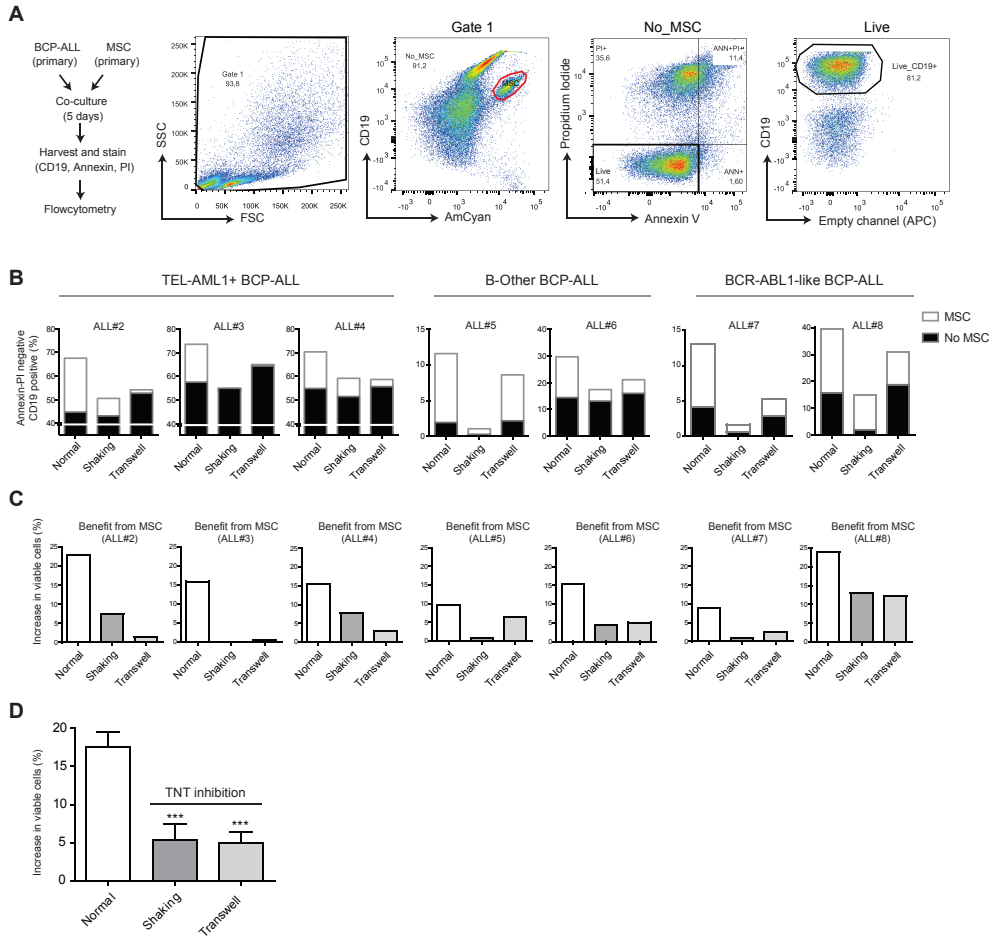

Figure 6. TNT signaling is important for the survival of primary BCP-ALL cells. (A) Flow chart and flow cytometrical gating strategy used to study the effect of TNTs on BCP-ALL cell survival. Co-cultures of $CD19^{positive}$ leukemic cells and $CD19^{negative}$ MSCs were stained with Brilliant Violet 421™ anti-human CD19 antibody, FITC Annexin V, and Propidium Iodide (PI). MSCs were excluded (red gate), and the percentage of viable BCP-ALL blasts ($AnnexinV^{neg}/PI^{neg}/CD19^{pos}$ cells) was determined within the MSC-negative fraction. (B) Percentage of viable primary leukemic patient cells ($n = 3$ TEL-AML1, $n = 2$ B-Other, $n = 2$ BCR-ABL1-like) in mono-culture (black bars) or co-culture with patient MSCs (white bars) after 5-day co-culture. (C) The survival benefit for primary leukemic patient cells ($n = 3$ TEL-AML1, $n = 2$ B-Other, $n = 2$ BCR-ABL1-like) in co-culture with patient MSCs. (D) The mean survival benefit for primary leukemic patient cells in co-culture with patient MSCs ($n = 7$; one-tailed t-test, paired). Data are means ± SEM; *** $p \leq 0.001$.

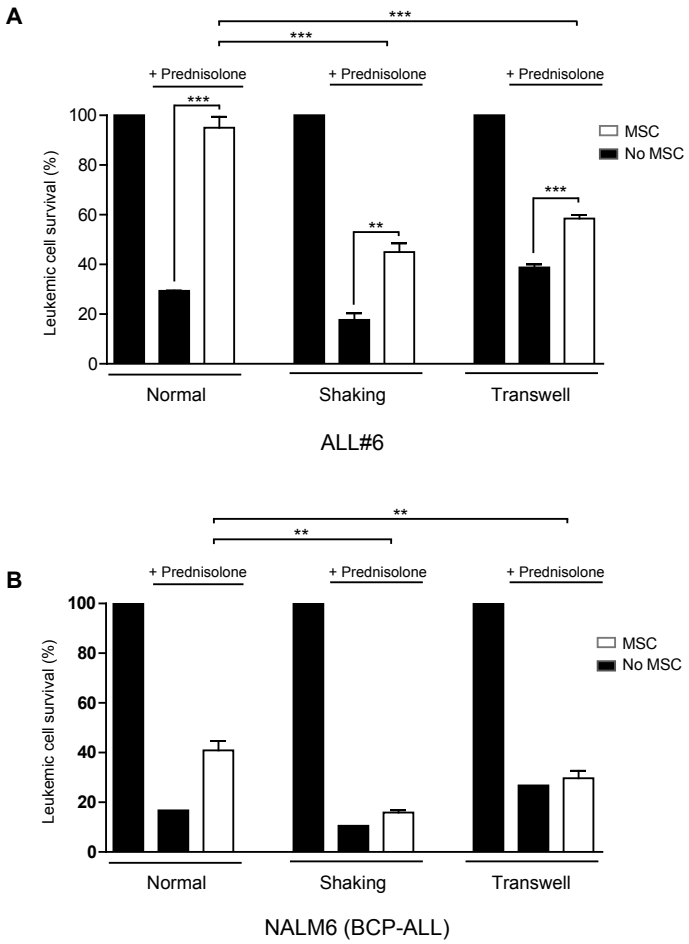

Figure 7. Inhibition of TNTs sensitizes BCP-ALL cells to prednisolone. (A) Leukemic cell survival of patient ALL#6 cells cultured with or without MSCs after 5 days of prednisolone exposure (0.3 µg/mL). All graphs show percentage compared to untreated control. TNT signaling was inhibited by shaking or transwell conditions (one-tailed t-test, unpaired). Quadruplicates represent four different sources of MSCs (MSC#1, MSC#2, MSC#6, MSC#7). (B) Leukemic cell survival of BCP-ALL cell line NALM6 cultured with or without MSCs after 5 days of prednisolone exposure. All graphs show percentage compared to untreated control. TNT signaling was inhibited by shaking or transwell conditions (one-tailed t-test, unpaired). Triplicates represent three different sources of MSCs (hTERT, MSC#1, and MSC#2). Data are means ± SEM; * $p \leq 0.05$, ** $p \leq 0.01$. See also supplemental Figure 10.

niche. Importantly, primary BCP-ALL cells use TNTs to modulate their microenvironment, identifying the leukemic cell, and not MSCs, as the driver of niche modulation.

Although less pronounced as seen between ALL cells and MSCs, TNTs are also used for communication between leukemic cells. This discovery may reveal a new aspect of tumor heterogeneity. In many cancer types, clonal evolution has been observed[50]. A recent study in T-ALL by Blackburn et al. shows that leukemia subclones acquire mutations, that can mediate chemotherapy resistance even without prior drug exposure[51]. Leukemic cells might exploit TNTs, which can transfer a broad spectrum of molecules and organelles like membrane-associated signaling molecules (e.g. H-Ras[19]), to transfer mutant proteins and subsequently chemotherapy resistance between subclones.

Several studies report that the leukemic niche can induce drug resistance for both classical chemotherapeutic agents and newly developed targeted therapies[9,44-46,52-54]. The seminal papers by Strausmann et al, and Wilson et al. revealed the widespread potential for growth-factor-driven resistance to kinase inhibitors in several tumor types. A recent study by Manshouri et al., showed the induction of resistance against JAK2 inhibitors by bone marrow stroma-secreted cytokines in JAK2-mutated primary hematopoietic cells. BCP-ALL cells use TNTs to induce a pro-inflammatory cytokine signature within their microenvironment[55]. These cytokines have been reported to be involved in leukemia survival and resistance to therapy, like IP10/CXCL10[54], IL-8[56], and MCP-1/CCL2[57]. When TNTs were inhibited, this signature was partly reversed and simultaneously leukemic cell survival was decreased. Since these cytokines also have a chemoattractive function, it is likely that migration towards the stromal compartments of the niche and subsequent induction of contact-dependent signaling modules, like integrins and gap junctions, also play a role in this process. Further, we observed TNT signaling from MSCs towards leukemic cells, which might also influence drug resistance of leukemic cells. For example, TNTs have been shown to transport drug-efflux pumps such as P-glycoproteins[24], and to transport mitochondria preferentially towards cancer cells[28].

Interestingly, we observed leukemia-specific cytokine patterns in MSC-ALL co-cultures that were affected by abrogation of TNT signaling. This observation opens the discussion how TNT signaling can lead to the upregulation of different soluble factors. The broad spectrum of signaling molecules that are transported by TNTs potentially allows the ALL to convey specific messages to MSCs in order to differentially regulate the secretion of soluble factors by its microenvironment. In addition, leukemia is a highly heterogeneous disease consisting of different (cyto)genetic subtypes that also have individual heterogeneity with regards to their transcriptome and proteome[58]. These factors are all likely to contribute to leukemia-unique demands for microenvironmental support.

Targeting TNT-directed communication between leukemic cells and their supportive niche may be a promising new approach to kill leukemic cells and prevent drug resistance in clinical practice. As of yet, no agents are available that induce specific inhibition of TNT signaling, but our data point to the importance to develop such agents. TNT signaling can be disrupted through shear stress, applying a physical distance between the cells, actin inhibition, and in some cases tubulin inhibition. In additional experiments, we observed that tubulin inhibition did not inhibit TNT signaling between BCP-ALL cells and MSCs (data not shown). The common building block for all TNTs reported in literature is F-actin, making it an obvious target for TNT disruption. Actin inhibitors are derived from fungi, plants and sponges, which developed these toxins as a defense mechanism.

Consequently, these compounds inhibit TNT formation (Figure 1E-F) and induce cell death (data not shown). Therefore, it is important to develop more specific and less-toxic small molecule inhibitors that target elements of the actin cytoskeleton important for TNT formation. We propose our primary patient-derived *ex vivo* model system as a highly suitable platform to identify such inhibitors. Once identified, these TNT-specific agents will allow us to investigate TNT signaling also *in vivo*.

In conclusion, the discovery of TNT signaling between BCP-ALL cells and mesenchymal stromal cells adds significant insight into the mechanisms of communication in the leukemic niche. BCP-ALL cells use TNT networks to modify their healthy microenvironment and hereby create a leukemic niche that induces survival and drug resistance. Current chemotherapeutic regimens are primarily focused on combating tumor intrinsic properties. Our data provide a new concept to develop alternative therapeutic strategies that include targeting of the leukemic niche in B-cell acute lymphoblastic leukemia.

ACKNOWLEDGEMENTS

We thank all members of the research laboratory Pediatric Oncology of the Erasmus MC for their help in processing leukemic and mesenchymal stromal cell samples, in particular L.C.J. van den Berk, C. van de Ven, and F. Meijers-Stalpers; M. Buitenhuis and M. Bierings for critical discussions and reading of the manuscript; D. Geerts for scientific input and critical discussions; The Erasmus Optical Imaging Centre for providing support of CLSM; The Department of Hematology of the Erasmus MC for providing the use of CLSM and Flow Cytometers; The Vlietland Ziekenhuis for collecting and providing cord blood. The work described in this paper was funded by the KiKa Foundation (Stichting Kinderen Kankervrij – Kika-39), the Dutch Cancer Society (UVA 2008; 4265, EMCR 2010; 4687), the Netherlands Organization for Scientific Research (NWO – VICI M.L. den Boer) and the Pediatric Oncology Foundation Rotterdam.

AUTHOR CONTRIBUTIONS

Co-first authors R. Polak and B. de Rooij contributed equally to the study and are listed alphabetically. R. Polak and B. de Rooij designed the study, performed the experiments, collected and analyzed all data, and wrote the paper. M.L. den Boer designed the study, analyzed data, and wrote the paper. R. Pieters analyzed data and wrote the paper. All authors discussed the results and approved the submitted manuscript.

CONFLICT OF INTEREST DISCLOSURE

The authors declare no competing financial interests.

REFERENCES

1. Colmone A, Amorim M, Pontier AL, Wang S, Jablonski E, Sipkins DA. Leukemic cells create bone marrow niches that disrupt the behavior of normal hematopoietic progenitor cells. *Science*. 2008;322(5909):1861-1865.

2. Flynn CM, Kaufman DS. Donor cell leukemia: insight into cancer stem cells and the stem cell niche. *Blood*. 2007;109(7):2688-2692.

3. Raaijmakers MH, Mukherjee S, Guo S, et al. Bone progenitor dysfunction induces myelodysplasia and secondary leukaemia. *Nature*. 2010;464(7290):852-857.

4. Walkley CR, Olsen GH, Dworkin S, et al. A microenvironment-induced myeloproliferative syndrome caused by retinoic acid receptor gamma deficiency. *Cell*. 2007;129(6):1097-1110.

5. Walkley CR, Shea JM, Sims NA, Purton LE, Orkin SH. Rb regulates interactions between hematopoietic stem cells and their bone marrow microenvironment. *Cell*. 2007;129(6):1081-1095.

6. Yilmaz OH, Valdez R, Theisen BK, et al. Pten dependence distinguishes haematopoietic stem cells from leukaemia-initiating cells. *Nature*. 2006;441(7092):475-482.

7. Arai F, Hirao A, Ohmura M, et al. Tie2/angiopoietin-1 signaling regulates hematopoietic stem cell quiescence in the bone marrow niche. *Cell*. 2004;118(2):149-161.

8. Fujisaki J, Wu J, Carlson AL, et al. In vivo imaging of Treg cells providing immune privilege to the haematopoietic stem-cell niche. *Nature*. 2011;474(7350):216-219.

9. McMillin DW, Delmore J, Weisberg E, et al. Tumor cell-specific bioluminescence platform to identify stroma-induced changes to anticancer drug activity. *Nat Med*. 2010;16(4):483-489.

10. Nakasone ES, Askautrud HA, Kees T, et al. Imaging tumor-stroma interactions during chemotherapy reveals contributions of the microenvironment to resistance. *Cancer Cell*. 2012;21(4):488-503.

11. Jin L, Hope KJ, Zhai Q, Smadja-Joffe F, Dick JE. Targeting of CD44 eradicates human acute myeloid leukemic stem cells. *Nat Med*. 2006;12(10):1167-1174.

12. Matsunaga T, Takemoto N, Sato T, et al. Interaction between leukemic-cell VLA-4 and stromal fibronectin is a decisive factor for minimal residual disease of acute myelogenous leukemia. *Nat Med*. 2003;9(9):1158-1165.

13. Nervi B, Ramirez P, Rettig MP, et al. Chemosensitization of acute myeloid leukemia (AML) following mobilization by the CXCR4 antagonist AMD3100. *Blood*. 2009;113(24):6206-6214.

14. Sipkins DA, Wei X, Wu JW, et al. In vivo imaging of specialized bone marrow endothelial microdomains for tumour engraftment. *Nature*. 2005;435(7044):969-973.

15. Tavor S, Petit I, Porozov S, et al. CXCR4 regulates migration and development of human acute myelogenous leukemia stem cells in transplanted NOD/SCID mice. *Cancer Res*. 2004;64(8):2817-2824.

16. Zeng Z, Shi YX, Samudio IJ, et al. Targeting the leukemia microenvironment by CXCR4 inhibition overcomes resistance to kinase inhibitors and chemotherapy in AML. *Blood*. 2009;113(24):6215-6224.

17. Chauveau A, Aucher A, Eissmann P, Vivier E, Davis DM. Membrane nanotubes facilitate long-distance interactions between natural killer cells and target cells. *Proc Natl Acad Sci U S A*. 2010;107(12):5545-5550.

18. Onfelt B, Nedvetzki S, Yanagi K, Davis DM. Cutting edge: Membrane nanotubes connect immune cells. *J Immunol*. 2004;173(3):1511-1513.

19. Rainy N, Chetrit D, Rouger V, et al. H-Ras transfers from B to T cells via tunneling nanotubes. *Cell Death Dis*. 2013;4:e726.

20. Rustom A, Saffrich R, Markovic I, Walther P, Gerdes HH. Nanotubular highways for intercellular organelle transport. *Science*. 2004;303(5660):1007-1010.

21. Sowinski S, Jolly C, Berninghausen O, et al. Membrane nanotubes physically connect T cells over long distances presenting a novel route for HIV-1 transmission. *Nat Cell Biol*. 2008;10(2):211-219.

22. Watkins SC, Salter RD. Functional connectivity between immune cells mediated by tunneling nanotubules. *Immunity*. 2005;23(3):309-318.

23. Arkwright PD, Luchetti F, Tour J, et al. Fas stimulation of T lymphocytes promotes rapid intercellular exchange of death signals via membrane nanotubes. *Cell Res*. 2010;20(1):72-88.

24. Pasquier J, Galas L, Boulange-Lecomte C, et al. Different modalities of intercellular membrane exchanges mediate cell-to-cell p-glycoprotein transfers in MCF-7 breast cancer cells. *J Biol Chem*. 2012;287(10):7374-7387.

25. Chinnery HR, Pearlman E, McMenamin PG. Cutting edge: Membrane nanotubes in vivo: a feature of MHC class II+ cells in the mouse cornea. *J Immunol*. 2008;180(9):5779-5783.

26. Marzo L, Gousset K, Zurzolo C. Multifaceted roles of tunneling nanotubes in intercellular communication. *Front Physiol*. 2012;3:72.

27. Seyed-Razavi Y, Hickey MJ, Kuffova L, McMenamin PG, Chinnery HR. Membrane nanotubes in myeloid cells in the adult mouse cornea represent a novel mode of immune cell interaction. *Immunol Cell Biol*. 2013;91(1):89-95.

28. Pasquier J, Guerrouahen BS, Al Thawadi H, et al. Preferential transfer of mitochondria from endothelial to cancer cells through tunneling nanotubes modulates chemoresistance. *J Transl Med*. 2013;11:94.

29. Lou E, Fujisawa S, Morozov A, et al. Tunneling nanotubes provide a unique conduit for intercellular transfer of cellular contents in human malignant pleural mesothelioma. *PLoS One*. 2012;7(3):e33093.

30. Gousset K, Schiff E, Langevin C, et al. Prions hijack tunnelling nanotubes for intercellular spread. *Nat Cell Biol*. 2009;11(3):328-336.

31. Den Boer ML, Harms DO, Pieters R, et al. Patient stratification based on prednisolone-vincristine-asparaginase resistance profiles in children with acute lymphoblastic leukemia. *J Clin Oncol*. 2003;21(17):3262-3268.

32. van den Berk LC, van der Veer A, Willemse ME, et al. Disturbed CXCR4/CXCL12 axis in paediatric precursor B-cell acute lymphoblastic leukaemia. *Br J Haematol*. 2014;166(2):240-249.

33. Sowinski S, Alakoskela JM, Jolly C, Davis DM. Optimized methods for imaging membrane nanotubes between T cells and trafficking of HIV-1. *Methods*. 2011;53(1):27-33.

34. Schindelin J, Arganda-Carreras I, Frise E, et al. Fiji: an open-source platform for biological-image analysis. *Nat Methods*. 2012;9(7):676-682.

35. Sourisseau M, Sol-Foulon N, Porrot F, Blanchet F, Schwartz O. Inefficient human immunodeficiency virus replication in mobile lymphocytes. *J Virol*. 2007;81(2):1000-1012.

36. Gyorgy B, Szabo TG, Pasztoi M, et al. Membrane vesicles, current state-of-the-art: emerging role of extracellular vesicles. *Cell Mol Life Sci*. 2011;68(16):2667-2688.

37. Lo Celso C, Fleming HE, Wu JW, et al. Live-animal tracking of individual haematopoietic stem/progenitor cells in their niche. *Nature*. 2009;457(7225):92-96.

38. Alon R, Dustin ML. Force as a facilitator of integrin conformational changes during leukocyte arrest on blood vessels and antigen-presenting cells. *Immunity*. 2007;26(1):17-27.

39. Alon R, Ley K. Cells on the run: shear-regulated integrin activation in leukocyte rolling and arrest on endothelial cells. *Curr Opin Cell Biol*. 2008;20(5):525-532.

40. Huang FY, Mei WL, Li YN, et al. The antitumour activities induced by pegylated liposomal cytochalasin D in murine models. *Eur J Cancer*. 2012;48(14):2260-2269.

41. Salu KJ, Bosmans JM, Huang Y, et al. Effects of cytochalasin D-eluting stents on intimal hyperplasia in a porcine coronary artery model. *Cardiovasc Res*. 2006;69(2):536-544.

42. Obermajer N, Jevnikar Z, Doljak B, Sadaghiani AM, Bogyo M, Kos J. Cathepsin X-mediated beta2 integrin activation results in nanotube outgrowth. *Cell Mol Life Sci*. 2009;66(6):1126-1134.

43. Ruoslahti E, Pierschbacher MD. New perspectives in cell adhesion: RGD and integrins. *Science*. 1987;238(4826):491-497.

44. Straussman R, Morikawa T, Shee K, et al. Tumour micro-environment elicits innate resistance to RAF inhibitors through HGF secretion. *Nature*. 2012;487(7408):500-504.

45. Wilson TR, Fridlyand J, Yan Y, et al. Widespread potential for growth-factor-driven resistance to anticancer kinase inhibitors. *Nature*. 2012;487(7408):505-509.

46. McMillin DW, Negri JM, Mitsiades CS. The role of tumour-stromal interactions in modifying drug response: challenges and opportunities. *Nat Rev Drug Discov*. 2013;12(3):217-228.

47. Medyouf H, Mossner M, Jann JC, et al. Myelodysplastic Cells in Patients Reprogram Mesenchymal Stromal Cells to Establish a Transplantable Stem Cell Niche Disease Unit. *Cell Stem Cell*. 2014.

48. Schepers K, Pietras EM, Reynaud D, et al. Myeloproliferative neoplasia remodels the endosteal bone marrow niche into a self-reinforcing leukemic niche. *Cell Stem Cell*. 2013;13(3):285-299.

49. Zhang B, Ho YW, Huang Q, et al. Altered microenvironmental regulation of leukemic and normal stem cells in chronic myelogenous leukemia. *Cancer Cell*. 2012;21(4):577-592.

50. Greaves M, Maley CC. Clonal evolution in cancer. *Nature*. 2012;481(7381):306-313.

51. Blackburn JS, Liu S, Wilder JL, et al. Clonal Evolution Enhances Leukemia-Propagating Cell Frequency in T Cell Acute Lymphoblastic Leukemia through Akt/mTORC1 Pathway Activation. *Cancer Cell*. 2014.

52. Konopleva MY, Jordan CT. Leukemia stem cells and microenvironment: biology and therapeutic targeting. *J Clin Oncol*. 2011;29(5):591-599.

53. Pallasch CP, Leskov I, Braun CJ, et al. Sensitizing protective tumor microenvironments to antibody-mediated therapy. *Cell*. 2014;156(3):590-602.

54. Manshouri T, Estrov Z, Quintas-Cardama A, et al. Bone marrow stroma-secreted cytokines protect JAK2(V617F)-mutated cells from the effects of a JAK2 inhibitor. *Cancer Res*. 2011;71(11):3831-3840.

55. Bernardo ME, Fibbe WE. Mesenchymal stromal cells: sensors and switchers of inflammation. *Cell Stem Cell*. 2013;13(4):392-402.

56. Francia di Celle P, Mariani S, Riera L, Stacchini A, Reato G, Foa R. Interleukin-8 induces the accumulation of B-cell chronic lymphocytic leukemia cells by prolonging survival in an autocrine fashion. *Blood*. 1996;87(10):4382-4389.

57. Burgess M, Cheung C, Chambers L, et al. CCL2 and CXCL2 enhance survival of primary chronic lymphocytic leukemia cells in vitro. *Leuk Lymphoma*. 2012;53(10):1988-1998.

58. Roberts KG, Mullighan CG. Genomics in acute lymphoblastic leukaemia: insights and treatment implications. *Nat Rev Clin Oncol*. 2015;12(6):344-357.

SUPPLEMENTAL TABLES

Supplemental Table 1. Characteristics of primary BCP-ALL cells

Name	Subtype	Remarks
ALL#1	BCR-ABL1	-
ALL#2	TEL-AML1	-
ALL#3	TEL-AML1	-
ALL#4	TEL-AML1	-
ALL#5	B-Other	E2A-rearranged subclone (21%)
ALL#6	B-Other	-
ALL#7	BCR-ABL1-like	-
ALL#8	BCR-ABL1-like	Down syndrome
ALL#9	BCR-ABL1-like	-
ALL#10	B-Other	ETV6 loss

Supplemental Table 2. Characteristics of primary MSCs

Name	Subtype	Remarks
MSC#1	B-Other	-
MSC#2	TEL-AML1	-
MSC#3	B-Other	-
MSC#4	Remission	1 year after treatment
MSC#5	AML	-
MSC#6	Healthy	-
MSC#7	Healthy	-
MSC#8	Healthy	-
MSC#9	Healthy	-
MSC#10	Healthy	-
MSC#11	B-Other	-
MSC#12	TEL-AML1	-
MSC#13	CML	-

Supplemental Table 3. Cytokine secretion in mono and co-cultures of ALL and MSCs

Cytokine	MSCs	ALL	Co-culture
6Ckine			
BCA-1			
CTACK			
EGF	x	x	
ENA-78			
Eotaxin		x	
Eotaxin-2			
Eotaxin-3	x		
FGF-2	x		
Flt3 Ligand			
Fractalkine			
G-CSF			
GM-CSF	x		
GRO	x		
I-309			
IFNalpha2			
IFNgamma			
IL10			
IL12			
p70			
IL13			
IL15			
IL16			
IL17A			
IL1alpha			
IL1beta			
IL1-ra			
IL2			
IL20			
IL21			
IL23			
IL28a			
IL3			
IL33			
IL4			
IL5			
IL6	x		
IL7			
IL8	x	x	x
IL9			
IP10			x
LIF			
MCP-1	x	x	

Supplemental Table 3. (continue)

Cytokine	MSCs	ALL	Co-culture
MCP-2			
MCP-3			
MCP-4			
MDC		x	
MIP-1alpha		x	
MIP-1beta		x	
MIP-1delta			
PDGF-AA	x	x	
PDGF-BB		x	
RANTES			
sCD40L			
SCF	x		
SDF1-alpha/beta	x		
TARC			x
TGFalpha			
TNFalpha		x	
TNFbeta			
TPO			
TRAIL			
TSLP			
VEGF	x	x	x

Supplemental Figure 1. TNTs between BCP-ALL cells and MSCs. (A-H) Interleukemic TNT networks (exemplified by white arrowheads) and exchange of lipophilic dye (exemplified by arrows) between NALM6 (A-D) or REH (E-H) cells (DiI, yellow; DiO, green) were observed after 24 hours of co-culture. White arrows indicate transfer of dye to recipient cell. (I-L) TNT networks were formed and dye transfer was present between hTERT-immortalized MSCs (DiI, yellow; DiO, green). TNT-like structures also attached to the fibronectin-coated substratum (exemplified by orange arrowheads; right panel). Red arrowheads (left panel) represent 'midbodies'. These midbodies look similar to TNTs, but are a short-lasting remainder of cell division. (M-P) Co-cultures of hTERT-immortalized MSCs (indicated by MSC) and BCP-ALL cell line NALM6 (indicated by LC) showed elaborate TNT networks and dye transfer after 3 hours of co-culture. (Q-R) Phalloidin-FITC staining of F-actin, shows the presence of F-Actin in TNTs between BCP-ALL cells (NALM6) and MSCs (primary MSC#1). White arrowheads indicate TNTs. DAPI-staining (blue) was used to stain nuclei. Images M-P are 3D image stacks. Scale bars represent 10 µm.

SUPPLEMENTAL FIGURES

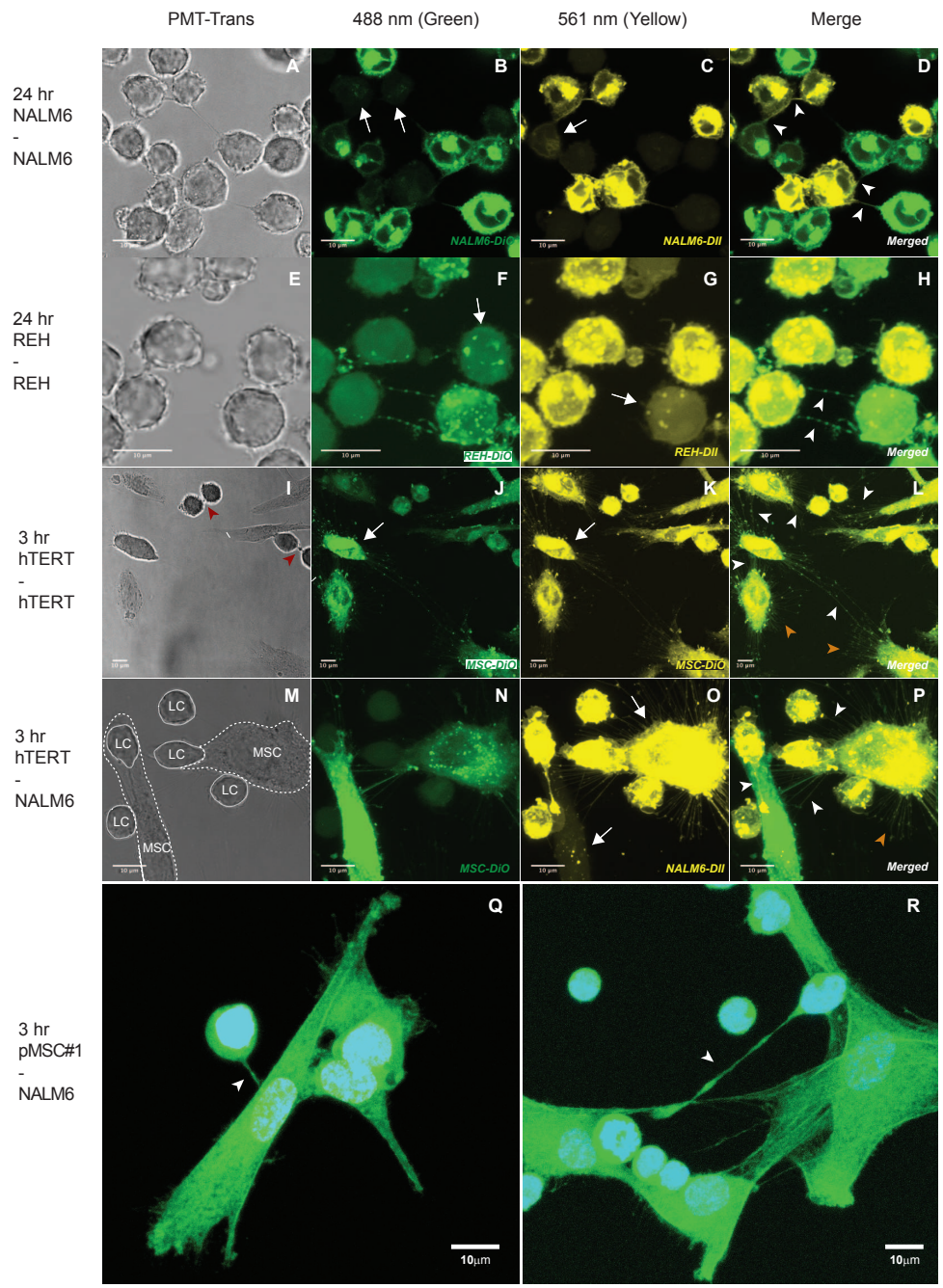

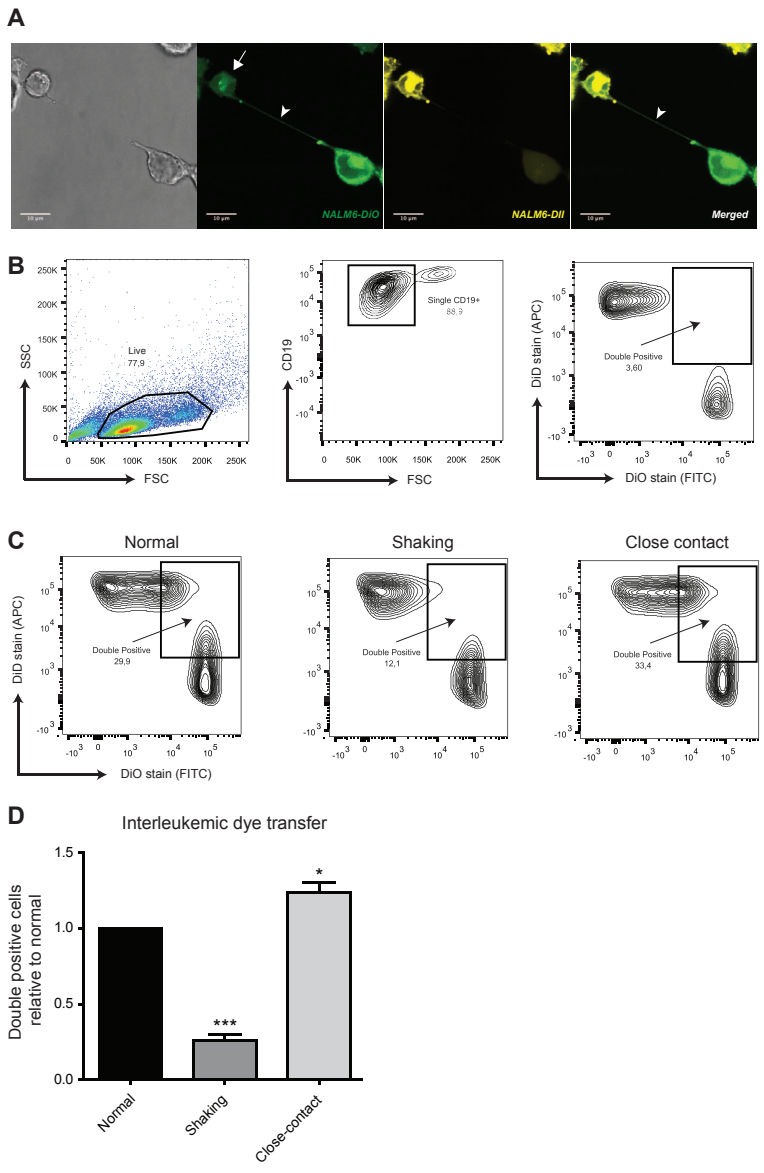

Supplemental Figure 2. TNT signaling between BCP-ALL cells. (A) Representative confocal images showing TNT formation (white arrowhead) between two NALM6 cells (DiI, yellow; DiO, green) after co-culture for 24 hours. White arrow indicates transfer of dye to recipient cell. (B) DiD-stained BCP-ALL NALM6 cells were cultured in a 1:1 ratio with DiO-stained BCP-ALL NALM6 cells for 24 hours. Double positive cells (DiD+/DiO+) were quantified and used as a measure of interleukemic signaling. Right panel represents the start of the experiment. (C) Graphs showing quantification of interleukemic dye transfer between NALM6 cells. Gentle shaking reduced interleukemic TNT signaling whereas culture in a 3.0 μm transwell system – in which leukemic cells reside in close contact - increased interleukemic TNT signaling. (D) Bar graphs representing interleukemic dye transfer in TNT-inhibiting and TNT-inducing conditions, exemplified in (C), compared to dye transfer in normal co-culture (n = 4; one-tailed t-test, paired). Data are means ± SEM; * $p \leq 0.05$, ** $p \leq 0.01$, *** $p \leq 0.001$.

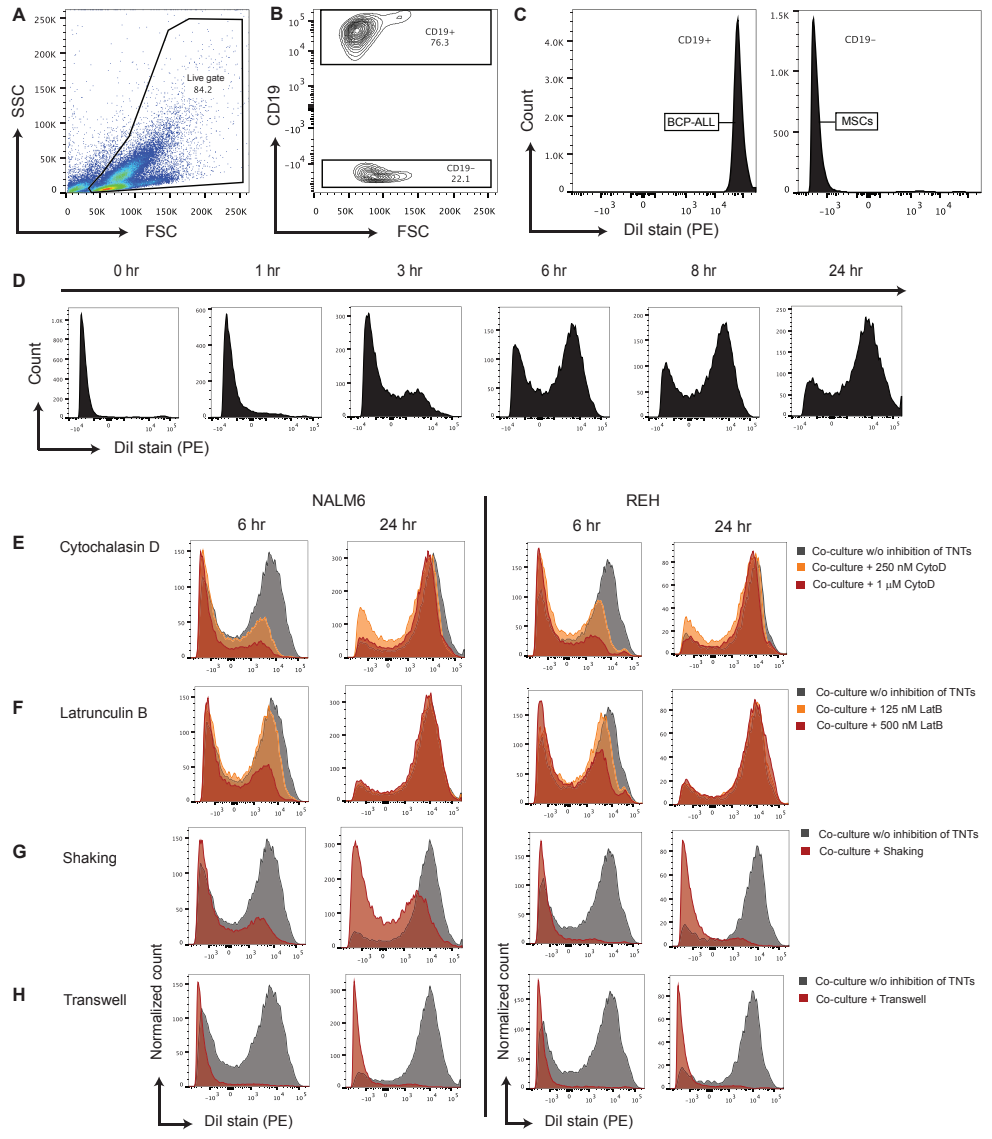

Supplemental Figure 3. Lipophilic dye transfer is caused by TNT signaling. DiI-stained $CD19^{pos}$ BCP-ALL cells (NALM6 and REH) were co-cultured with unstained $CD19^{neg}$ hTERT-MSCs and transfer of DiI staining to hTERT-MSCs was analyzed by flow cytometry at the indicated time points. (A-C) Gating strategy for analysis of dye transfer from leukemic cells towards MSCs. Panel C represents the start of the experiment. (D) Quantification of dye transfer showing efficient transfer from DiI-stained REH cells towards unstained hTERT-MSCs in time (cultured in 4:1 ratio). Data is representative of three independent experiments. (E-H) After 6 hours of co-culture, dye transfer from DiI –stained NALM6 cells towards unstained hTERT-MSCs was decreased using three independent TNT inhibiting conditions: actin inhibition (E: cytochalasin D, F: latrunculin B), physical disruption by gentle shaking (G), or culture in a 3.0 μm transwell system (H). TNT inhibition by gentle shaking, or culture in a 3.0 μm transwell system was continuous, while the inhibition of TNT signaling with actin inhibitors (observed after 6 hours of co-culture) was reversed after 24 hours, due to the short half-life of these inhibitors. Data is representative of three independent experiments.

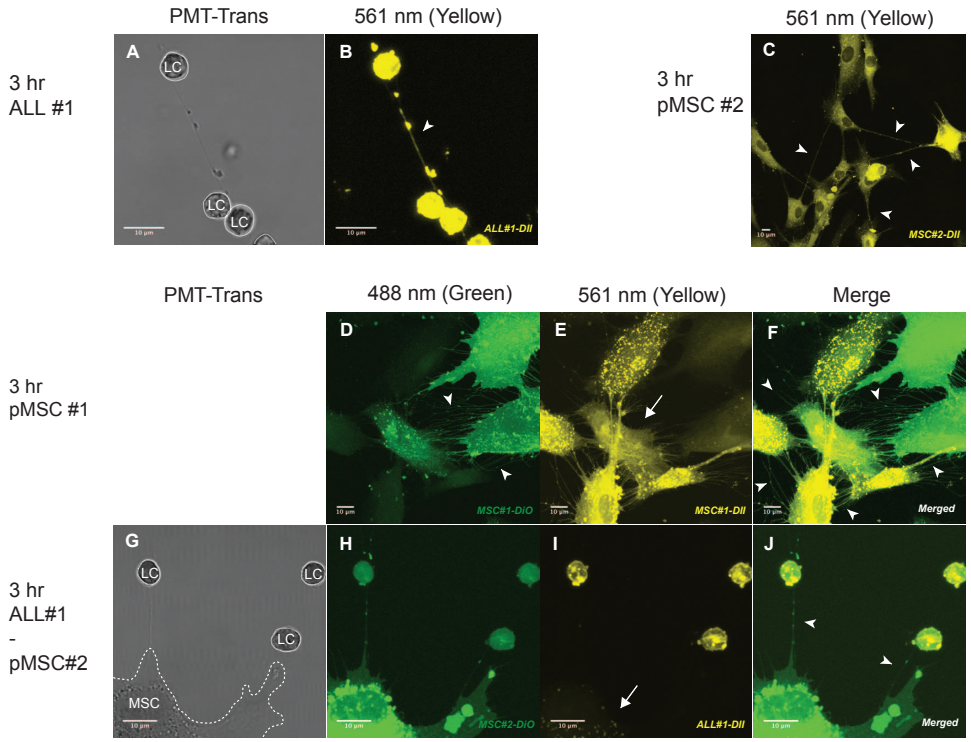

Supplemental Figure 4. TNT networks between primary cells. (A-B) Culture of BCP-ALL patient cells showed interleukemic TNT formation (arrowhead) after 3 hours. (C-F) Culture of BCP-ALL patient MSCs (c: MSC#1, d-f: MSC#2) showed the formation of intermesenchymal TNT networks (arrowheads) which have transferred dye (arrow) after 3 hours. (G-J) TNT signaling between primary BCP-ALL cells (DiI; yellow) and primary MSCs (DiO; green) after co-culture for 3 hours showed bidirectional exchange of lipophilic dye (arrows) via TNTs (white arrowheads). Images are 3D image stacks. Data is representative of at least 3 experiments. Scale bars represent 10 μm.

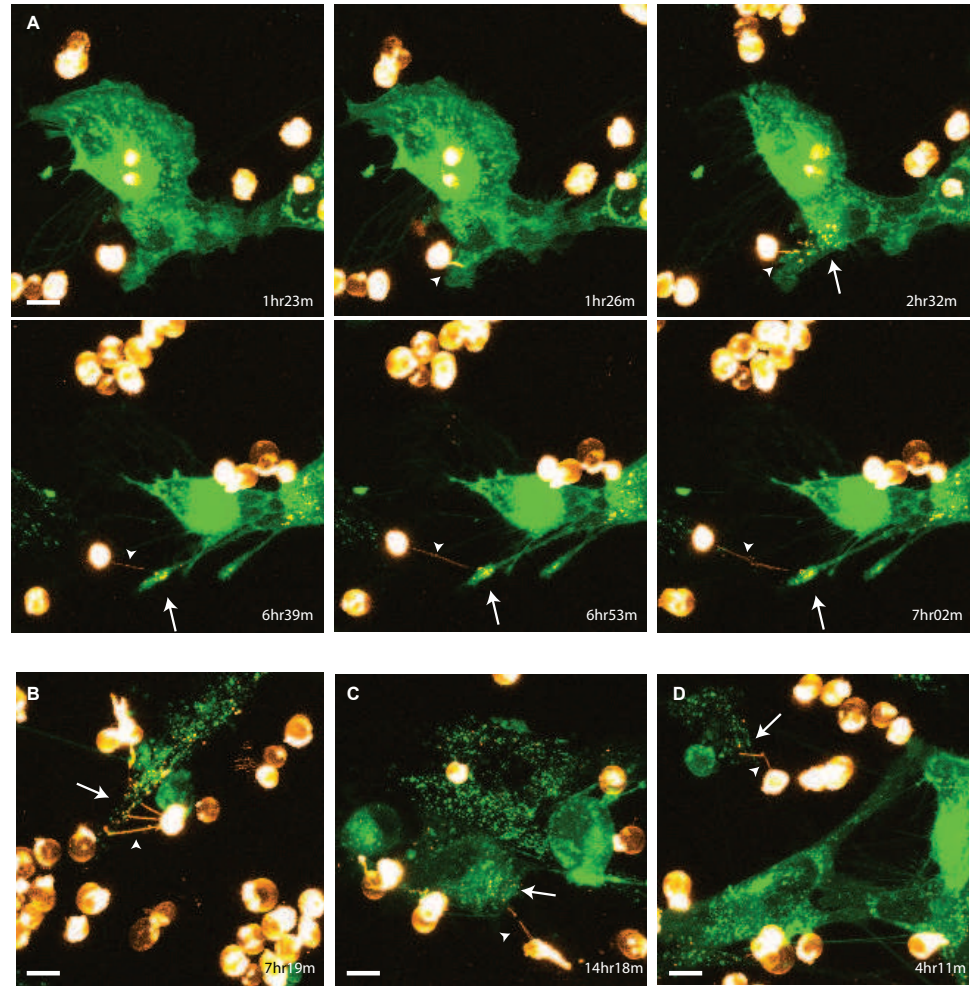

Supplemental Figure 5. Dynamics of TNT formation between primary cells. (A) Time-lapse confocal images (3D image stacks) showing TNT formation (white arrowhead) between primary BCP-ALL cells (ALL#10; DiI, yellow) and primary MSCs (pMSC#1; DiO, green) at multiple time points. White arrow indicates transfer of dye to recipient cell. Time indicated in the right lower corner is the duration from start of the experiment. Orange Hot look-up table (LUT) was used to visualize DiI. Scale bars represent 10 μm. (B-D) Single frames of time-lapse confocal microscopy experiments (3D image stacks) showing TNT formation and signaling from primary BCP-ALL cells (ALL#10; DiI, yellow) and primary MSCs (pMSC#1; DiO, green).

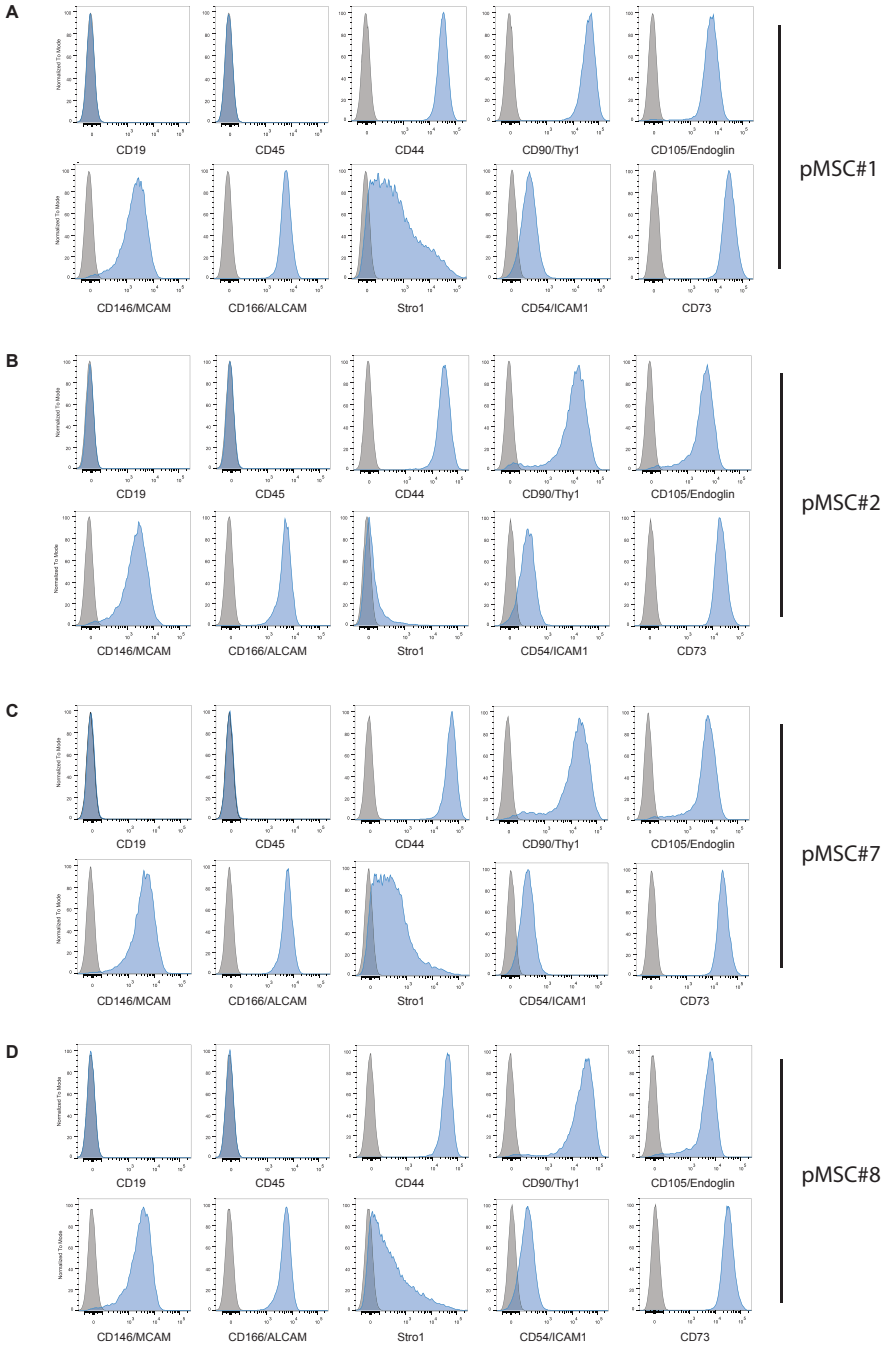

Supplemental Figure 6. Surface marker expression of primary human MSCs. All primary human MSCs were characterized using positive (CD44/ CD90/ CD105/ CD54/ CD73/ CD146/ CD166/ STRO-1) and negative surface markers (CD19/ CD45/ CD34). (A-D) Representative graphs showing the expression of surface markers on 4 primary MSCs. Blue graphs represent surface marker expression. Gray graphs represent expression of isotype controls.

A

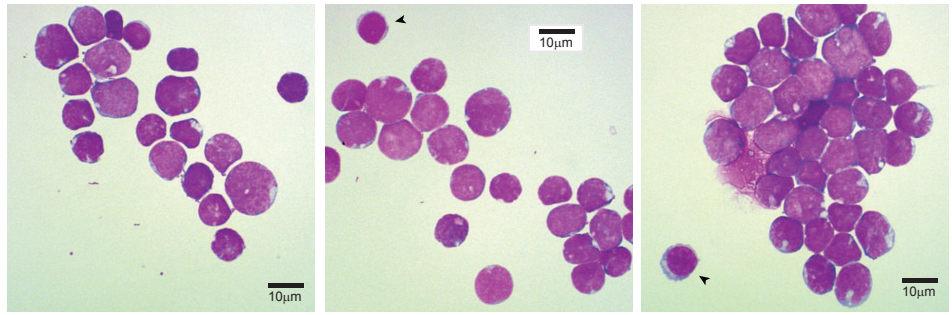

B

	Subgroup	Blasts	Lympho	Mono	Neutro	Me/My
ALL#1	*TA*	98%	-	-	-	2%
ALL#2	*TA*	99%	1%	-	-	-
ALL#3	*TA*	97%	3%	-	-	-
ALL#4	*TA*	98%	1%	-	-	1%
ALL#5	*BO*	98%	1%	1%	-	-
ALL#6	*BO*	97%	3%	-	-	-
ALL#7	*BAL*	99%	1%	-	-	-
ALL#8	*BAL*	97%	1%	-	1%	1%

C

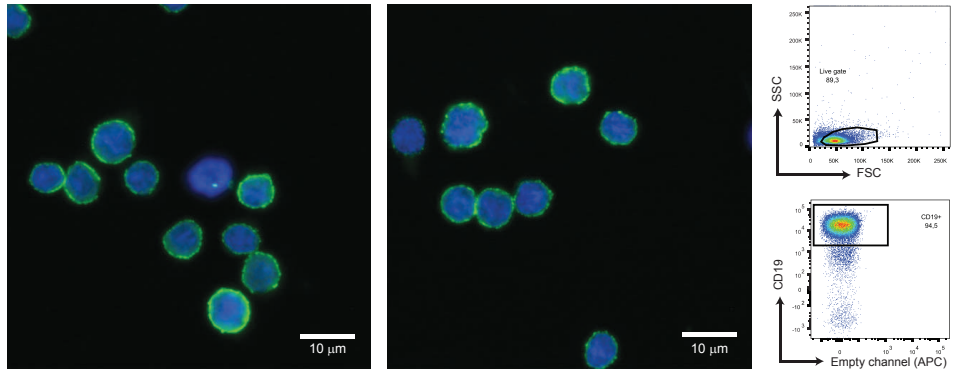

Supplemental Figure 7. Characterization of primary leukemic blasts. (A) The percentage of processed leukemic cells was determined using May-Grünwald-Giemsa staining of cytospin preparations. Images show representative cytospin preparation of leukemic blasts of patient ALL#3. Black arrowheads indicate lymphocytes. All other cells are scored as leukemic blasts. (B) Table containing blast percentages of primary BCP-ALL samples obtained by scoring at least 200 cells per sample. (C) CD19-expression of leukemic blasts was determined for all samples with flow cytometry or fluorescence microscopy. Images are representative and show CD19 surface marker expression of leukemic blasts of patient ALL#3. Dot plots show CD19 surface marker expression of leukemic blasts of patient ALL#3 using flow cytometry.

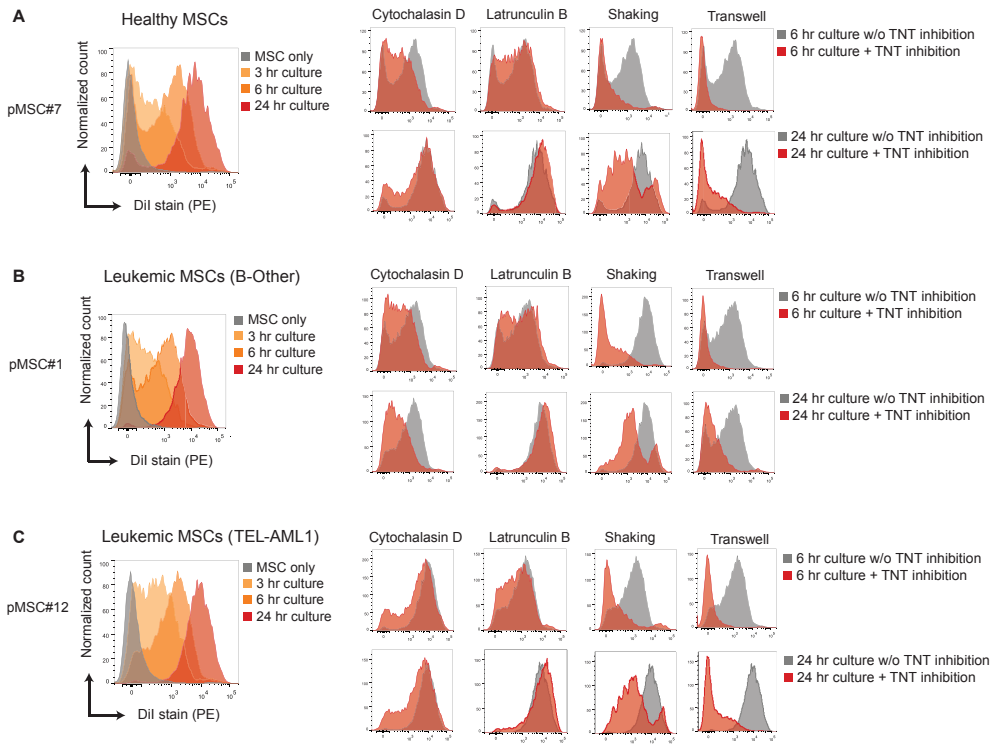

Supplemental Figure 8. TNT signaling to healthy and leukemic MSCs is similarly efficient. Quantification of dye transfer indicating similarly efficient transfer from DiI-stained REH cells towards unstained primary healthy and primary leukemic MSCs (cultured in 4:1 ratio) in time. (A) Dye transfer from DiI –stained NALM6 cells towards unstained primary MSCs of a healthy donor. Three independent TNT inhibiting conditions (actin inhibition (cytochalasin D; 1µM, latrunculin B; 500 nM), physical disruption by gentle shaking, or culture in a 3.0 µm transwell system) decreased dye transfer from leukemic cells towards primary MSCs. (B) Same as (A) for transfer towards unstained primary MSCs of a BCP-ALL patient (B-Other). (C) Same as (A) for transfer towards unstained primary MSCs of a BCP-ALL patient (TEL-AML1).

Supplemental Figure 9. Secretion of cytokines induced by primary BCP-ALL cells. (A) MCP-1 (CCL2) supernatant levels in co-culture of primary leukemic patient ALL#7 cells with primary MSC#1 (left panel), MSC#2 (middle panel), or MSC#3 (right panel). TNT signaling was inhibited by gentle shaking or culture in a transwell system. *p<0.05, **p<0.01 (one-tailed t-test, unpaired). (B) Same as (A) for GRO levels. (C) MCP-1 (CCL2) supernatant levels in co-culture of primary leukemic patient ALL#9 cells with primary MSC#4 (left panel), or MSC#5 (right panel). (D) Same as (C) for GRO levels. (E) IL8 supernatant levels in co-culture of BCP-ALL cells (NALM6) with primary MSC#1 (left panel) or MSC#2 (right panel). TNT signaling was inhibited by gentle shaking or culture in a transwell system. (F) VEGF supernatant levels in co-culture of BCP-ALL cells (NALM6) with primary MSC#1 (left panel) or MSC#2 (right panel). (G) IL8 measurements as seen in (F) relative to the 'Normal' condition (one-tailed t-test, paired). (H) VEGF measurements as seen in (C) relative to the 'Normal' condition (one-tailed t-test, paired). Data are means ± SEM. * p ≤ 0.05, ** p ≤ 0.01, *** p ≤ 0.001 (one-tailed t-test, unpaired). nd = not detectable (below detection level).

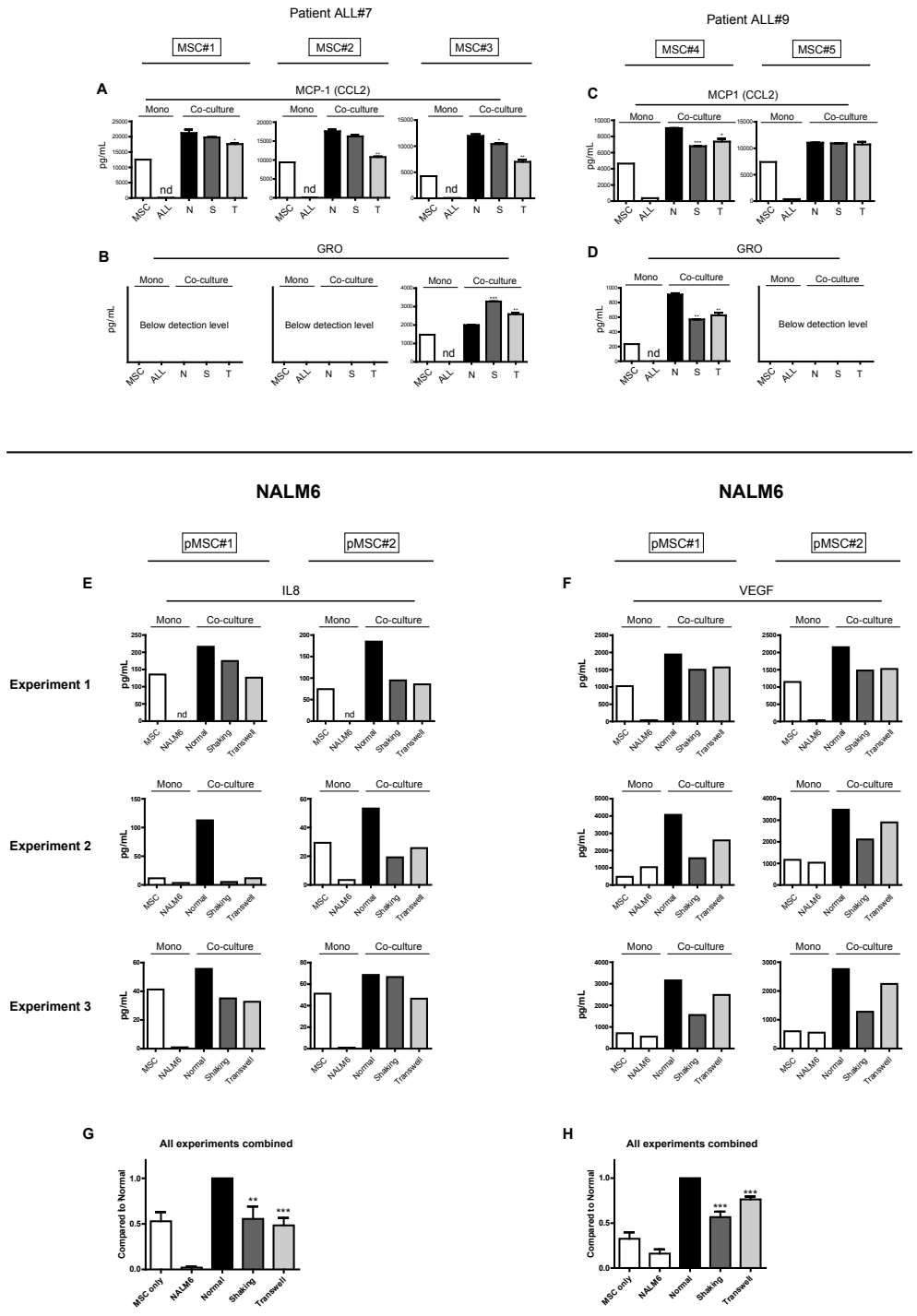

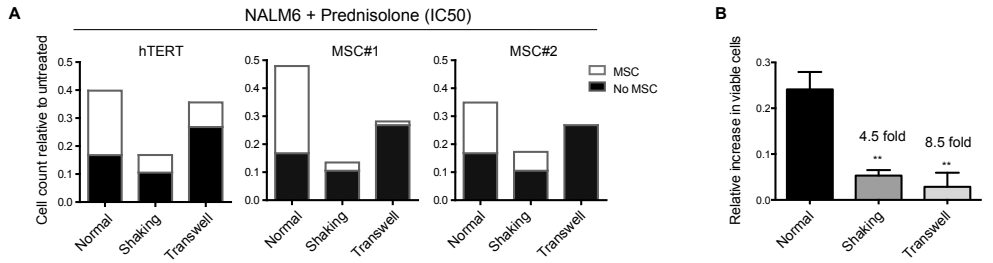

Supplemental Figure 10. TNTs contribute to drug resistance. These data represent the same experiment as shown in Figure 7B. (A) BCP-ALL cell line NALM6 was cultured with (white bars) or without (black bars) MSCs (of three different sources) and cultures were exposed to prednisolone. Bars represent the cell count relative to an untreated control. (B) The relative survival benefit for NALM6 cells in co-culture with MSCs. Inhibition of TNT signaling (by gentle shaking or culture in a 3.0 µm transwell system) re-sensitized to prednisolone (n = 3; one-tailed t-test, unpaired). Data are means ± SD. ** $p \leq 0.01$ (one-tailed t-test, unpaired).

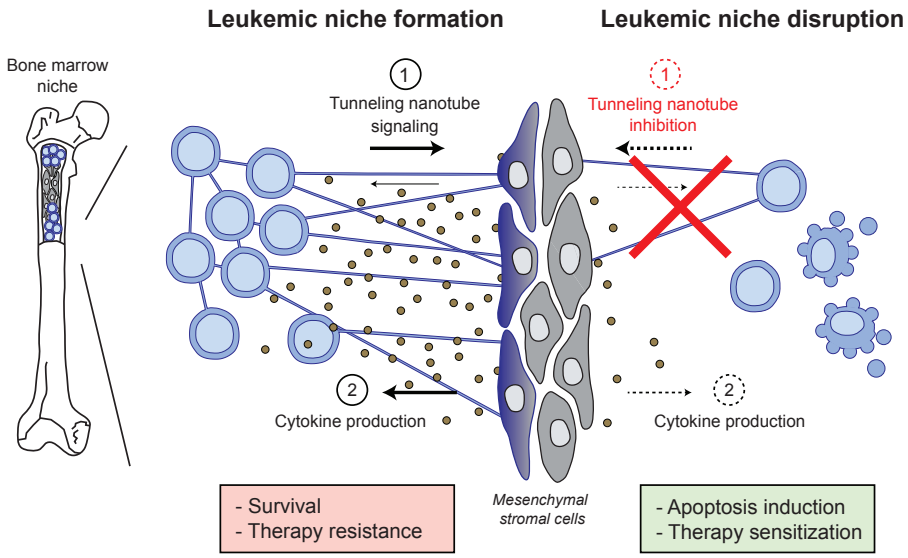

Supplemental Figure 11. Model of the TNT-driven leukemic niche. Model depicting the role of TNT signaling in leukemic niche formation. Leukemic cells use TNTs to modulate their microenvironment by directing non-malignant stromal cells to produce pro-survival cytokines and chemokines. This leukemic niche promotes cell survival and drug resistance and can be disrupted by inhibiting TNT signaling.

SUPPLEMENTAL VIDEOS

Supplemental Video 1. TNT formation between BCP-ALL cells and MSCs.

TNTs are thin membrane tethers containing F-Actin that do not contact the substratum. These videos show that membrane tethers between BCP-ALL cells and MSCs do not touch the substratum. (A) Video showing all z-stacks of images shown in Figure 1A-D. Video starts at the highest Z-stack and moves towards the fibronectin-coated glass slide. (B) Video showing 3D projections of all z-stacks of images in Figure 1A-D.

Supplemental Video 2. TNT connecting a BCP-ALL cell and a MSC

Video showing a thin membrane tether between a BCP-ALL cell (NALM6; DiI; in red) and a MSC (hTERT-MSC; in green) that does not touch the substratum. Dye transfer from the BCP-ALL cell to the MSC is illustrated by the presence of red dye in the MSC.

Supplemental Video 3. Time lapse analysis of TNT formation between BCP-ALL cells and MSCs

Time-lapse confocal imaging showing TNT formation from NALM6 cells (DiI; yellow) towards primary MSCs (DiO; green) in time (red arrows). NALM6 cells were labeled with the fluorescent lipophilic dye DiI, and primary MSCs were labeled with the fluorescent lipophilic dye DiO. Frames were collected every 3 minutes and 19 seconds and the video runs at 3 frames/second, except between 0:09 and 0:15 seconds, where the playback speed is increased 1.5 times. All frames are 3D image stacks as described in Figure 3 and Supplemental Methods. 3D projections of start and end of experiment are included to show the amount of dye transfer and are confocal signals of 561-nm laser overlaid to bright field images.

Supplemental Video 4. Time lapse analysis of TNT formation between BCP-ALL cells and MSCs

(A) Time-lapse confocal imaging showing TNT formation from NALM6 cells (DiI; yellow) towards primary MSCs (DiO; green) in time (red arrows). Blue arrow indicates a TNT formed by MSCs. NALM6 cells were labeled with the fluorescent lipophilic dye DiI, and primary MSCs were labeled with the fluorescent lipophilic dye DiO. Frames were collected every 3 minutes and 19 seconds and the video runs at 3 frames/second. (B) 3D projections of start (0 hr) and end (10 hr) of experiment to illustrate the amount of dye transfer. Confocal signals of 561-nm laser are overlaid to bright field images.

Supplemental videos available online: www.bloodjournal.org.

Chapter 3

DISRUPTING TUNNELING NANOTUBE SIGNALING IN THE LEUKEMIC NICHE USING ACTIN INHIBITORS

Bob de Rooij, Roel Polak, Femke Stalpers,
Rob Pieters & Monique L. den Boer

Submitted

ABSTRACT

Acute lymphoblastic leukemia (ALL) cells use tunneling nanotubes (TNT) to communicate with mesenchymal stromal cells (MSCs) and thereby induce cellular drug resistance and the secretion of pro-survival cytokines. However, it is currently unclear how to inhibit these cytoskeletal structures in the leukemic niche. Here we investigated 6 tubulin and 11 actin inhibitors for their potency to disrupt signaling in ALL-MSC co-cultures using flow cytometric analysis. Our data show that microtubule inhibitors were cytotoxic to both ALL cells and MSCs but paradoxically *increased* TNT signaling up to 2.7-fold ($p < 0.05$). In contrast, inhibiting actin polymerization (swinholide A, cytochalasin D, mycalolide B, or latrunculin B), inhibiting actin disassembly (cucurbitacin E or jasplakinolide), or inhibiting actin nucleation by targeting formins or the Arp2/3 complex (SMIFH2, CK548), strongly *reduced* TNT signaling up to 20-fold ($p < 0.001$). Interestingly, combining inhibitors of actin stabilization and polymerization as well as simultaneous targeting of actin stabilization and nucleation significantly reduced TNT signaling compared to single agents. Similar to Vinca alkaloids, actin inhibitors reduced the viability of primary ALL cells. These findings provide novel insights into the biology of TNTs in the leukemic niche and indicate that cytoskeleton-interfering drugs other than Vinca alkaloids may be of additional benefit in the treatment of ALL.

KEY POINTS

Tunneling nanotube signaling between leukemic cells and mesenchymal stromal cells is inhibited by disrupting actin not tubulin.

Simultaneously targeting actin disassembly and actin nucleation or polymerization reduces TNT signaling in a synergistic-like manner.

INTRODUCTION

The structure of eukaryotic cells is regulated by a dynamic cytoskeletal matrix, mainly composed of three polymers: microtubules, microfilaments (or actin filaments) and intermediate filaments. These cytoskeletal proteins spatially organize the contents of the cell, physically and biochemically connect the cell to its microenvironment and facilitate cell shape and movement[1]. Each type of filament has unique characteristics and regulates specific biological processes. For example, actin filaments drive cellular protrusions which are involved in chemotaxis and cell-cell communication[1]. Recently, new cytoskeletal structures called tunneling nanotubes (TNTs) have been discovered. TNTs reach lengths of multiple cell diameters, protrude from the cell membrane, and connect the cytoskeleton of two cells[2]. These structures are driven by the polymerization of monomeric, or globular, actin into filamentous actin (F-actin)[2,3]. TNTs facilitate intercellular transport of pathogens, organelles, proteins and calcium fluxes[2,4-7]. They have been identified in multiple cell types, including cancer cells[2,3,6,8-12]. We recently showed that TNTs support leukemic cell survival and drug resistance in acute lymphoblastic leukemia (ALL)[13]. In addition, TNT signaling between ALL cells and mesenchymal stromal cells (MSCs) induced the secretion of pro-survival cytokines in the tumor microenvironment[13]. TNT inhibition reversed this cytokine signature and subsequently sensitized leukemic cells toward chemotherapeutic drugs[13]. These findings suggest that TNT inhibition may offer a promising new therapeutic option. Unfortunately, agents that specifically inhibit TNTs have not yet been identified. Since TNT signaling depends on actin and/or tubulin[2,13-15], we investigated 6 tubulin and 11 actin inhibitors for their potency to disrupt TNT signaling between ALL cells and MSCs. In addition, we studied how these compounds affect the viability of primary ALL cells, $CD34^+$ hematopoietic progenitor cells (HPCs), hematopoietic mononuclear cells (MNCs), and MSCs.

METHODS

BCP-ALL cells

BCP-ALL cell line NALM6 (B-Other), obtained from DSMZ (Braunschweig, Germany), was used at low cell passages and routinely verified by DNA fingerprinting. Patient cells were obtained from bone marrow aspirates from children with newly diagnosed BCP-ALL prior to treatment. Mononuclear leukemic cells were collected and processed as previously described[16]. All samples used in this study contained ≥ 95% leukemic blasts.

Isolation and characterization of healthy cells

Mesenchymal stromal cells (MSCs) were isolated from bone-marrow aspirates and characterized as previously described[13,17]. In short, MSCs were confirmed to have multilineage potential for adipocyte, osteocyte and chondrocyte differentiation and characterized using positive (CD44/ CD90/CD105/CD54/CD73/CD146/CD166/STRO-1) and negative surface markers (CD19/CD45/CD34).

Human mononuclear cells (MNCs) were obtained from umbilical cord blood (UBC) based on a density gradient using Lymphoprep (Stemcell Technologies, Köln, Germany). $CD34^+$ hematopoietic progenitor cells (HPCs) were obtained from UBC using the Direct CD34 Progenitor Cell Isolation kit, human (Miltenyi Biotec, Gladback, Germany). $CD34^+$ HPCs were positively selected by magnetic microbeads using the MACS LS column (Miltenyi Biotec) in combination with a MACS separator (Miltenyi Biotec). Isolated cells were confirmed to be $CD34^+$ by flow cytometry using the CD34-PE fluorescent antibody (BD Pharmingen, San Diego, USA).

Confocal laser scanning microscopy

NALM6 cells were stained with 1,1'-dioctadecyl-3,3,3'3'-tetramethylindocarbocyanine perchlorate (DiI; yellow) and MSCs were stained with 3,3'-dioctadecyloxacarbocyanine (DiO; green; both from Life Technologies, Breda, The Netherlands) according to the manufacturer's protocol. NALM6 cells and MSCs were co-cultured in a 4:1 ratio on a glass slide coated with 10 µg/mL fibronectin (Sigma-Aldrich, Saint Louis, USA) at 37 °C and 5% CO_2 for 3 hours and fixated as previously described[13,18]. Confocal images were acquired as previously described using a Leica SP5[13]. In short, we used sequential scanning of different channels at a resolution of 1024 x 1024 pixels in the x ^{x} y plane and 0.15 µm steps in z-direction. DiO and DiI were excited with a 488-nm Argon laser and a 561-nm Diode-Pumped Solid-State laser, respectively. Image processing was done with Fiji software[19].

Dye transfer experiments

CD19-positive BCP-ALL cells were stained with DiI and co-cultured with unstained CD19-negative MSCs for 3 or 24 hours in a 4:1 ratio. ALL-MSC co-cultures were either untreated (control) or treated with tubulin or actin inhibitors (Table 1). At the end of each experiment, cells were harvested and stained with brilliant violet 421-labelled anti-human CD19 antibody (Biolegend, San Diego, USA) to separate cell types, and stained with Sytox Red (Sigma-Aldrich) to distinguish live and apoptotic events (See supplemental Figure 1 for gating strategy). The median intensity of DiI-label was determined for viable MSCs using the PE-channel and taken as a measure of dye transfer. Target populations were analyzed before and after co-culture with flow cytometry (BD Bioscience, San Jose, USA).

Cell viability assay

The effect of tubulin and actin inhibitors on multiple cell types was assessed using a colorimetric assay. All cells were cultured in round-bottom 96-well plates and incubated with inhibitors for 48 hours, except MSCs which were cultured on flat-bottom 96-well plates. At the end of experiment, MTS (3-(4,5-dimethylthiazol-2-yl)-5-(3-carboxymethoxyphenyl)-2-(4-sulfophenyl)-2H-tetrazolium) was added to each well (20 µL / well) and conversion of MTS was detected by a spectrophotometer at 490 nm. The amount of MTS conversion in the presence of inhibitors was normalized relative to an untreated control and used as a measure of cell viability. For primary BCP-ALL cells, MTT (3-(4,5-dimethylthiazol-2-yl)-2,5-diphenyltetrazolium bromide) was used.

Statistical analysis

Student's t-test was used as a statistical test and a Student's paired t-test was used when applicable (indicated in figure legends). Error bars show as standard error of the mean (SEM).

Table 1. Overview of tubulin and actin inhibitors

Name	Target	Mechanism of action
Taxol[a]	tubulin	Enhances tubulin polymerization and stabilization[20]
Colchicine[a]	tubulin	Inhibits microtubule polymerization[21]
Nocodazole[a]	tubulin	Inhibits microtubule polymerization[22]
Vinblastine[a]	tubulin	Inhibits microtubule polymerization[21]
Colcemid[a]	tubulin	Inhibits microtubule polymerization[23]
Vincristine[a]	tubulin	Inhibits microtubule polymerization[23]
Swinholide A[a,b]	actin	Stabilizes actin dimers and severs actin[24]
Mycalolide B[c,d]	actin	Stabilizes actin dimers and severs actin[25,26]
Latrunculin B[a]	actin	Alters the actin-monomer subunit interface[27]
Cytochalasin D[a]	actin	Blocks fast growing end of actin filaments[28]
Cucurbitacin E[a]	actin	Inhibits depolymerization by binding to F-actin[29]
Jasplakinolide[c]	actin	Decreases sequestering of actin[30,31]
ML141[a]	actin	Cdc42 inhibitor[32]
SMIFH2[a]	actin	Formin inhibitor
CK548[a,d]	actin	Arp2/3 inhibitor
Wiskostatin[a]	actin	N-wasp inhibitor[33]
Blebbistatin[d]	actin	Myosin-II inhibitor[34]

Company information: a = Sigma-Aldrich (Saint Louis USA), b = AG Scientific (San Diego, USA), c = Abcam (Cambridge, UK), d = Enzo Life Sciences (New York, USA).

RESULTS

TNT signaling is accurately quantified by lipophilic dye transfer

Confocal microscopy was used to visualize the presence of TNTs between B-cell precursor ALL (BCP-ALL) cells and MSCs as earlier described[13]. TNTs connecting BCP-ALL cells (NALM6, stained with DiI-yellow) and primary MSCs (stained with DiO-green) were visible after 3 hours of co-culture and showed transport of lipophilic dye toward MSCs (Figure 1A, supplemental Figure 2). 3D reconstruction of confocal images confirmed that these TNTs did not connect with the substratum (i.e. the fibronectin-coated glass slide; see supplemental Video 1A-D and supplemental Video 2A-D). Confocal microscopy visualizes

TNT structures, but is less suited to measure the signaling through TNTs. Measuring lipophilic dye transfer from ALL cells toward MSCs using flow cytometry is an accurate way to quantify TNT signaling[2,3,13]. Within 3 hours of co-culture, DiI-labeled NALM6 cells transferred dye to more than 50% of MSCs and this increased to > 95% after 24 hours (Figure 1B).

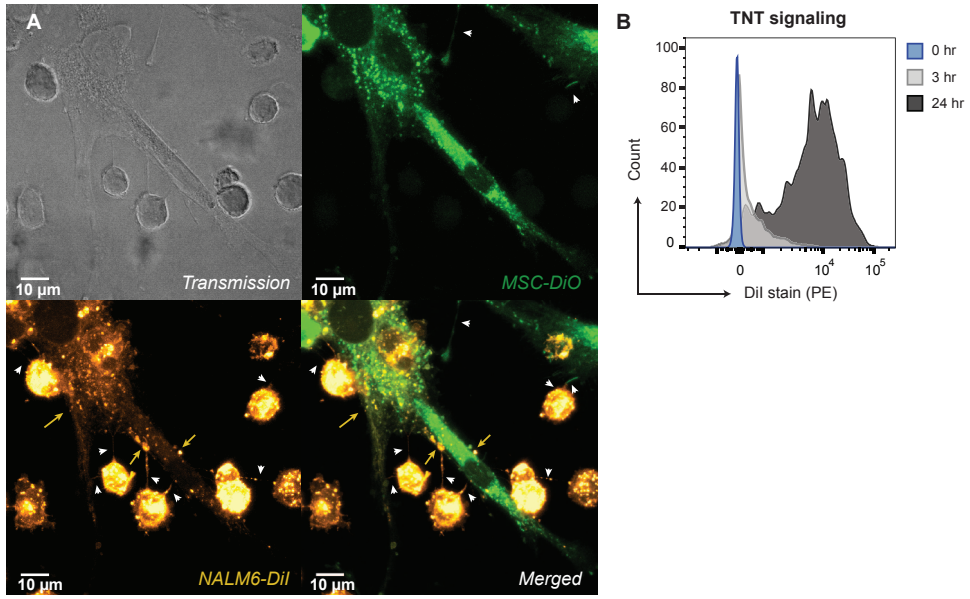

Figure 1. TNT signaling is accurately quantified by measuring lipophilic dye transfer. (A) Representative confocal images (Z-stack) showing TNT networks (white arrowheads) between BCP-ALL cell line NALM6 (DiI, yellow) and primary MSCs (DiO, green) after co-culture for 3 hours (n = 4). Lipophilic dye transfer toward MCSs via TNTs was observed (yellow dye in green MSCs). (B) Graph showing quantification of dye transfer from DiI-stained NALM6 cells toward unstained MSCs after 3 (light-grey histogram) and 24 hours (grey histogram) of co-culture (n = 20). See also supplemental Figures 1 and 2 and supplemental Video 1A-D and 2A-D.

Tubulin inhibitors do not inhibit TNT signaling between BCP-ALL cells and MSCs

Next, we assessed the effect of tubulin inhibitors on lipophilic dye transfer by flow cytometry. We used a broad range of concentrations based on those reported to be effective in literature (for references see Table 1). Tubulin disruption for 48 hours by six different tubulin inhibitors caused a marked decrease in cell viability of leukemic cells and MSCs (supplemental Figure 3). However, this was not preceded by reduced lipophilic dye transfer. Instead, dye transfer was increased by all tubulin inhibitors (Figure 2, ≤ 2.7-fold increase, $p < 0.05$). These data show that TNT signaling between BCP-ALL cells and MSCs cannot be inhibited by interference with microtubules. In addition, these data suggest that TNT signaling is enhanced during treatment with tubulin inhibitors.

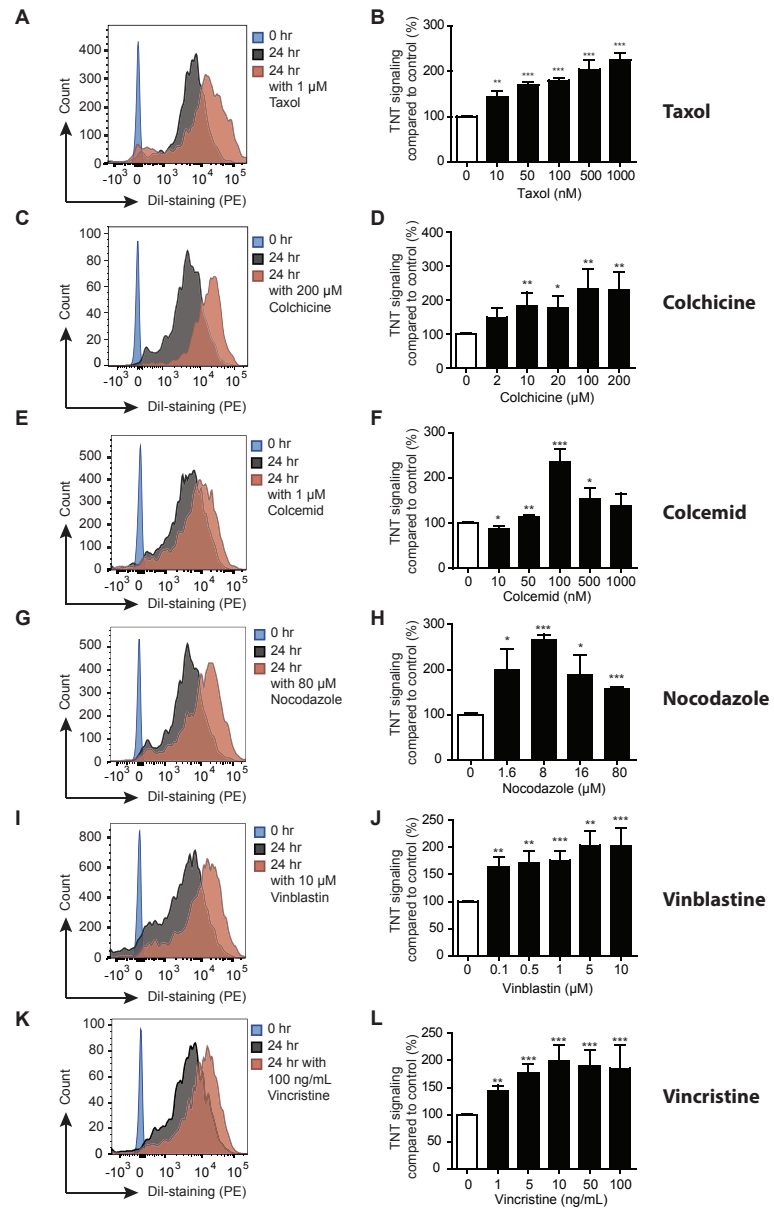

Figure 2. Tubulin inhibitors do not inhibit TNT signaling between BCP-ALL cells and MSCs. (A) Graph showing quantification of dye transfer from DiI-stained NALM6 cells toward unstained MSCs with (red histogram) or without (grey histogram) treatment with 1 µM taxol for 24 hours (n = 2). (B) Graph showing quantification of dye transfer from DiI-stained NALM6 cells toward unstained MSCs. Co-cultures were treated with or without taxol using multiple concentrations (two-tailed t-test, unpaired) (n = 2). (C) Same as (A) for 200 µM colchicine (n = 3). (D) Same as (B) for colchicine (n = 3). (E) Same as (A) for 1 µM colcemid (n = 2). (F) Same as (B) for colcemid (n = 2). (G) Same as (A) for 80 µM nocodazole (n = 2). (H) Same as (B) for nocodazole (n = 2). (I) Same as (A) for 10 µM vinblastine (n = 2). (J) Same as (B) for vinblastine (n = 2). (K) Same as (A) for 100 ng/mL vincristine (n = 2). (L) Same as (B) for vincristine (n = 2). Data are means ± SEM; ** $p \leq 0.01$, *** $p \leq 0.001$. See also supplemental Figure 1 and 3.

TNT signaling between BCP-ALL cells and MSCs is dependent on actin polymerization, disassembly and nucleation

Next, we used the ALL-MSC co-culture model to investigate the ability of 11 actin disrupting molecules to inhibit TNT signaling. Actin inhibitors can be subdivided into four different classes, namely those affecting the polymerization, the disassembly, the nucleation or the rearrangement of actin molecules (Figure 3). The concentration range of the inhibitors was based upon those reported to be effective in literature (for references see Table 1). Like tubulin inhibitors, all actin inhibitors caused a decrease in cell viability of leukemic cells and MSCs after 48 hours of exposure (supplemental Figure 4).

All four actin polymerization inhibitors significantly reduced dye transfer from BCP-ALL cells toward MSCs within 24 hours of exposure (Figure 4A-B, ≤ 92% reduction, $p < 0.001$). This is in line with literature showing that inhibition of actin polymerization inhibits TNT formation[2,35-37]. Next we assessed the effect of the actin disassembly inhibitors cucurbitacin E and jasplakinolide. Interestingly, both molecules strongly reduced lipophilic dye transfer toward MSCs (Figure 4C-D; ≤ 95% reduction at 250 nM cucurbitacin E or jasplakinolide, $p < 0.001$). Jasplakinolide has been reported to affect the length of TNTs in microvascular endothelial cells and to reduce the formation of TNTs between cells[38,39]. Our data show that stabilization of the actin cytoskeleton also reduces signaling via TNTs. Actin nucleation factors mimic actin monomers and hereby create a stable starting point for actin polymerization. Inhibiting actin nucleation by either SMIFH2 (formin inhibitor)[40] or CK548 (Arp2/3 inhibitor)[41] strongly reduced dye transfer from BCP-ALL cells toward MSCs, although only at high concentrations (96% reduction at 37.5 μM SMIFH2 or 200 μM CK548, $p < 0.001$; Figure 4E-F). To our knowledge, this is the first report showing that actin nucleation is important for TNT signaling. Finally, we explored the effects of small-molecule inhibitors interfering with proteins that rearrange the actin cytoskeleton. ML141 (Cdc42 inhibitor)[32] was unable to reduce lipophilic dye transfer, wiskostatin (N-wasp inhibitor)[33] slightly affected dye transfer (32% reduction at 12.5 μM, $p < 0.05$) and (±)-blebbistatin (Myosin II inhibitor)[34] stimulated dye transfer at higher concentrations (2.1-fold at 50 μM, $p < 0.001$; Figure 4G-H). These findings show that actin nucleation, polymerization, and disassembly are important for TNT signaling between ALL cells and MSCs.

Inhibitors identified in NALM6 cells also inhibit TNT signaling in primary BCP-ALL cells

Next we tested the most promising compounds in our cell line studies using co-cultures of patient-derived BCP-ALL cells and MSCs. We selected these compounds based on TNT inhibiting capacity and cytotoxicity. Cytochalasin D, cucurbitacin E, jasplakinolide and CK548 significantly reduced the dye transfer from primary BCP-ALL cells toward MSCs in 24 hours (Figure 5A-B, $p < 0.001$). Interestingly, both jasplakinolide and CK548 were less potent in inhibiting dye transfer in primary BCP-ALL cells compared to NALM6 cells

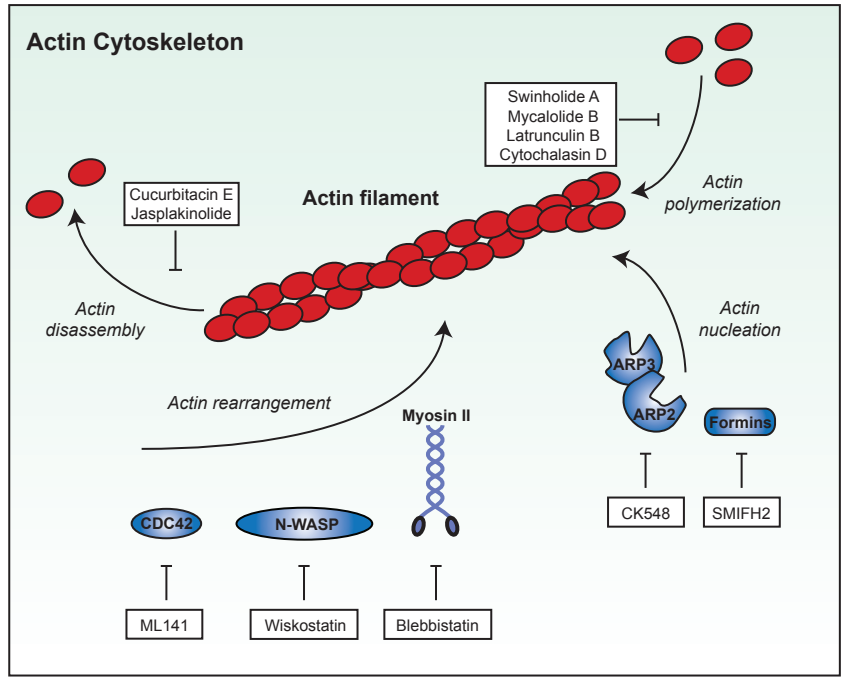

Figure 3. Schematic overview of compounds disrupting actin biosynthesis and breakdown. Schematic overview showing the regulation of the actin cytoskeleton by actin nucleation, polymerization, rearrangement, and disassembly. White boxes show actin inhibitory molecules. See also Table 1.

(61% versus 95% reduction at 500 nM jasplakinolide; 27% versus 96% reduction at 200 μM CK548; Figure 4 and 5). These data show that inhibitors of actin nucleation, polymerization, and disassembly also effectively reduce TNT signaling between primary BCP-ALL cells and primary MSCs.

Inhibiting the actin cytoskeleton reduces cell viability in healthy and leukemic cells

We tested the cytotoxic effect of cytochalasin D, cucurbitacin E, jasplakinolide and CK548 exposure for 48 hours in primary BCP-ALL cells (n = 6), primary MSCs (n = 3), umbilical cord-blood derived $CD34^+$ HPCs (n = 2) and umbilical cord-blood derived MNCs (n = 6). Red areas indicate the drug concentrations resulting in profound inhibition of dye transfer via TNTs after 24 hours of exposure (Figure 6). Exposure to cytochalasin D had no effect on the viability of MNCs and $CD34^+$ HPCs, and only a limited effect on BCP-ALL cells (21% reduction in cell viability at 1000 nM), compared to MSCs (65% reduction in cell viability at 1000 nM; Figure 6A). Cucurbitacin E had a limited effect on MNCs (28% reduction at 1000 nM; Figure 6B), but strong effects on the viability of primary

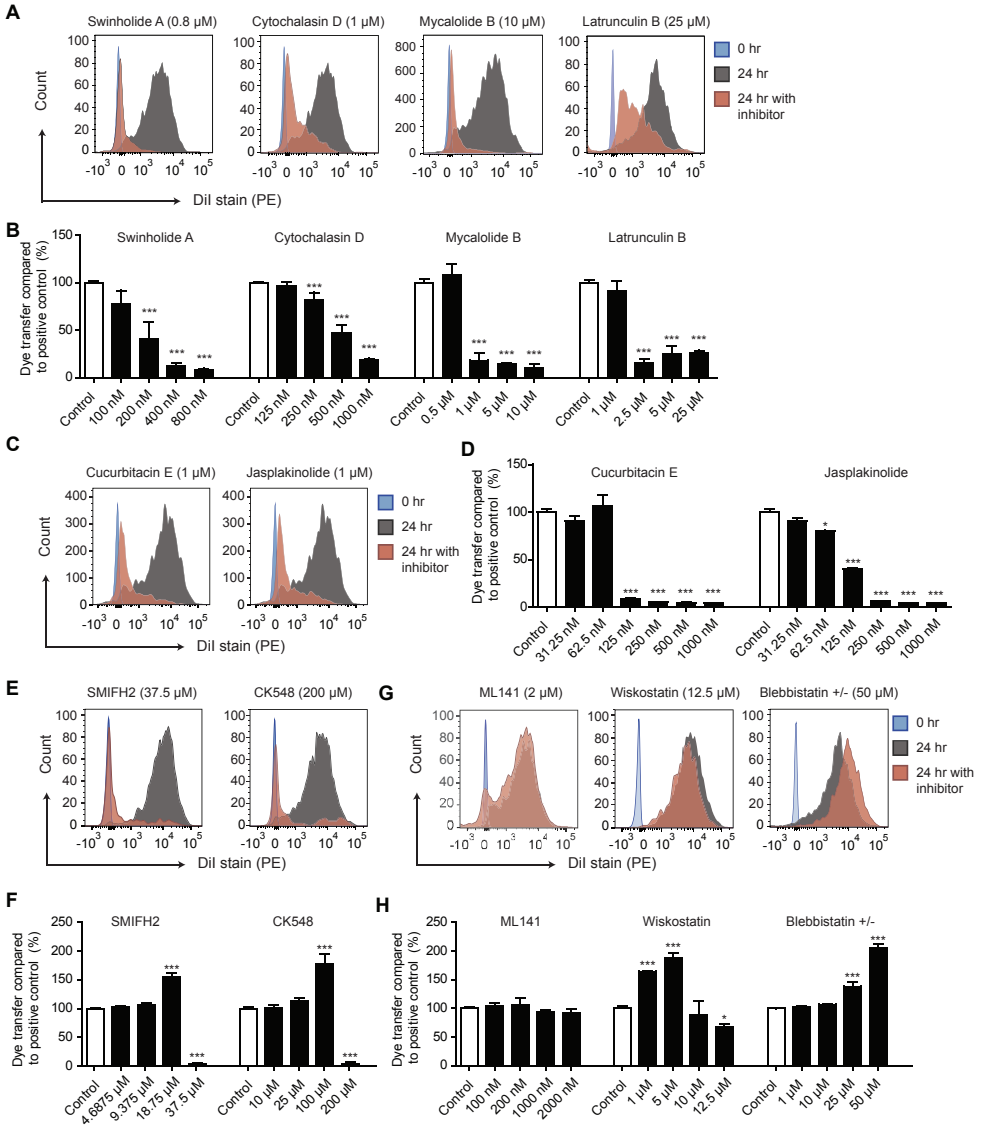

Figure 4. TNT signaling between BCP-ALL cells and MSCs is dependent on actin polymerization, actin disassembly and actin nucleation. (A) Graphs showing quantification of dye transfer from DiI-stained NALM6 cells towards unstained MSCs with (red histograms) or without (grey histograms) treatment by inhibitors depicted in (B). (B) Graph showing quantification of dye transfer after 24 hours from DiI-stained NALM6 cells toward unstained MSCs. Co-cultures were treated with or without the actin polymerization. inhibitors swinholide A, cytochalasin D, mycalolide B or latrunculin B. Data is representative of at least three independent experiments (two-tailed t-test, unpaired). (C) Same as (A) for actin disassembly inhibitors cucurbitacin E and jasplakinolide. (D) Same as (B) for actin disassembly inhibitors cucurbitacin E and jasplakinolide. (E) Same as (A) for actin nucleation inhibitors SMIFH2 and CK548. (F) Same as (B) for actin rearrangement inhibitors SMIFH2 and CK548. (G) Same as (A) for actin rearrangement inhibitors ML141, wiskostatin and (±)-blebbistatin. (H) Same as (B) for actin rearrangement inhibitors ML141, wiskostatin and (±)-blebbistatin. Data are means ± SEM; * $p \leq 0.05$, ** $p \leq 0.01$, *** $p \leq 0.001$. See also supplemental Figures 1 and 4.

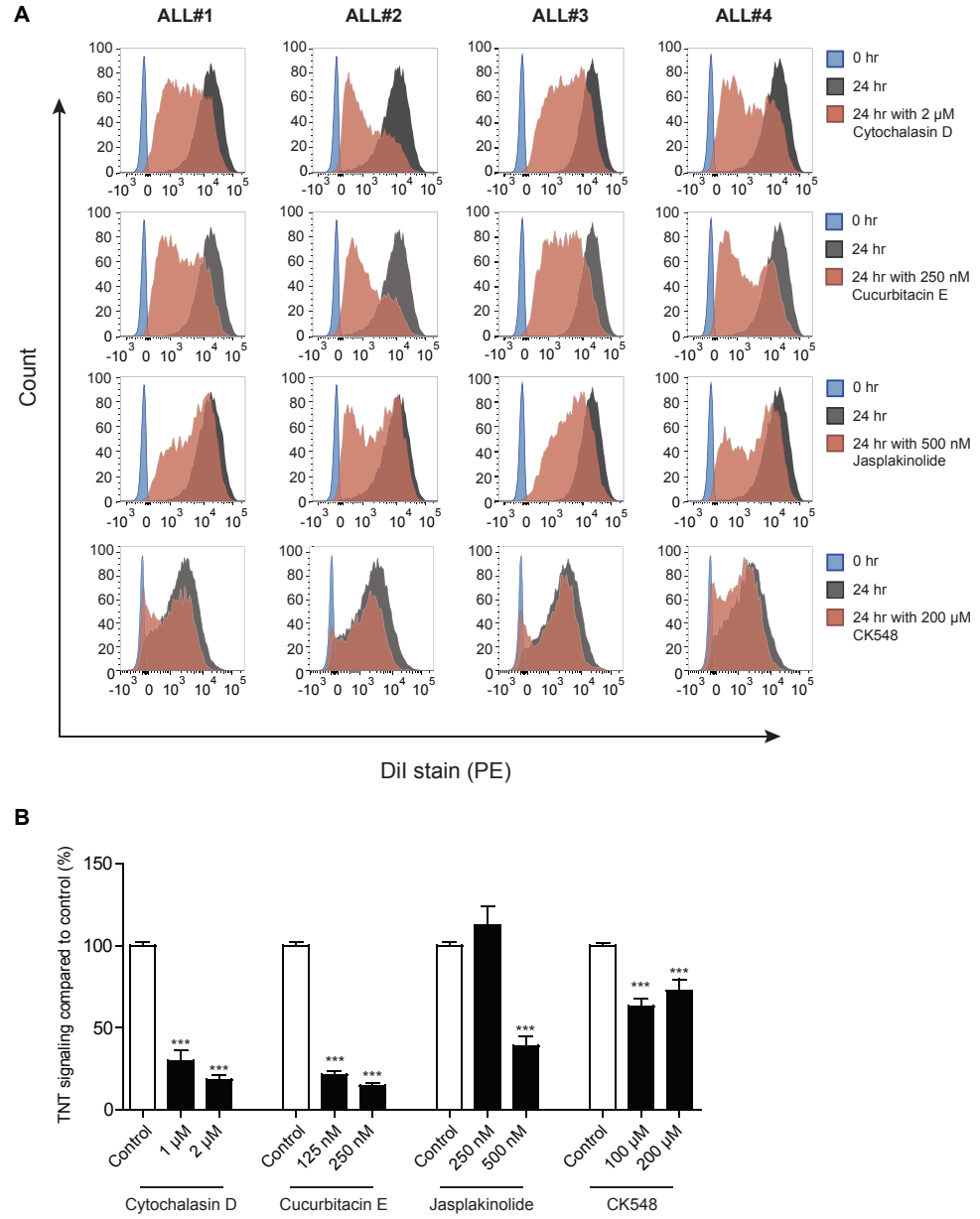

Figure 5. Inhibitors identified in NALM6 cells also inhibit TNT signaling in primary BCP-ALL cells. (A) Graphs showing quantification of dye transfer from primary BCP-ALL cells from 4 different patients toward unstained MSCs with (red histograms) or without (grey histograms) treatment by inhibitors cytochalasin D, cucurbitacin E, jasplakinolide or CK548. (B) Quantification of dye transfer experiment exemplified in (A) performed with 2 different concentrations for each inhibitor (one-tailed t-test, paired; n = 4). Data are means ± SEM; *** $p \leq 0.001$. See also supplemental Figure 1 and Figure 6.

BCP-ALL cells, MSCs and CD34+ HPCs (81% reduction for BCP-ALL, 78% reduction for MSCs and 72% reduction for CD34+ HPCs at 1000 nM; Figure 6B). Jasplakinolide strongly affected MSC viability (87% reduction at 1000 nM), whereas the toxic effect was less pronounced for primary BCP-ALL cells, CD34+ HPCs (59% reduction at 1000 nM), and MNCs (19% reduction at 1000 nM; Figure 6C). The actin nucleation inhibitor CK548 was detrimental to all cell types at high concentrations (> 100 µM CK548, ≤ 88% reduction in cell viability; Figure 6D). These data show that actin inhibitors are toxic to leukemic and healthy hematopoietic and stromal cells, which is in line with previous findings for tubulin inhibitors[21,42,43].

Actin nucleation and actin polymerization regulate TNT signaling together with actin disassembly

Next, we determined if actin nucleation, polymerization, and/or disassembly cooperate or independently regulate TNT signaling. For each inhibitor a concentration was used that had limited effect in inhibiting TNT signaling as a single agent in ALL-MSC co-cultures (50 nM cytochalasin D ,120 nM jasplakinolide and 25 µM CK548; Figure 7A). Targeting both actin

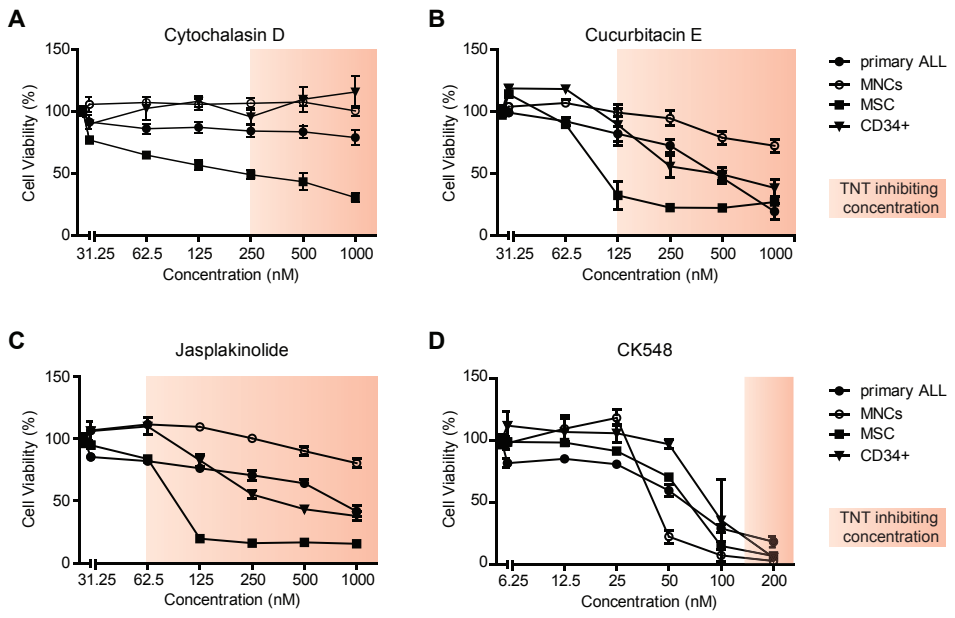

Figure 6. Inhibiting the actin cytoskeleton reduces cell viability in healthy and leukemic cells. (A) Graph showing the effect of cytochalasin D on cell viability of BCP-ALL cells (n = 6), MNCs (n = 6), CD34+ HPCs (n = 2) and MSCs (n = 3) derived from patients as measured by a MTS assay (primary BCP-ALL cells were measured using a MTT assay). The red area represents concentrations at which cytochalasin D inhibits dye transfer from BCP-ALL cells toward MSCs. (B) Same as (A) for cucurbitacin E. (C) Same as (A) for jasplakinolide. (D) Same as (A) for CK548. Data are means ± SEM. See also supplemental Figure 4.

nucleation and polymerization by co-treatment with CK548 and cytochalasin D did not reduce dye transfer (Figure 7B). Interestingly, simultaneous inhibition of actin disassembly by jasplakinolide in combination with inhibition of actin polymerization (cytochalasin D) or nucleation (CK548) was more effective than each of the single agents (Figure 7B-D, $p < 0.05$). These data suggest synergism between actin disassembly inhibitors and inhibitors of actin polymerization and actin nucleation.

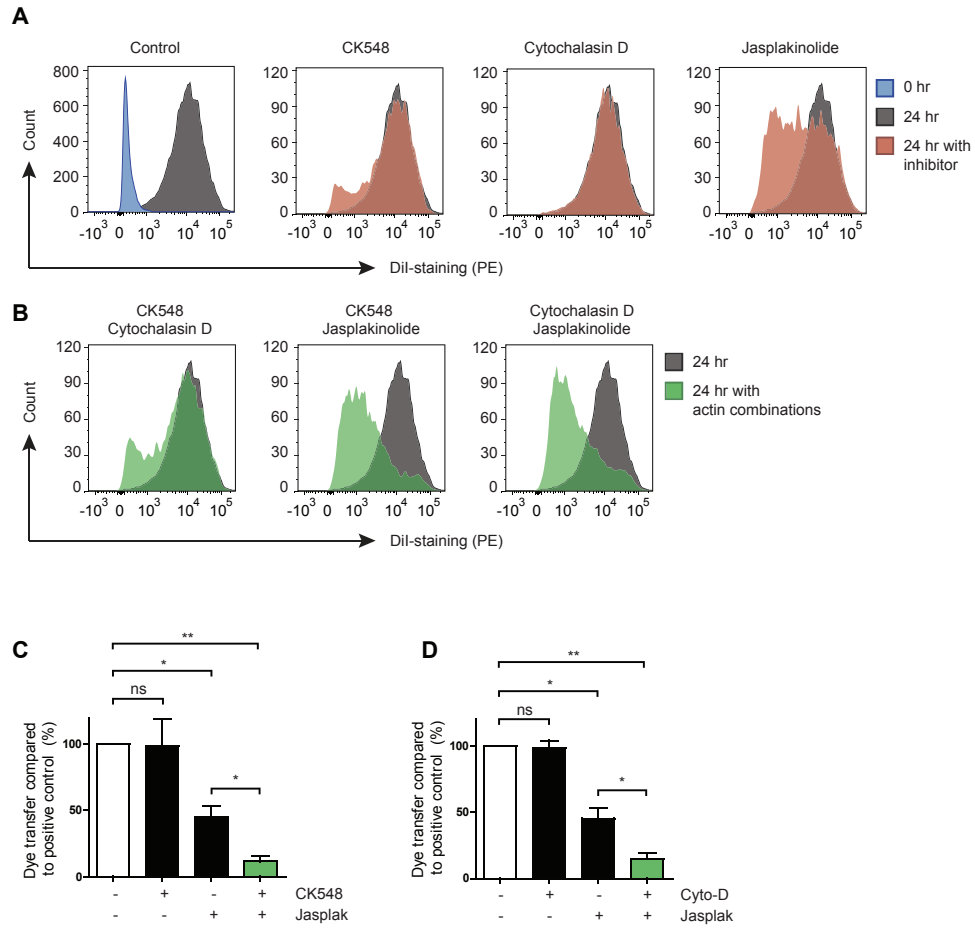

Figure 7. Simultaneous inhibition of actin disassembly and actin polymerization or nucleation synergistically inhibits TNTs. (A) Graphs showing quantification of dye transfer from DiI-stained NALM6 cells towards unstained MSCs with (red histograms) or without (grey histograms) single treatment of actin inhibitors CK548 (25 µM), cytochalasin D (50 nM) or jasplakinolide (120 nM). Blue histogram shows DiI-positivity of MSCs at the start of experiment (n = 3). (B) Graphs showing quantification of dye transfer from DiI-stained NALM6 cells towards unstained MSCs with (green histograms) or without (grey histograms) combination treatment of actin inhibitors CK548, cytochalasin D or jasplakinolide (n = 3). (C) Quantification of dye transfer experiments exemplified in (A) and (B) performed with CK548 and jasplakinolide (n = 3; one-tailed t-test paired). (D) Same as (C) for cytochalasin D and jasplakinolide (n = 3; one-tailed t-test paired). Data are means ± SEM; * $p \leq 0.05$, ** $p \leq 0.01$. See also supplemental Figure 1.

DISCUSSION

TNTs regulate the resistance of tumor cells to chemotherapeutic agents in multiple cancers, showing the strong need for TNT inhibitors[11,13,14]. Disruption of TNTs through physical separation of cells or mechanical disruption has been shown to sensitize leukemic cells to prednisolone and prevent the secretion of pro-survival factors[13]. Unfortunately, these techniques cannot be used in *in vivo* models and cancer patients. There is a large variety in the composition, length, width, and lifespan of TNTs across cell types[2,3,13,38,44]. However, the main components of TNTs are reported to be actin and or tubulin. We therefore assessed the effect of tubulin and actin disrupting agents on the exchange of a lipophilic dye that it is transported by TNTs from BCP-ALL cells toward MSCs[13]. In previous experiments, we showed that the contribution of other cell-cell communication mechanisms to dye transfer is negligible[13].

Importantly, our study revealed that interference with microtubules induces dye transfer via TNTs (Figure 2). This increase is not explained by the release of dye by apoptotic cells, since similar toxicity induced by actin inhibitors did not promote dye transfer (Figure 4-6, supplemental Figures 3 and 4). The induction of TNT signaling by tubulin inhibitors supports earlier observations that TNT formation is increased in response to cellular stress[12,45]. Importantly, tubulin inhibitors are used in the treatment of ALL patients worldwide. The finding that these drugs induce TNT signaling possibly uncovers a rescue mechanism triggered in leukemic cells in response to treatment.

In contrast to tubulin, all TNTs have been reported to contain actin. Therefore, we assessed actin perturbing compounds with different working mechanisms for their ability to inhibit TNT signaling between BCP-ALL cells and MSCs (Table 1). Inhibitors of actin nucleation, actin polymerization and actin disassembly were all effective in disrupting TNT signaling. To increase our insight in how these mechanisms are intertwined, we investigated the effect of combining actin inhibitors of different classes. Simultaneous inhibition of actin polymerization (cytochalasin D) and actin nucleation (CK548) did not reveal a synergistic effect (Figure 7). This can be explained by the fact that actin nucleation is directly responsible for the initiation of actin polymerization and hence both inhibitors affect the same process. In contrast, simultaneous targeting of actin disassembly and actin nucleation or actin polymerization did affect TNT signaling more than would be expected if the effect was additive (Figure 7). These results show that TNT signaling is driven by the interplay of fundamental actin regulating processes in leukemic cells.

The actin cytoskeleton is often transformed in malignant cells[46-48], for example by deregulation of formins[49]. Consequently, actin inhibitors are being investigated as novel anti-cancer drugs[50,51]. Actin is present in all eukaryotic cells and hence might lead to toxicity of these compounds[52-54]. We observed that MNCs were relatively more resistant to actin inhibition than BCP-ALL cells, while primary MSCs and $CD34^+$ HPCs were also affected. Therefore, actin inhibitors should be used with caution. Likewise, tubulin inhibitors induce significant side-effects, like peripheral neuropathy[42], cardiovascular and thromboembolic events[43]. Nevertheless, it has been argued that tubulin inhibitors represent the most successful class of anti-cancer agents thus far, and they will likely remain important even as more selective drugs are developed[21,28,55]. Therefore, actin inhibitors might become an important novel class of anti-leukemic agents which induce cytotoxicity and disrupt the intercellular communication between leukemic cells and the bone marrow microenvironment.

ACKNOWLEDGEMENTS

We thank all members of the research laboratory Pediatric Oncology of the Erasmus MC for their help in processing leukemic and mesenchymal stromal cell samples. The Erasmus Optical Imaging Centre for providing support of CLSM; The Department of Immunology, especially J.G. te Marvelde, A.C. Bijkerk and V.H.J. van der Velden of the Erasmus MC for providing the use of Flow Cytometers; The Vlietland Ziekenhuis for collecting and providing cord blood. The work described in this paper was funded by the KiKa Foundation (Stichting Kinderen Kankervrij – Kika-39), the Dutch Cancer Society (UVA 2008; 4265, EMCR 2010; 4687), the Netherlands Organization for Scientific Research (NWO – VICI M.L. den Boer) and the Pediatric Oncology Foundation Rotterdam.

AUTHOR CONTRIBUTIONS

B. de Rooij and R. Polak designed the study, performed experiments, collected and analyzed all data, and wrote the paper. F. Stalpers performed experiments, collected and analyzed data. M.L. den Boer designed the study, analyzed data, and wrote the paper. R. Pieters analyzed data and wrote the paper. All authors discussed the results and approved the submitted manuscript.

CONFLICT OF INTEREST DISCLOSURE

The authors declare no competing financial interests.

REFERENCES

1. Fletcher DA, Mullins RD. Cell mechanics and the cytoskeleton. *Nature*. 2010;463(7280):485-492.

2. Rustom A, Saffrich R, Markovic I, Walther P, Gerdes HH. Nanotubular highways for intercellular organelle transport. *S cience*. 2004;303(5660):1007-1010.

3. Sowinski S, Jolly C, Berninghausen O, et al. Membrane nanotubes physically connect T cells over long distances presenting a novel route for HIV-1 transmission. *Nat Cell Biol*. 2008;10(2):211-219.

4. Watkins SC, Salter RD. Functional connectivity between immune cells mediated by tunneling nanotubules. *Immunity*. 2005;23(3):309-318.

5. Arkwright PD, Luchetti F, Tour J, et al. Fas stimulation of T lymphocytes promotes rapid intercellular exchange of death signals via membrane nanotubes. *Cell Res*. 2010;20(1):72-88.

6. Pasquier J, Galas L, Boulange-Lecomte C, et al. Different modalities of intercellular membrane exchanges mediate cell-to-cell p-glycoprotein transfers in MCF-7 breast cancer cells. *J Biol Chem*. 2012;287(10):7374-7387.

7. Rainy N, Chetrit D, Rouger V, et al. H-Ras transfers from B to T cells via tunneling nanotubes. *Cell Death Dis*. 2013;4:e726.

8. Chinnery HR, Pearlman E, McMenamin PG. Cutting edge: Membrane nanotubes in vivo: a feature of MHC class II+ cells in the mouse cornea. *J Immunol*. 2008;180(9):5779-5783.

9. Marzo L, Gousset K, Zurzolo C. Multifaceted roles of tunneling nanotubes in intercellular communication. *Front Physiol*. 2012;3:72.

10. Seyed-Razavi Y, Hickey MJ, Kuffova L, McMenamin PG, Chinnery HR. Membrane nanotubes in myeloid cells in the adult mouse cornea represent a novel mode of immune cell interaction. *Immunol Cell Biol*. 2013;91(1):89-95.

11. Pasquier J, Guerrouahen BS, Al Thawadi H, et al. Preferential transfer of mitochondria from endothelial to cancer cells through tunneling nanotubes modulates chemoresistance. *J Transl Med*. 2013;11:94.

12. Lou E, Fujisawa S, Morozov A, et al. Tunneling nanotubes provide a unique conduit for intercellular transfer of cellular contents in human malignant pleural mesothelioma. *PLoS One*. 2012;7(3):e33093.

13. Polak R, de Rooij B, Pieters R, den Boer ML. B-cell precursor acute lymphoblastic leukemia cells use tunneling nanotubes to orchestrate their microenvironment. *Blood*. 2015;126(21):2404-2414.

14. Osswald M, Jung E, Sahm F, et al. Brain tumour cells interconnect to a functional and resistant network. *Nature*. 2015;528(7580):93-98.

15. Antanaviciute I, Rysevaite K, Liutkevicius V, et al. Long-distance communication between laryngeal carcinoma cells. *PLoS One*. 2014;9(6):e99196.

16. Den Boer ML, Harms DO, Pieters R, et al. Patient stratification based on prednisolone-vincristine-asparaginase resistance profiles in children with acute lymphoblastic leukemia. *J Clin Oncol*. 2003;21(17):3262-3268.

17. van den Berk LC, van der Veer A, Willemse ME, et al. Disturbed CXCR4/CXCL12 axis in paediatric precursor B-cell acute lymphoblastic leukaemia. *Br J Haematol*. 2014;166(2):240-249.

18. Sowinski S, Alakoskela JM, Jolly C, Davis DM. Optimized methods for imaging membrane nanotubes between T cells and trafficking of HIV-1. *Methods*. 2011;53(1):27-33.

19. Schindelin J, Arganda-Carreras I, Frise E, et al. Fiji: an open-source platform for biological-image analysis. *Nat Methods*. 2012;9(7):676-682.

20. Schiff PB, Horwitz SB. Taxol stabilizes microtubules in mouse fibroblast cells. *Proc Natl Acad Sci U S A*. 1980;77(3):1561-1565.

21. Jordan MA, Wilson L. Microtubules as a target for anticancer drugs. *Nat Rev Cancer*. 2004;4(4):253-265.

22. Samson F, Donoso JA, Heller-Bettinger I, Watson D, Himes RH. Nocodazole action on tubulin assembly, axonal ultrastructure and fast axoplasmic transport. *J Pharmacol Exp Ther*. 1979;208(3):411-417.

23. Banerjee AC, Bhattacharyya B. Colcemid and colchicine binding to tubulin. Similarity and dissimilarity. *FEBS Lett*. 1979;99(2):333-336.

24. Bubb MR, Spector I, Bershadsky AD, Korn ED. Swinholide A is a microfilament disrupting marine toxin that stabilizes actin dimers and severs actin filaments. *J Biol Chem*. 1995;270(8):3463-3466.

25. Hori M, Saito S, Shin YZ, Ozaki H, Fusetani N, Karaki H. Mycalolide-B, a novel and specific inhibitor of actomyosin ATPase isolated from marine sponge. *FEBS Lett*. 1993;322(2):151-154.

26. Saito S, Watabe S, Ozaki H, Fusetani N, Karaki H. Mycalolide B, a novel actin depolymerizing agent. *J Biol Chem*. 1994;269(47):29710-29714.

27. Morton WM, Ayscough KR, McLaughlin PJ. Latrunculin alters the actin-monomer subunit interface to prevent polymerization. *Nat Cell Biol*. 2000;2(6):376-378.

28. Jordan MA, Wilson L. Microtubules and actin filaments: dynamic targets for cancer chemotherapy. *Curr Opin Cell Biol*. 1998;10(1):123-130.

29. Sorensen PM, Iacob RE, Fritzsche M, et al. The natural product cucurbitacin E inhibits depolymerization of actin filaments. *ACS Chem Biol*. 2012;7(9):1502-1508.

30. Bubb MR, Senderowicz AM, Sausville EA, Duncan KL, Korn ED. Jasplakinolide, a cytotoxic natural product, induces actin polymerization and competitively inhibits the binding of phalloidin to F-actin. *J Biol Chem*. 1994;269(21):14869-14871.

31. Bubb MR, Spector I, Beyer BB, Fosen KM. Effects of jasplakinolide on the kinetics of actin polymerization. An explanation for certain in vivo observations. *J Biol Chem*. 2000;275(7):5163-5170.

32. Surviladze Z, Waller A, Strouse JJ, et al. A Potent and Selective Inhibitor of Cdc42 GTPase. 2010.

33. Guerriero CJ, Weisz OA. N-WASP inhibitor wiskostatin nonselectively perturbs membrane transport by decreasing cellular ATP levels. *Am J Physiol Cell Physiol*. 2007;292(4):C1562-1566.

34. Kovacs M, Toth J, Hetenyi C, Malnasi-Csizmadia A, Sellers JR. Mechanism of blebbistatin inhibition of myosin II. *J Biol Chem*. 2004;279(34):35557-35563.

35. Liu K, Ji K, Guo L, et al. Mesenchymal stem cells rescue injured endothelial cells in an in vitro ischemia-reperfusion model via tunneling nanotube like structure-mediated mitochondrial transfer. *Microvasc Res*. 2014;92:10-18.

36. Luchetti F, Canonico B, Arcangeletti M, et al. Fas signalling promotes intercellular communication in T cells. *PLoS One*. 2012;7(4):e35766.

37. Takahashi A, Kukita A, Li YJ, et al. Tunneling nanotube formation is essential for the regulation of osteoclastogenesis. *J Cell Biochem*. 2013;114(6):1238-1247.

38. Osteikoetxea-Molnar A, Szabo-Meleg E, Toth EA, et al. The growth determinants and transport properties of tunneling

nanotube networks between B lymphocytes. *Cell Mol Life Sci*. 2016.

39. Astanina K, Koch M, Jungst C, Zumbusch A, Kiemer AK. Lipid droplets as a novel cargo of tunnelling nanotubes in endothelial cells. *Sci Rep*. 2015;5:11453.

40. Rizvi SA, Neidt EM, Cui J, et al. Identification and characterization of a small molecule inhibitor of formin-mediated actin assembly. *Chem Biol*. 2009;16(11):1158-1168.

41. Nolen BJ, Tomasevic N, Russell A, et al. Characterization of two classes of small molecule inhibitors of Arp2/3 complex. *Nature*. 2009;460(7258):1031-1034.

42. Wienecke A, Bacher G. Indibulin, a novel microtubule inhibitor, discriminates between mature neuronal and nonneuronal tubulin. *Cancer Res*. 2009;69(1):171-177.

43. Lu Y, Chen J, Xiao M, Li W, Miller DD. An overview of tubulin inhibitors that interact with the colchicine binding site. *Pharm Res*. 2012;29(11):2943-2971.

44. Hase K, Kimura S, Takatsu H, et al. M-Sec promotes membrane nanotube formation by interacting with Ral and the exocyst complex. *Nat Cell Biol*. 2009;11(12):1427-1432.

45. Wang Y, Cui J, Sun X, Zhang Y. Tunneling-nanotube development in astrocytes depends on p53 activation. *Cell Death Differ*. 2011;18(4):732-742.

46. Stevenson RP, Veltman D, Machesky LM. Actin-bundling proteins in cancer progression at a glance. *J Cell Sci*. 2012;125(Pt 5):1073-1079.

47. Rao JY, Hemstreet GP, 3rd, Hurst RE, Bonner RB, Min KW, Jones PL. Cellular F-actin levels as a marker for cellular transformation: correlation with bladder cancer risk. *Cancer Res*. 1991;51(11):2762-2767.

48. Heng YW, Koh CG. Actin cytoskeleton dynamics and the cell division cycle. *Int J Biochem Cell Biol*. 2010;42(10):1622-1633.

49. Sahai E. Mechanisms of cancer cell invasion. *Curr Opin Genet Dev*. 2005;15(1):87-96.

50. Foerster F, Braig S, Moser C, et al. Targeting the actin cytoskeleton: selective antitumor action via trapping PKCvarepsilon. *Cell Death Dis*. 2014;5:e1398.

51. Stournaras C, Stiakaki E, Koukouritaki SB, et al. Altered actin polymerization dynamics in various malignant cell types: evidence for differential sensitivity to cytochalasin B. *Biochem Pharmacol*. 1996;52(9):1339-1346.

52. Trendowski M, Wong V, Wellington K, Hatfield S, Fondy TP. Tolerated doses in zebrafish of cytochalasins and jasplakinolide for comparison with tolerated doses in mice in the evaluation of pre-clinical activity of microfilament-directed agents in tumor model systems in vivo. *In Vivo*. 2014;28(6):1021-1031.

53. Sierra-Paredes G, Oreiro-Garcia T, Nunez-Rodriguez A, Vazquez-Lopez A, Sierra-Marcuno G. Seizures induced by in vivo latrunculin a and jasplakinolide microperfusion in the rat hippocampus. *J Mol Neurosci*. 2006;28(2):151-160.

54. Tian B, Kiland JA, Kaufman PL. Effects of the marine macrolides swinholide A and jasplakinolide on outflow facility in monkeys. *Invest Ophthalmol Vis Sci*. 2001;42(13):3187-3192.

55. Giannakakou P, Sackett D, Fojo T. Tubulin/microtubules: still a promising target for new chemotherapeutic agents. *J Natl Cancer Inst*. 2000;92(3):182-183.

SUPPLEMENTAL FIGURES

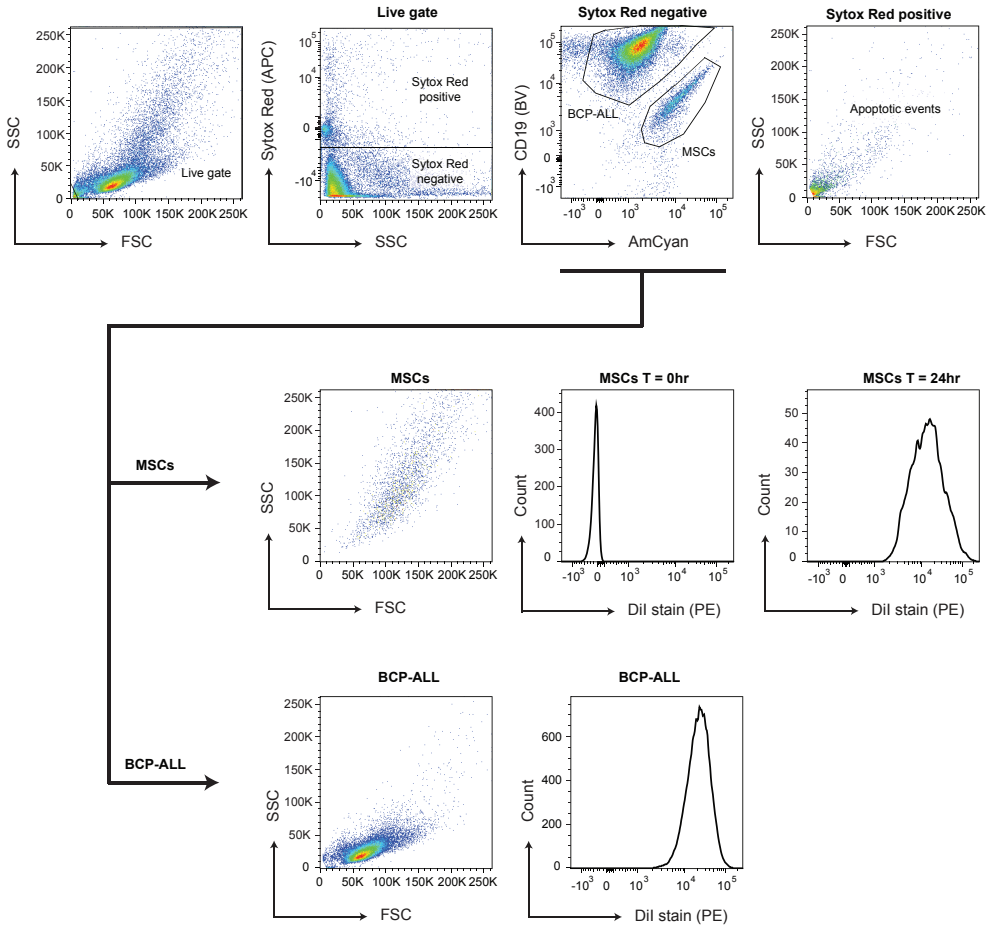

Supplemental Figure 1. Gating strategy to measure dye transfer from BCP-ALL toward MSCs. Flow cytometric gating strategy used to study TNT signaling from BCP-ALL cells toward MSCs. Co-cultures of CD19-positive leukemic cells and CD19-negative MSCs were stained with Sytox Red and Brilliant Violet 421 anti-human CD19 antibody. Sytox Red-positive events (apoptotic events) were excluded and CD19 positivity was evaluated to distinguish BCP-ALL cells and MSCs. At the start of each experiment, MSCs were confirmed to be negative for DiI and NALM6 cells were confirmed to be positive for DiI using the PE-channel. At the end of the experiment, median intensity of viable MSCs for the PE-channel was used as a measure of dye transfer.

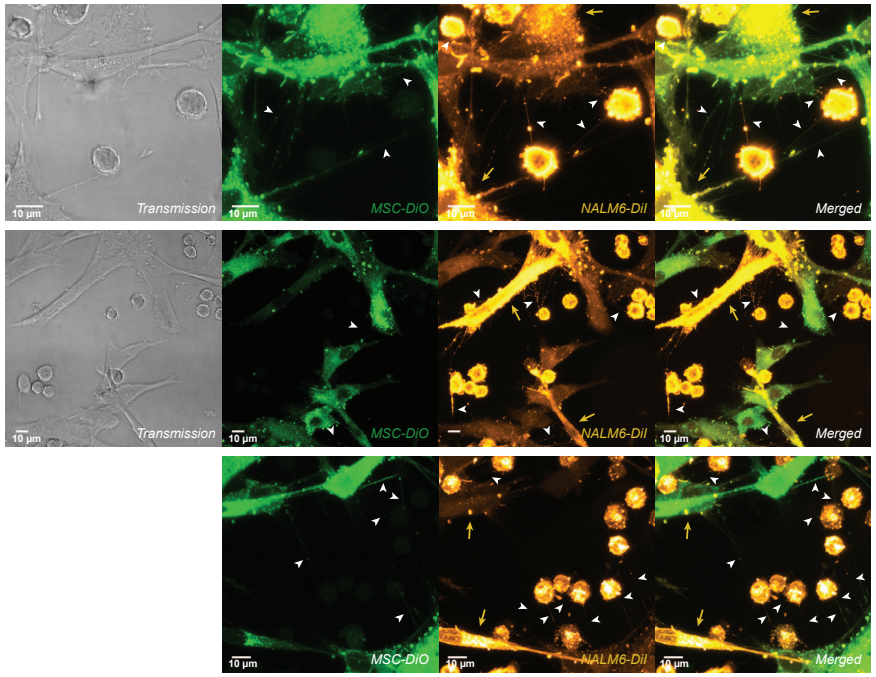

Supplemental Figure 2. Tunneling nanotube formation between BCP-ALL cells and MSCs. Confocal images (Z-stack) showing TNT networks (white arrowheads) between BCP-ALL cell line NALM6 (DiI, yellow) and primary MSCs (DiO, green) after co-culture for 3 hours. Lipophilic dye transfer toward MCSs via TNTs was observed (yellow dye in green MSCs). See also supplemental Video 1A-D and supplemental Video 2A-D.

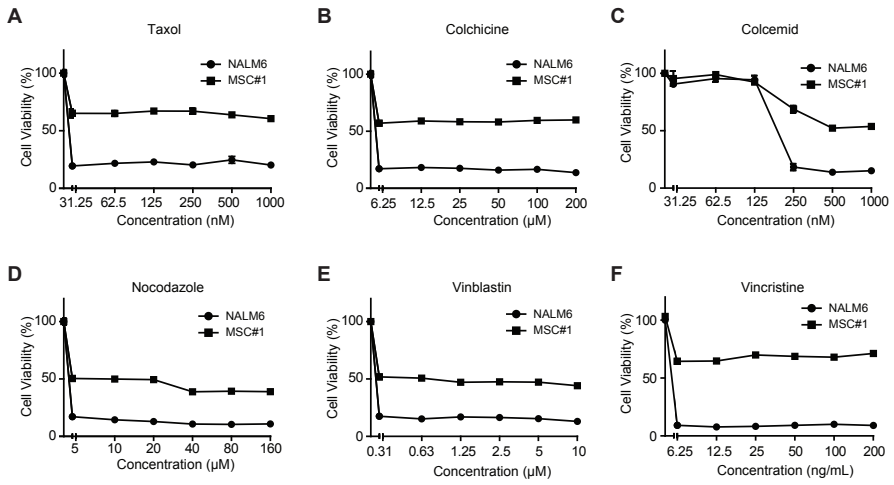

Supplemental Figure 3. Tubulin inhibition decreases cell viability of NALM6 cells and MSCs. (A) Graph showing the effect of tubulin inhibitor Taxol on cell viability of NALM6 cells and MSCs. (B) Same as (A) for colchicine. (C) Same as (A) for colcemid. (D) Same as (A) for nocodazole. (E) Same as (A) for vinblastine. (F) Same as (A) for vincristine.

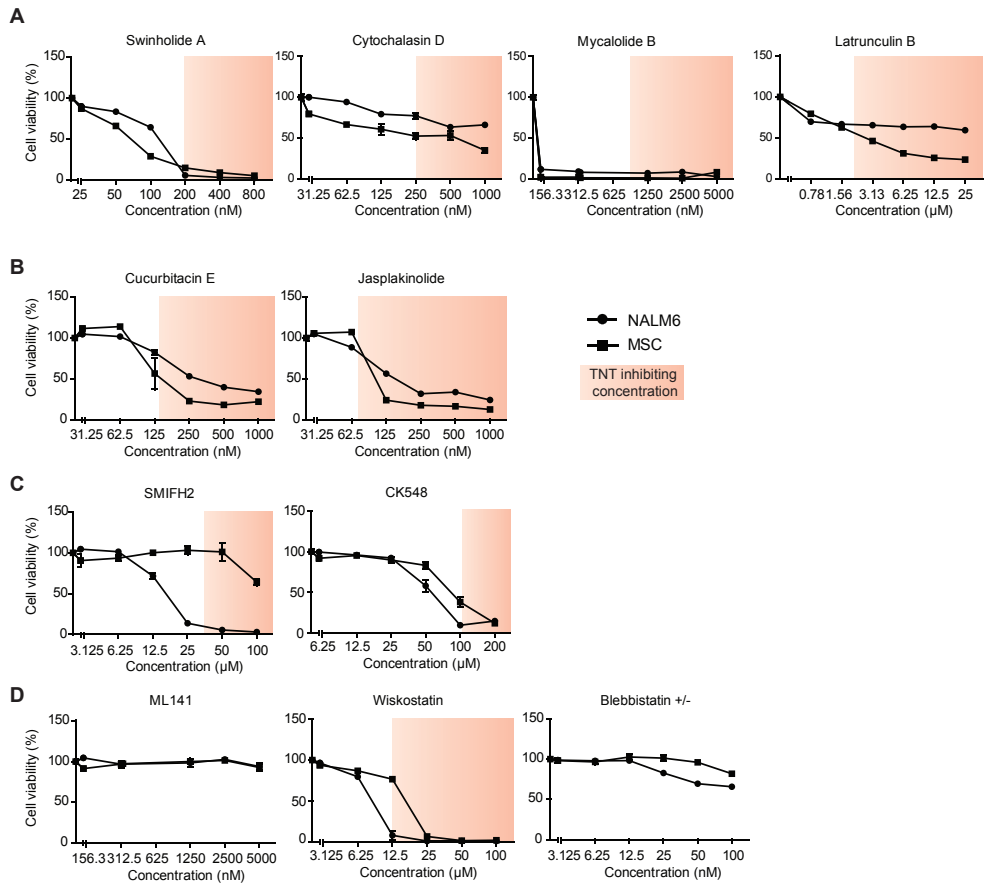

Supplemental Figure 4. Actin inhibition decreases cell viability of NALM6 cells and MSCs. (A) Graphs showing the effect of actin polymerization inhibitors swinholide A, cytochalasin D, mycalolide B or latrunculin B on cell viability of NALM6 cells and MSCs. The red area represents concentrations at which TNT signaling is inhibited. (B) Same as (A) for actin disassembly inhibitors cucurbitacin E and jasplakinolide. (C) Same as (A) for actin nucleation inhibitors SMIFH2 and CK548. (D) Same as (A) for actin rearrangement inhibitors ML141, wiskostatin, and (±)-blebbistatin.

Chapter 4

TUNNELING NANOTUBES FACILITATE AUTOPHAGOSOME TRANSFER IN THE LEUKEMIC NICHE

Bob de Rooij, Roel Polak, Femke Stalpers,
Rob Pieters & Monique L. den Boer

Accepted as Letter to the Editor in Leukemia

ABSTRACT

Acute lymphoblastic leukemia (ALL) cells create a leukemic niche with mesenchymal stromal cells (MSCs). Cytoskeletal structures called tunneling nanotubes (TNTs) facilitate communication between ALL cells and MSCs by transporting molecules and inducing the secretion of pro-survival cytokines. The identity of the molecules driving these malignant processes are currently unknown. Here we investigate which structures are transported from ALL cells toward MSCs by quantifying the transfer of ectopically expressed fluorescent marker proteins using flow cytometry. Our results indicate that actin, endoplasmatic reticulum, ICAM1, autophagosomes, mitochondria, and endosomes are contact-dependently transferred from leukemic cells toward MSCs. Transfer of mitochondria, adhesion molecule ICAM1, and autophagosomes were significantly reduced (≤ 9.6-fold) when TNT signaling was inhibited. Autophagosomes and mitochondria are known inducers of cytokine signaling and hence their transfer might unveil an important mechanism that ALL cells use to affect their microenvironment. Importantly, transfer of autophagosomes was 3.0-fold greater than the other molecules tested in ALL-MSC co-cultures, and has not been previously associated with TNT signaling. These data provide insight into intercellular signaling in the leukemic niche and implicate autophagosomes as novel TNT cargo.

Authors declare that there are no competing financial interests in relation to the work described.

Acute lymphoblastic leukemia (ALL) cells disrupt the healthy bone marrow microenvironment to create a leukemic niche that is crucial for facilitating leukemogenesis and protects leukemic cells from chemotherapeutic agents and immune cells[1, 2]. However, the functional mechanisms that regulate this malignant process are largely unknown. Recently, we showed that tunneling nanotubes (TNTs) play an important role in the communication between leukemic cells and bone-marrow derived mesenchymal stromal cells (MSCs)[3, 4]. TNTs are thin membrane protrusions that are driven by the actin cytoskeleton[5]. We recently showed that ALL cells use TNTs to signal toward MSCs and subsequently induce the secretion of pro-survival cytokines, leukemic cell survival and drug resistance[4]. B-cell precursor ALL (BCP-ALL) cells and MSCs exchange lipophilic molecules using TNTs[4]. However, the identity of the transported cargo needs further elucidation. In this study, we describe that autophagosomes, mitochondria and the transmembrane protein ICAM1 are transferred from B-cell precursor ALL (BCP-ALL) cells toward MSCs in a TNT-dependent manner.

To identify which structures are transferred from leukemic cells to MSCs via TNTs, we ectopically (i.e. non-endogenously) expressed fluorescently tagged proteins that mark specific cellular structures in BCP-ALL cells (NALM6) using lentiviral vectors (Figure 1A and supplemental Figure 1). After lentiviral transduction, we obtained stable BCP-ALL cell clones expressing turbo RFP (tRFP)-tagged marker proteins. The tRFP-positive BCP-ALL cells were stained with a nucleus specific dye (NucBlue), after which specific subcellular localization of fluorescent marker proteins was confirmed by confocal microscopy (Figure 1B). For example, CALR, which marks the endoplasmatic reticulum (ER), was expressed at the nuclear border (Figure 1B second panel from the top).

Next, we co-cultured tRFP-marker protein expressing BCP-ALL cells with tRFP-negative MSCs (Figure 1C) and quantified the transfer of tRFP by flow cytometry (Figure 1D). The B-cell marker CD19 was used to distinguish between BCP-ALL cells and MSCs (Figure 1D, second panel). Actin, ER, cytoplasm, ICAM1, autophagosomes, mitochondria, and early/late/recycle endosomes were transferred from BCP-ALL cells to MSCs, since MSCs became increasingly positive for tRFP signal after co-culture with tRFP-tagged leukemic clones for 24, 48, and 72 hours (Figure 2A). To exclude that tRFP transfer was nonspecific, we plotted the intensity of tRFP in BCP-ALL cells, that differed 6.9-fold between the brightest and dimmest clone (cytoplasm versus ER; supplemental Figure 2), against the intensity of tRFP in MSCs after co-culture for 48 hours (Figure 2B). No correlation was found between the amount of transfer and the intensity of the tRFP signal in the leukemic clone from which the tRFP-tagged molecule originated (Figure 2B; $p = 0.48$, Pearson correlation test), showing that the observed transfer is not explained by nonspecific leakage of tRFP label. This implies that tRFP transfer from BCP-ALL cells toward MSCs is representative for transfer of tagged cellular structures. Autophagosomes appeared to be the most highly transported structure from BCP-ALL cells to MSCs (3.0-fold more than other proteins after 48 hours; Figure 2C). To assess the contribution of TNTs to the transfer of cellular structures, we performed ALL-MSC co-cultures in the absence or

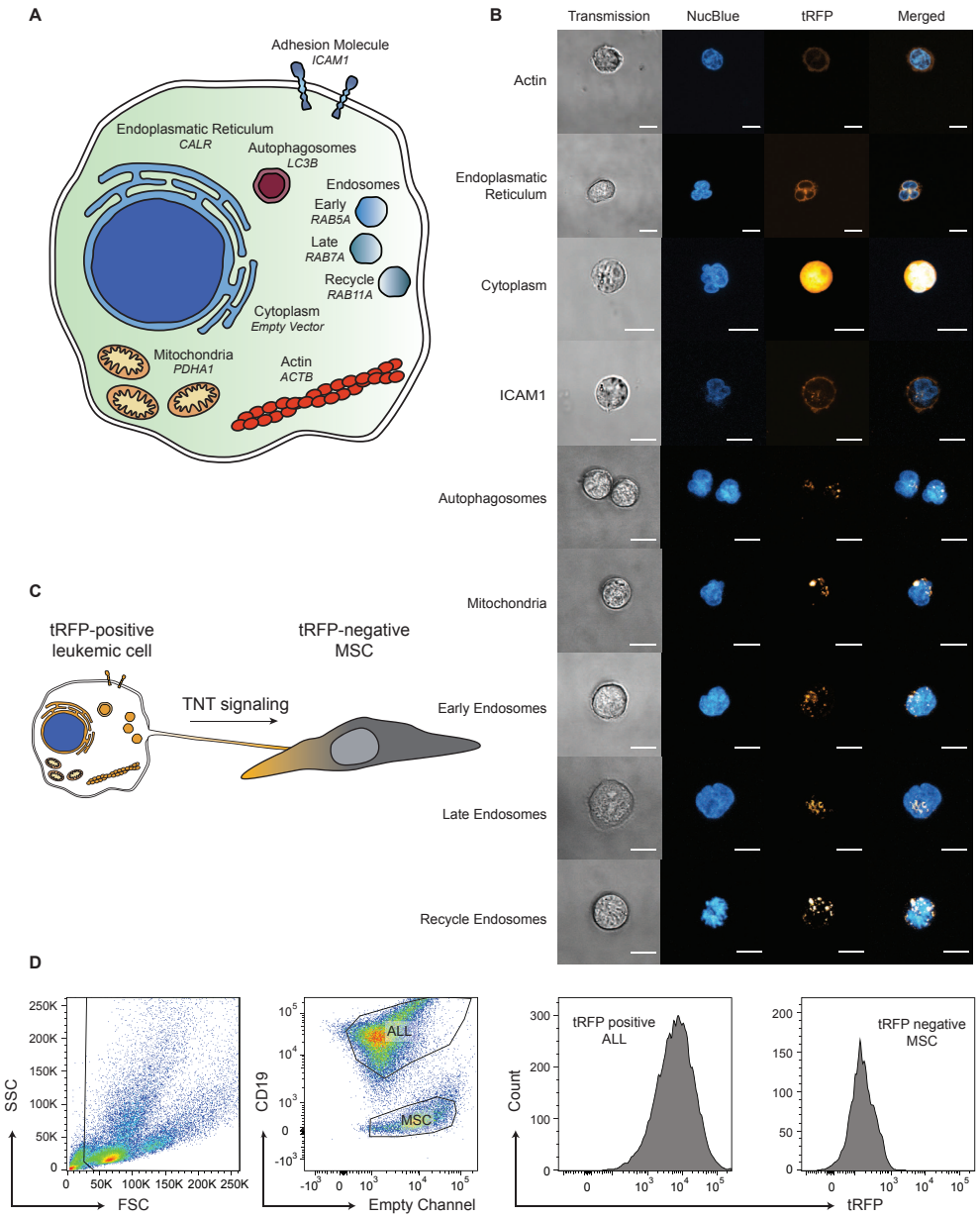

Figure 1. Identifying TNT cargo using fluorescently tagged proteins. (A) Schematic overview of ectopically expressed marker proteins that were used to visualize specific cellular structures in BCP-ALL cells (NALM6). (B) Representative confocal images showing the subcellular localization of tRFP-positive marker proteins relative to the nucleus in live NALM6 cells. A transmission image is provided to show the shape of the leukemic cell (left panel). (C) Experimental setup for visualizing protein transfer from BCP-ALL cells toward MSCs. Leukemic clones that express tRFP-positive marker proteins were co-cultured with tRFP-negative MSCs and transfer of protein toward was quantified by flow cytometry. (D) Gating strategy that was used to quantify transfer of tRFP-positive marker protein from leukemic cells toward MSCs by flow cytometry. BCP-ALL cells and MSCs are gated

based on their forward and sideward scatter (first panel) and separated based on CD19 expression (second panel). Finally, the median tRFP signal in MSCs was quantified with the PE-channel and used as a measure of tRFP-positive marker protein transfer (last panel). See also supplemental Figure 1.

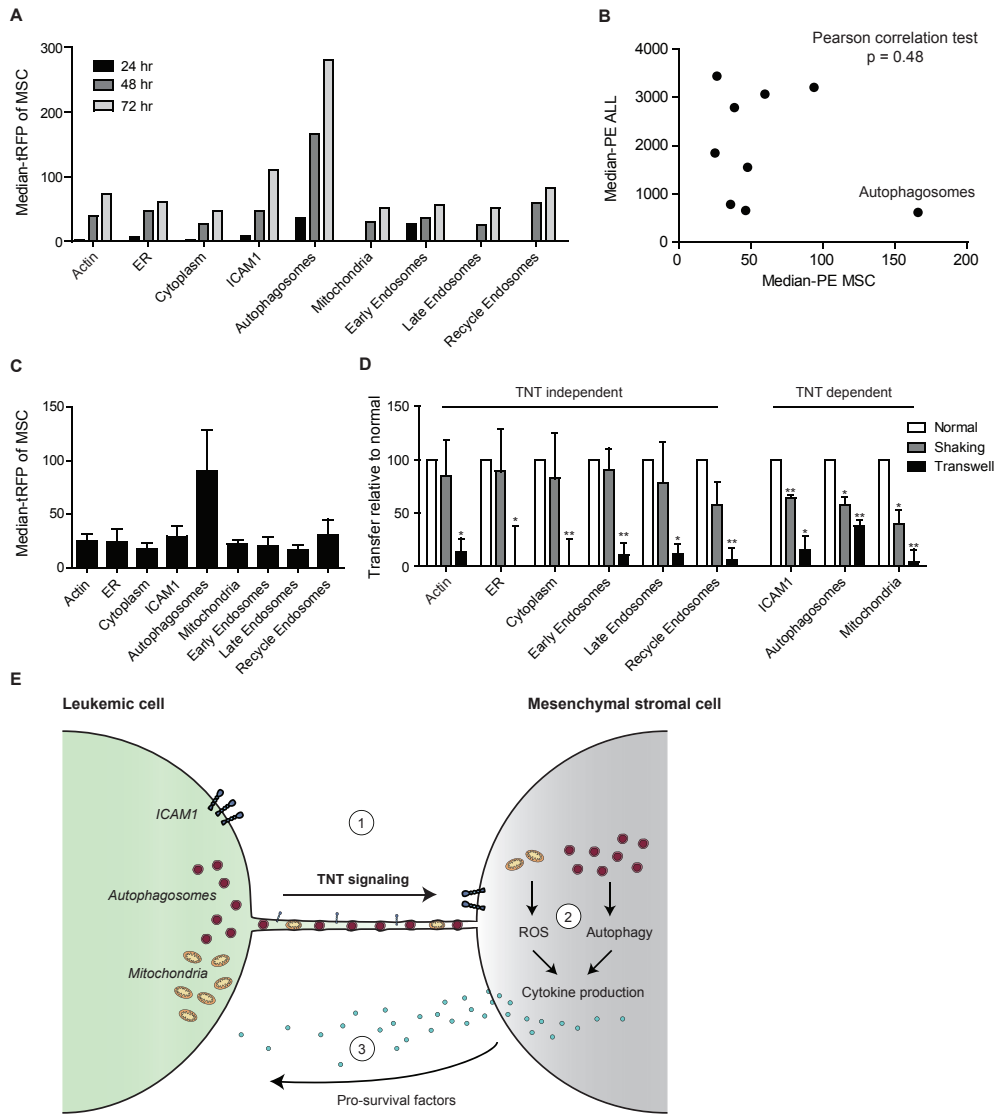

Figure 2. Autophagosomes, mitochondria and ICAM1 are transferred via tunneling nanotubes. (A) BCP-ALL cells expressing tRFP-markers were co-cultured with tRFP-negative MSCs for 24 (black bars), 48 (dark-grey bars), and 72 hours (light-grey bars). Median intensity of MSCs for tRFP is shown. (B) Graph showing the median tRFP intensity of MSCs (X-axis) compared to BCP-ALL tRFP intensity (Y-axis) after co-culture for 48 hours as depicted in Figure 2A. No correlation was found indicating that transfer of tRFP was protein specific (n = 3, p = 0.48, Pearson correlation test). (C) Graph showing the transfer of tRFP from BCP-ALL cells toward MSCs after 48 hours of co-culture

(n = 3). (D) Graph showing the transfer of tRFP from BCP-ALL cells toward MSCs after TNT inhibition (grey and black bars), compared to normal co-culture conditions (white bars; n = 3; one-tailed t-test, paired). (E) Model of TNT signaling in the leukemic niche: 1: Leukemic cells use TNT signaling to transfer autophagosomes, mitochondria and ICAM1 toward MSCs in their microenvironment. 2: Increased reactive oxygen species (ROS) and autophagy in MSCs induces the production of cytokines, 3: Supportive and nurturing factors are released into the tumor microenvironment, which induce survival and drug resistance in leukemic cells. Data are means ± SEM; * $p \leq 0.05$, ** $p \leq 0.01$. See also supplemental Figure 2.

presence of TNT inhibiting conditions for 48 hours. TNTs were inhibited by two established approaches in literature: mechanical disruption of TNTs through gentle shaking of cell cultures and physical separation of BCP-ALL cells and MSCs using a transwell system (3.0 µm pore size)[4, 6]. While actin inhibitors are often used to inhibit TNTs, their short half-time and high cytotoxicity prevented their use in these experiments[4]. Transfer of actin (ACTB), endoplasmatic reticulum (CALR), cytoplasmic content (Empty Vector), and endosome markers (RAB family) were inhibited by transwell conditions, but not by gentle shaking (Figure 2D). This implicates that transfer of these proteins is driven by cell-cell signaling modules other than TNTs. For example by gap junctional protein Cx43, which has been shown to be involved in transfer of extracellular vesicles[7]. Interestingly, transfer of transmembrane protein ICAM1, autophagosomes (LC3B), and mitochondria (PDHA1) were significantly inhibited by both TNT inhibiting conditions (shaking and transwell; $p < 0.05$, Figure 2D). Transmembrane proteins and mitochondria have previously been observed to be transferred via TNTs by other cell types[8, 9]. Our data show that this is also true for TNT signaling between BCP-ALL cells and MSCs. Strikingly, transfer of autophagosomes was 3.0-fold higher than ICAM1 and PDHA1 transfer (Figure 2C). To our knowledge, this is the first time that autophagosome transfer is observed between ALL cells and MSC in a TNT-dependent manner.

Autophagy is a process that degrades and recycles unwanted or damaged cellular components, like proteins and organelles[10]. This process has been implicated as an important regulator of both tumor-initiation and tumor-suppression[11]. Autophagy is driven by double-membraned vesicles known as autophagosomes, which are shaped through the actin cytoskeleton[12]. TNT formation is also dependent on actin[4, 5] and this co-dependence might be important for autophagosome transport through the TNT machinery. Interestingly, autophagy induction through starvation of cells has been shown to increase the formation of TNTs[13], suggesting a correlation between these processes. Recently, we observed that TNT signaling induces the secretion of pro-survival cytokines[4]. Autophagy is a known regulator of cytokine signaling and this process is influenced by mitochondrial reactive oxygen species and/or mitochondrial DNA[14].The transfer of mitochondria and autophagosomes from leukemic cells toward MSCs might therefore explain the release of supportive factors by the tumor microenvironment, as we recently reported elsewhere (Figure 2E)[4]. Interestingly, the transcription of ICAM1, a transmembrane protein involved in cell-cell adhesion, is known to be upregulated in response to cytokine signaling and reactive oxgen species[15]. Its transport toward MSCs may provide anchorage to facilitate TNT function.

In conclusion, these data show the potential of using fluorescently labeled marker proteins to characterize which cellular structures are transported by TNT signaling from ALL cells to MSCs. Our study confirmed several known TNT cargo (i.e. mitochondria and transmembrane proteins)[8, 9] and revealed novel structures (autophagosomes) that are transported through TNTs. The TNT-dependent transfer of autophagosomes and mitochondria from ALL cells toward MSCs might unveil an important mechanism that leukemic cells use to affect their microenvironment. Our study suggests that instead of upregulating autophagy in an indirect manner, leukemic cells transfer autophagosomes to MSCs in order to enhance autophagy-induced cytokine secretion. In addition, our study identifies autophagosomes, ICAM1 and mitochondria as important structures that are actively transported from leukemic cells toward their microenvironment via TNTs.

ACKNOWLEDGEMENTS

We thank all members of the research laboratory Pediatric Oncology of the Erasmus MC for their help in processing mesenchymal stromal cell samples, in particular F. Meijers-Stalpers; The Erasmus Optical Imaging Centre for providing support of CLSM, in particular G. Kremers; The work described in this paper was funded by the KiKa Foundation (Stichting Kinderen Kankervrij – Kika-39), the Dutch Cancer Society (UVA 2008; 4265, EMCR 2010; 4687), the Netherlands Organization for Scientific Research (NWO – VICI M.L. den Boer) and the Pediatric Oncology Foundation Rotterdam.

AUTHOR CONTRIBUTIONS

B. de Rooij and R. Polak designed the study, performed the experiments, collected and analyzed all data, and wrote the paper. F. Stalpers performed additional experiments. M.L. den Boer and R. Pieters analyzed data and wrote the paper. All authors discussed the results and approved the submitted manuscript.

4
AUTOPHAGOSOME TRANSFER VIA TNTS IN THE LEUKEMIC NICHE

REFERENCES

1. Colmone A, Amorim M, Pontier AL, Wang S, Jablonski E, Sipkins DA. Leukemic cells create bone marrow niches that disrupt the behavior of normal hematopoietic progenitor cells. *Science* 2008 Dec 19; 322(5909): 1861-1865.

2. Nakasone ES, Askautrud HA, Kees T, Park JH, Plaks V, Ewald AJ, *et al.* Imaging tumor-stroma interactions during chemotherapy reveals contributions of the microenvironment to resistance. *Cancer Cell* 2012 Apr 17; 21(4): 488-503.

3. Morrison SJ, Scadden DT. The bone marrow niche for haematopoietic stem cells. *Nature* 2014 Jan 16; 505(7483): 327-334.

4. Polak R, de Rooij B, Pieters R, den Boer ML. B-cell precursor acute lymphoblastic leukemia cells use tunneling nanotubes to orchestrate their microenvironment. *Blood* 2015 Nov 19; 126(21): 2404-2414.

5. Rustom A, Saffrich R, Markovic I, Walther P, Gerdes HH. Nanotubular highways for intercellular organelle transport. *Science* 2004 Feb 13; 303(5660): 1007-1010.

6. Sowinski S, Jolly C, Berninghausen O, Purbhoo MA, Chauveau A, Kohler K, *et al.* Membrane nanotubes physically connect T cells over long distances presenting a novel route for HIV-1 transmission. *Nat Cell Biol* 2008 Feb; 10(2): 211-219.

7. Soares AR, Martins-Marques T, Ribeiro-Rodrigues T, Ferreira JV, Catarino S, Pinho MJ, *et al.* Gap junctional protein Cx43 is involved in the communication between extracellular vesicles and mammalian cells. *Sci Rep* 2015; 5: 13243.

8. Wang X, Gerdes HH. Transfer of mitochondria via tunneling nanotubes rescues apoptotic PC12 cells. *Cell Death Differ* 2015 Jul; 22(7): 1181-1191.

9. Rainy N, Chetrit D, Rouger V, Vernitsky H, Rechavi O, Marguet D, *et al.* H-Ras transfers from B to T cells via tunneling nanotubes. *Cell Death Dis* 2013; 4: e726.

10. Mizushima N, Komatsu M. Autophagy: renovation of cells and tissues. *Cell* 2011 Nov 11; 147(4): 728-741.

11. Mathew R, Karantza-Wadsworth V, White E. Role of autophagy in cancer. *Nat Rev Cancer* 2007 Dec; 7(12): 961-967.

12. Mi N, Chen Y, Wang S, Chen M, Zhao M, Yang G, *et al.* CapZ regulates autophagosomal membrane shaping by promoting actin assembly inside the isolation membrane. *Nat Cell Biol* 2015 Sep; 17(9): 1112-1123.

13. Lou E, Fujisawa S, Morozov A, Barlas A, Romin Y, Dogan Y, *et al.* Tunneling nanotubes provide a unique conduit for intercellular transfer of cellular contents in human malignant pleural mesothelioma. *PLoS One* 2012; 7(3): e33093.

14. Harris J. Autophagy and cytokines. *Cytokine* 2011 Nov; 56(2): 140-144.

15. Hubbard AK, Rothlein R. Intercellular adhesion molecule-1 (ICAM-1) expression and cell signaling cascades. *Free Radic Biol Med* 2000 May 1; 28(9): 1379-1386.

SUPPLEMENTAL DATA

METHODS

Cell lines

BCP-ALL cell line NALM6 (B-Other) and human embryonic kidney cell line HEK293T were obtained from DSMZ (Braunschweig, Germany), used at low cell passages, and routinely verified by DNA fingerprinting.

Isolation and characterization of MSCs

Mesenchymal stromal cells (MSCs) were isolated from bone-marrow aspirates and characterized as previously described[13,17]. In short, MSCs were confirmed to have multilineage potential for adipocyte, osteocyte and chondrocyte differentiation and characterized using positive (CD44/ CD90/CD105/CD54/CD73/CD146/CD166/STRO-1) and negative surface markers (CD19/CD45/CD34).

Leukemic clones containing fluorescent cellular markers

HEK293T cells were transfected with lentiviral vectors coding for tRFP-positive marker proteins (Cellpainter™ Organelle Markers; Origene, USA), together with the helper plasmids VSVG and pPAX, using X-tremegene 9 (Sigma-Aldrich; Saint Louis, USA). Turbo-RFP (tRFP) was added either C- or N-terminally to the marker proteins, to minimize its influence on protein structure (supplemental Figure 1). Lentiviral particles produced by the HEK293T cells were collected by harvesting supernatant for three consecutive days and purified using a 0.45 µm cellulose acetate filter (GE Healthcare Life Sciences, Buckinghamshire, United Kingdom) and ultra-centrifugation (32.000 rounds per minute (RPM) for 2 hours at room temperature).

BCP-ALL cells (NALM6) were transduced with a serial dilution of lentivirus to ensure optimal cell viability and virus transduction. Subsequently, BCP-ALL cells were centrifuged at 1800 RPM for 45 minutes at room temperature and incubated overnight. Afterwards, single cells were plated out and positive leukemic clones were selected based on tRFP positivity using a MACSQuant analyzer (Miltenyi Biotec, Gladbach Germany). The proliferation capacity of leukemic clones was confirmed to be unaffected compared to wildtype cells, by prolonged cell culture.

Confocal laser scanning microscopy

Leukemic clones expressing tRFP-positive marker proteins were visualized using a confocal laser scanning microscope (Leica SP5). The nucleus of leukemic cells was stained using live cell stain "Nucblue", according to the manufacturer's protocol (Life Technologies, Breda, The Netherlands). Cells were imaged without fixation to retain optimal tRFP signal. Confocal images were acquired using sequential scanning of different channels at a resolution of 1024 x 1024 pixels in the x ^{x} y plane and 0.15 µm steps in z-direction. Nucblue and tRFP-positive marker proteins were excited with a 405-nm ultraviolet laser

and a 561-nm Diode-Pumped Solid-State laser, respectively. Image processing was done with Fiji software[19].

Transfer of tRFP protein markers

tRFP-positive BCP-ALL cells (NALM6) were co-cultured with tRFP-negative MSCs in a 4:1 ratio for 24, 48 or 72 hours with and without TNT inhibition. TNTs were inhibited by mechanical disruption via gentle shaking of cell cultures (250 RPM), or by physical separation of leukemic cells (cultured in a 3.0 µm pore-sized insert) and MSCs (cultured in the bottom compartment of a transwell system; Corning, New York, USA). BCP-ALL cells and MSCs were separated using Brilliant Violet 421 labeled anti-human CD19 antibody (Biolegend, San Diego, USA). Median intensity of MSCs for the PE-channel was used as a measure of tRFP protein transfer and was determined using flow cytometry (BD Biosciences, California, USA; see Figure 1D for gating strategy).

Statistical analysis

Student's t-test was used as a statistical test and a Student's paired t-test was used when applicable (indicated in figure legends). Pearson correlation testing was used to compare the median tRFP intensity of MSCs and BCP-ALL cells after co-culture. Error bars show as standard error of the mean (SEM). Sample size and statistical test methods are reported in the figure legends. Variance between groups that are statistically compared is similar.

SUPPLEMENTAL FIGURES

A

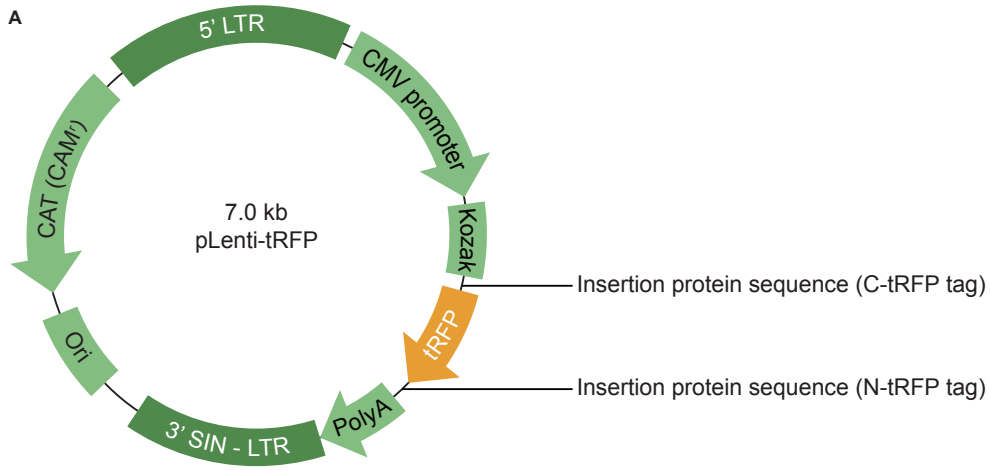

B

Marker protein	Cellular structure	GENENAME	Base pairs	Tag
Actin, beta	Actin filaments	ACTB	1852 bp	N-tRFP tag
Calreticulin	Endoplasmatic reticulum	CALR	1929 bp	C-tRFP tag
Empty vector	-	-		C-tRFP tag
Intercellular adhesion molecule 1	Integrin signalling	ICAM1	3249 bp	C-tRFP tag
Microtubule-associated protein 1 light chain 3 beta	Autophagosomes	MAP1LC3B	2304 bp	N-tRFP tag
Pyruvate dehydrogenase alpha 1	Mitochondria	PDHA1	3390 bp	C-tRFP tag
RAB5A, member RAS oncogene family	Early endosome	RAB5A	2548 bp	N-tRFP tag
RAB7A, member RAS oncogene family	Late endosome	RAB7A	2240 bp	N-tRFP tag
RAB11A, member RAS oncogene family	Recycle endosome	RAB11A	4943 bp	N-tRFP tag

Supplemental Figure 1. Transduction of leukemic cells with lentiviral vectors encoding for specific cellular markers. (A) Schematic overview of the lentiviral vector backbone in which specific cellular marker proteins were cloned. Two insertion sites were used in order to position the tRFP tag C or N-terminally. (B) Overview of the marker proteins depicting which cellular structures they visualize, their gene name, their length in base pairs (bp), and the position of the tRFP tag.

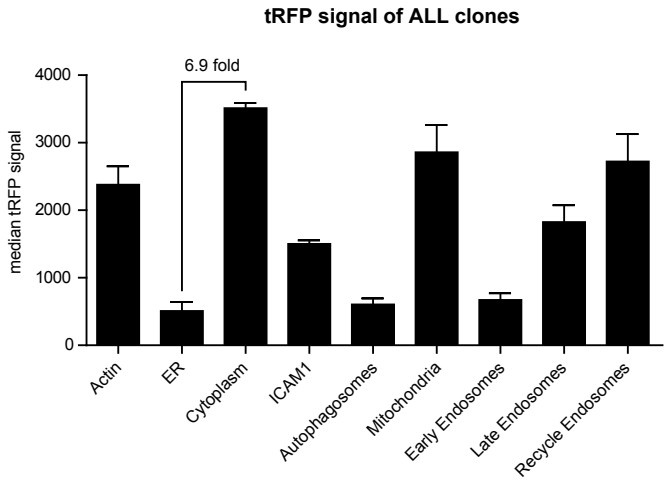

Supplemental Figure 2. tRFP positivity of BCP-ALL clones differs between markers. Graph showing the median tRFP intensity of tRFP-positive BCP-ALL cells for each cellular marker (n = 3). tRFP signal differs between clones and therefore transfer of tRFP protein from BCP-ALL cells toward MSCs should be corrected for the intensity of leukemic cells.

Chapter 5

ACUTE LYMPHOBLASTIC LEUKEMIA CELLS CREATE A LEUKEMIC NICHE WITHOUT AFFECTING THE CXCR4/CXCL12 AXIS

Bob de Rooij*, Roel Polak*, Lieke C.J. van den Berk,
Femke Stalpers, Rob Pieters & Monique L. den Boer

* Authors contributed equally

Minor revisions needed (Haematologica)

Acute lymphoblastic leukemia (ALL) is characterized by an outgrowth of malignant lymphoblasts that occupy the bone marrow microenvironment, where they reside with mesenchymal stromal cells (MSCs)[1]. Leukemic cells are able to disrupt the healthy microenvironment and create a leukemic niche that shelters malignant cells from elimination through cytostatic treatment and immune responses[2, 3]. Disrupting intercellular communication in this malignant microenvironment sensitizes leukemic cells to chemotherapeutic drugs[4]. Homing of ALL cells toward the bone marrow microenvironment is thought to be similar to that of hematopoietic stem cells (HSCs)[5]. Human $CD34^+$ progenitor cells, are attracted by stromal cell-derived factor 1 (SDF-1/CXCL12), a chemoattractant actively produced by MSCs in the bone marrow[5, 6]. CXCL12 binds to the CXCR4 receptor. Disturbance of the CXCR4/CXCL12 axis, by treatment with cytokines and/or CXCR4 antagonists, mobilizes HSCs to the peripheral blood[7], and shows promising pre-clinical results in AML patients[8]. Like HSCs, ALL cells have high CXCR4 surface expression and disruption of CXCR4/CXCL12 interaction reduces ALL engraftment in animal models[9, 10]. However, in mice suffering from ALL, CXCR4/CXCL12 inhibition as mono-treatment did not reduce the leukemic cell number in the bone marrow[9, 11]. In addition, CXCL12 expression was remarkably downregulated in murine bone marrow regions of extensive ALL growth[1]. Likewise, CXCL12 levels in the bone marrow of patients diagnosed with BCP-ALL were lower compared to those in the same patients at the time of remission and healthy controls[6]. This suggests that ALL cells use additional mechanisms to retain a protective microenvironment.

In this study, we used an *ex vivo* co-culture model in which we cultured B-cell precursor ALL (BCP-ALL) cells with bone marrow-derived primary MSCs. Several studies show that ALL cells home toward the bone marrow microenvironment in a CXCR4/CXCL12-dependent manner[1, 9, 10]. We confirmed these findings in our model by assessing the migration of GFP-positive BCP-ALL cells (NALM6) toward MSCs, using a transwell system. MSCs induced migration of BCP-ALL cells by 5-16 fold compared to medium controls ($p < 0.05$; Figure 1A and supplementary Figure 1A-B). The induction of migration was correlated with the level of CXCL12 produced by the primary MSCs (Figure 1B). Inhibition of the CXCR4/CXCL12 axis with AMD3100 significantly impaired migration of BCP-ALL cells toward MSCs (4.5-fold reduction, $p < 0.01$; Figure 1C).

Next, we hypothesized that BCP-ALL cells alter the chemoattractive properties of their microenvironment. To address this hypothesis, GFP-negative BCP-ALL cells (NALM6) were cultured with MSCs in the bottom compartment of a transwell system as a model of the leukemic niche. Migration of GFP-positive BCP-ALL cells (NALM6) from the upper to the bottom compartment was determined (supplementary Figure 1A-C). GFP-positive BCP-ALL cells migrated significantly more toward ALL-MSC co-cultures than toward MSCs in mono-culture (blue bars versus grey bars, $p < 0.01$; Figure 1D and supplementary Figure 1D-E). The leukemic niche induced migration of BCP-ALL cells by 2.2-fold (Figure 1E, $p < 0.001$). Surprisingly, CXCR4 inhibition by AMD3100 did not affect the preferential migration of BCP-ALL cells towards the leukemic niche (2.2-fold versus

2.5-fold, p = 0.52, Figure 1E and supplementary Figure 1F). In addition, we compared CXCL12 levels in the supernatant of mono- and co-cultures of primary BCP-ALL cells derived from 9 different BCP-ALL cases and 4 primary MSCs. CXCL12 levels were high in mono-cultures of MSCs, and below detection level in mono-cultures of primary BCP-ALL cells (supplementary Figure 2A-B). Co-culture of primary BCP-ALL cells and MSCs did not increase CXCL12 levels compared to the combined levels produced in both mono-

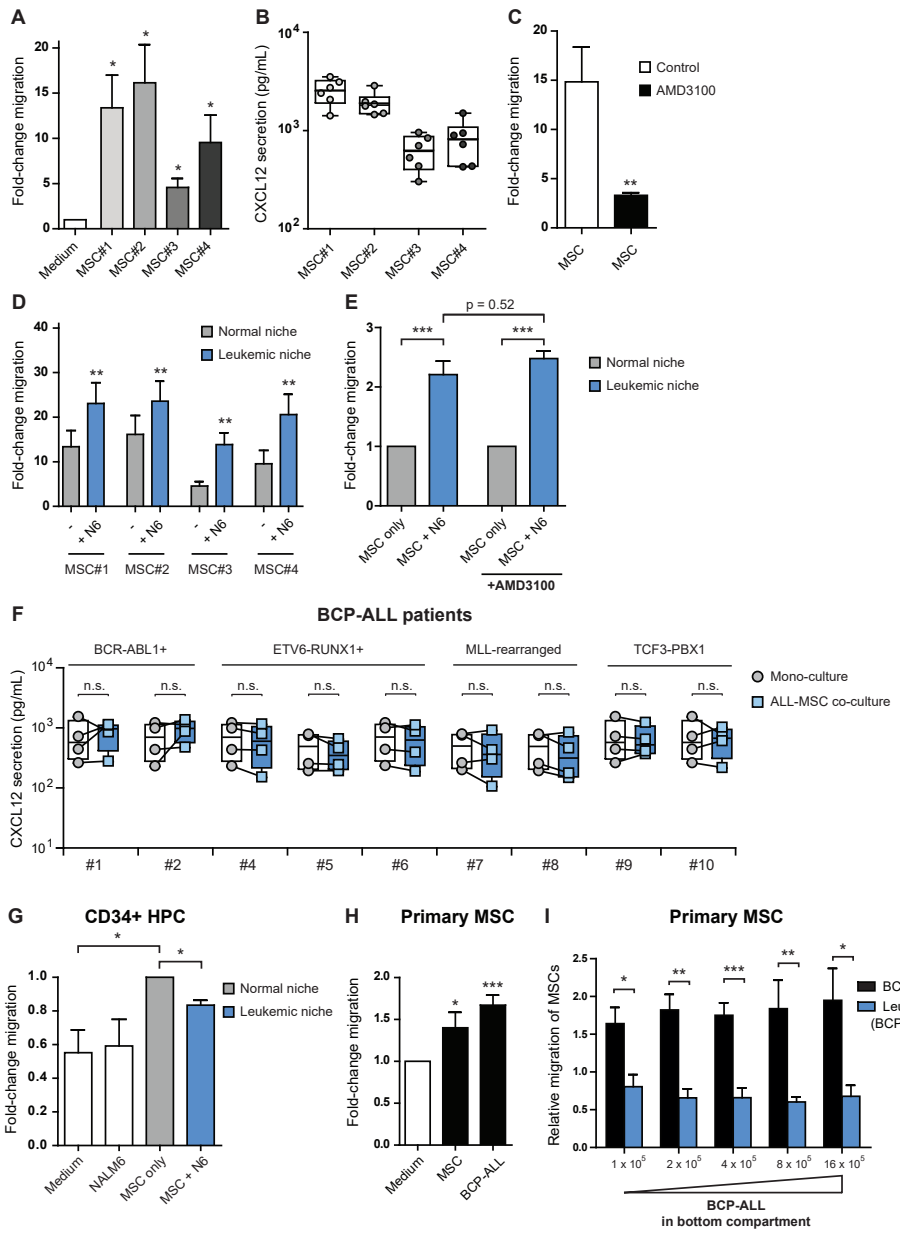

Figure 1. ALL-MSC co-cultures induce leukemic cell migration without affecting the CXCR4/CXCL12 axis. (**A**) Graph showing the fold-change in migration of GFP-positive BCP-ALL cells (NALM6) toward four distinct primary bone marrow-derived MSCs compared to background migration toward culture medium after 48 hours in a 3.0 µm transwell system (n = 5 for each MSC; one-tailed t-test, unpaired). We used MSCs derived from healthy controls (MSC#1 and MSC#2) and MSCs derived from leukemia patients at diagnosis (MSC#3 and MSC#4), see also supplementary Table 3. Migration towards culture medium was used to calculate the foldchange migration. (**B**) Graph showing the secretion of CXCL12 by primary MSCs as determined using a fluorescent bead-based immunoassay (n = 6 for each MSC). (**C**) Graph showing the effect of CXCR4 blockade with AMD3100 (10µM) on the migration of NALM6 cells toward primary MSCs after 48 hours in a 3.0 µm transwell system (n = 4; one-tailed t-test, paired). Migration towards culture medium was used to calculate the foldchange migration. For this experiment we combined the data of four distinct primary MSCs (MSC#1-4). (**D**) Graph showing the migration of NALM6 cells toward MSCs in mono-culture (normal niche, grey bars) or toward ALL-MSC co-cultures (leukemic niche, blue bars), after 48 hours in a 3.0 µm transwell system (n = 5 for each MSC; one-tailed t-test, paired). Migration towards culture medium was used to calculate the foldchange migration. Experiments were performed with MSCs from four different donors. (**E**) Graph showing that the leukemic niche affects the migration of BCP-ALL cells independent of CXCR4/CXCL12 signaling. Migration of NALM6 cells toward N6-MSC co-cultures (leukemic niche, blue bars) is compared to migration toward MSC mono-cultures (normal niche, grey bars) in absence or presence of AMD3100 (10 µM) after 48 hours using a 3.0 µm transwell system (n = 4; one-tailed t-test, paired). For this experiment we combined the data of four distinct primary MSCs (MSC#1-4). Data is shown as fold induction compared to migration towards MSC mono-culture. (**F**) Plots showing the secreted levels of CXCL12 by primary BCP-ALL cells and MSCs in mono-culture (circles represent the sum of cytokine secretion in mono-culture of BCP-ALL and mono-culture of MSC) compared to ALL-MSC co-culture (squares). Data was determined using a multiplexed fluorescent bead-based immunoassay. Boxes represent p25-p75 intervals. (**G**) Graph showing the migration of umbilical cord blood-derived healthy CD34$^+$ progenitor cells after 48 hours in a 3.0 µm transwell system. Bars represent migration toward culture medium, NALM6 cells, MSCs and NALM6-MSC cultures (n = 3; one-tailed t-test; paired). Migration towards MSC mono-culture was used to calculate the foldchange migration. Data are means ± SEM; * $p \leq 0.05$, HPC = hematopoietic progenitor cell. (**H-I**) Primary MSCs (experiments performed with MSC#1 and MSC#3) were allowed to migrate to the other side of a 8.0 µm transwell insert for 16 hours. Cells were fixed and subsequently stained with crystal violet. MSCs migrated toward a bottom compartment containing culture medium, MSCs or BCP-ALL cells (REH). The amount of migrated cells was measured by spectrophotometry of crystal violet stained cells. (**H**) Graph showing the migration of primary MSCs. Migration towards medium was used to calculate the foldchange migration (n = 4; one-tailed t-test; paired). (**I**) Graph showing the migration of primary MSCs toward REH cells (BCP-ALL, black bars) or REH-MSC co-cultures (leukemic niche, blue bars) (n = 4; one-tailed t-test, paired). Data are relative to control condition without BCP-ALL cells (medium-only or MSC-only control). Data are means ± SEM; * $p \leq 0.05$, ** $p \leq 0.01$, *** $p \leq 0.001$, N6 = NALM6. See also supplementary Figures 1-3.

cultures (Figure 1F). These results suggest that BC-PALL cells create a leukemic niche that attracts leukemic cells in a CXCR4/CXCL12 independent manner.

Next, we assessed the migration of healthy CD34$^+$ hematopoietic progenitor cells (HPCs) toward primary MSCs cultured with or without BCP-ALL cells. As expected, CD34$^+$ HPCs migrated more abundantly toward MSCs than to control medium without MSCs (1.8-fold, $p < 0.05$; Figure 1G). However, migration of CD34$^+$ HPCs toward ALL-MSC co-cultures was significantly reduced compared to migration toward MSCs in mono-

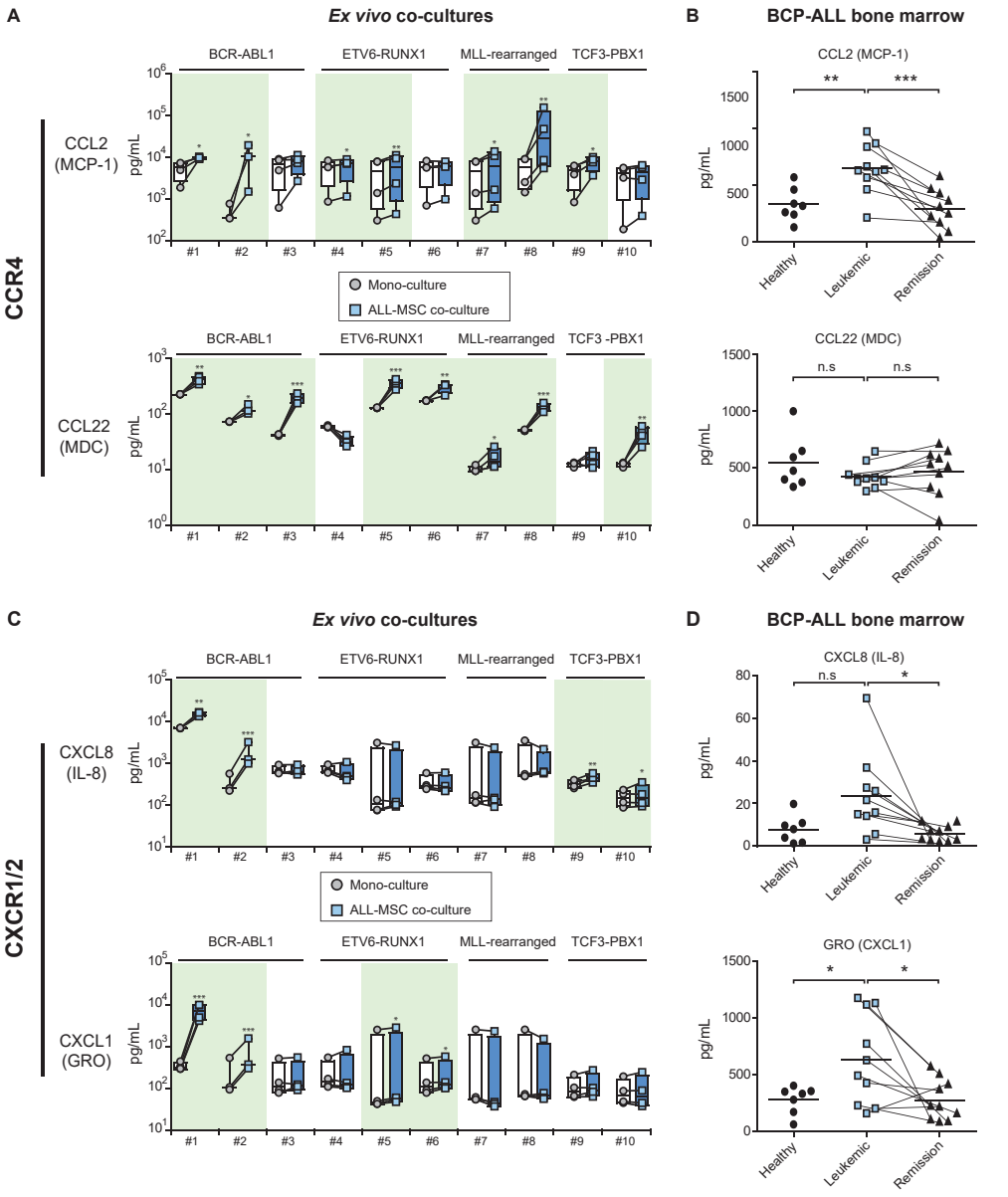

Figure 2. Chemokine inducing the CCR4 and CXCR1/2 axes are upregulated in the BCP-ALL niche. (**A**) Plots showing the secretion of CCL2/MCP-1 and CCL22/MDC by primary MSCs (n = 4) and primary BCP-ALL cells (n = 10) in mono-culture (circles represent the sum of cytokine secretion in mono-culture of BCP-ALL and mono-culture of MSC) compared to ALL-MSC co-cultures (squares). Data was obtained using a multiplexed fluorescent bead-based immunoassay. Boxes represent p25-p75 intervals. Raw data was logarithmically transformed to obtain a normal distribution of the data and upregulation of cytokines was tested using a one-tailed paired t-test * $p \leq 0.05$, ** $p \leq 0.01$, *** $p \leq 0.001$. (**B**) Plots showing the serum levels of CCL2/MCP-1 and CCL22/MDC in bone marrow aspirates from healthy controls (n = 7, circles), from untreated BCP-ALL patients at diagnosis (n = 10, blue squares) and from BCP-ALL patients after induction treatment (n = 10, triangles; lines indicate paired samples). Data was obtained using a multiplexed fluorescent bead-based immunoassay in which we measured the levels of 64 cytokines. Healthy (circles) and leukemic samples (blue squares) were compared using a two-tailed unpaired t-test. Leukemic samples before and after induction therapy (blue squares versus triangles) were compared using a one-tailed paired t-test * $p \leq 0.05$, ** $p \leq 0.01$, *** $p \leq 0.001$. (**C**) Same as (A) for CXCL8/IL-8 and CXCL1/GRO secretion. (**D**) Plots showing the serum levels of GRO/CXCL1 and CXCL8/IL-8. See also supplementary Figure 2 and 4 and supplementary Table 1 and 2.

cultures (20% reduction, $p < 0.05$; Figure 1G). In addition, we assessed the migratory behavior of healthy MSCs toward ALL-MSC co-cultures. We performed a transwell migration assay in which primary MSCs were allowed to migrate toward BCP-ALL cells or other MSCs in the bottom compartment. We observed that MSC migration was induced toward other MSCs compared to control medium ($p < 0.05$; Figure 1H). Strikingly, MSCs also actively migrated to BCP-ALL cells illustrating that BCP-ALL cells are able to recruit MSCs ($p < 0.001$; Figure 1H and supplementary Figure 3A). However, MSC migration was significantly inhibited toward the leukemic niche (ALL-MSC co-cultures) compared to a bottom compartment containing only BCP-ALL cells (2-3 fold reduction, $p < 0.001$, Figure 1I and supplementary Figure 3B-C). Interestingly, increasing the amount of ALL cells (up to 16fold) in ALL-MSC co-cultures did not re-induce MSC migration (Figure 1I). These results show that ALL-MSC co-cultures efficiently attract leukemic cells, but reduce migration of healthy CD34$^+$ HPCs and primary MSCs, suggesting that ALL-MSC co-cultures produce chemokines that specifically attract BCP-ALL cells.

To address which cytokines/chemokines may be altered in the leukemic niche, we quantified the levels of 64 cytokines known to be important in immunology/hematology in the supernatant of *ex vivo* co-cultures of patient-derived BCP-ALL cells (n = 10, representing major BCP-ALL subgroups) and MSCs (n = 4) (supplementary Table 1). Cytokine/chemokine profiles of mono-cultures of primary BCP-ALL cells and primary MSCs are depicted in supplementary Figure 2. Cocu-ltures of BCP-ALL cells with MSCs revealed the induction of unique secretion patterns per patient. These patterns were similar for different sources of MSC, i.e. MSCs obtained at the time of leukemia and those obtained from healthy controls. The unique profile per BCP-ALL patient suggests that leukemic cells govern the observed cytokine secretion (Figure 2, supplementary Figure 4A-B and supplementary Table 2). These unique cytokine/chemokine profiles suggest the need for patientspecific approaches to disrupt the leukemic niche. However, we also found recurrently induced signaling pathways. All ALL-MSC co-cultures showed increased levels of CCL2/MCP-1 and/or CCL22/MDC (Figure 2A), both ligands for the CCR4 receptor. This chemokine receptor is implicated in T cell leukemia and lymphoma, but has not yet been implicated as an important factor in BCP-ALL[13]. In addition, analysis of previously published microarray-based gene expression data showed that CCR4 expression levels in pediatric ALL cells were significantly higher compared to healthy hematopoietic cells (Supplementary Figure 4C).

Further, we observed recurrent induction of CXCL8/IL-8 and CXCL1/GRO secretion, ligands of the CXCR1 and CXCR2 receptor. CXCR1/2 ligands were induced by BCP-ALL cells from six out of ten patients (Figure 2C). In contrast to CCR4 expression, CXCR1 and CXCR2 expression levels were lower in pediatric ALL compared to healthy hematopoietic cells (supplementary Figure 3C).

We validated the cytokine/chemokine patterns identified in our co-culture model using serum derived from bone marrow aspirates from 10 ALL patients at diagnosis. We compared the cytokine/chemokine patterns in these samples with serum obtained from bone marrow aspirates of the same patients taken at the end of induction chemotherapy. At this stage of treatment the patients were in remission. Furthermore, we used bone marrow aspirates of 7 healthy controls to analyze cytokine/chemokine patterns of the healthy niche. Levels of the CCR4 ligand CCL2/MCP-1 were significantly higher in the bone marrow of untreated, newly diagnosed BCP-ALL patients compared to healthy controls (2.0-fold increase, $p < 0.01$; Figure 2B). Interestingly, after induction therapy, the CCL2/MCP-1 levels in the bone marrow of ALL patients decreased to levels observed in healthy controls (2.2 fold decrease, $p < 0.01$; Figure 2B). This suggests that the induced CCL2/MCP-1 levels at diagnosis are causally linked to the presence of leukemic cells. CCL22/MDC levels were similar between BCP-ALL patients and healthy controls (Figure 2B). Like CCL2/MCP-1, CXCL1/GRO levels were also increased in the bone marrow of BCP-ALL patients (2.3-fold increase, $p < 0.05$; Figure 2D) and CXCL8/IL8 levels showed a trend towards upregulation (2.5fold, $p = 0.052$; Figure 2D). Similar to CCL2/MCP-1 levels, the secreted levels of these CXCR1/2 ligands were significantly reduced after induction chemotherapy (2.3 fold and 3.1-fold respectively, $p < 0.05$; Figure 2D). These data implicate that CCR4 and CXCR1/2 signaling are important in the bone marrow of BCP-ALL patients and suggest that CCR4 inhibition (e.g. by mogamulizumab(14)) or CXCR1/2 inhibition might be an alternative or additional way to disrupt the BCP-ALL niche

In conclusion, our data indicate that the BCP-ALL niche is highly potent in attracting BCP-ALL cells and repelling the influx of healthy hematopoietic cells and MSCs in a CXCL12 independent manner. Instead, we show the recurrent induction of CCR4 and CXCR1/2 ligands by BCP-ALL cells in the leukemic niche (Figure 3). Our data point to CCR4 and CXCR1/2 as valuable future therapeutic targets to interfere with the leukemic niche in ALL.

ACKNOWLEDGEMENTS

We thank all members of the research laboratory Pediatric Oncology of the Erasmus MC for their help in processing leukemic and mesenchymal stromal cell samples; M. Buitenhuis for critical discussions and reading of the manuscript; the Vlietland Ziekenhuis for collecting and providing cord blood; the Amsterdam Medical Center for providing the R2 gene genomic analysis and visualization platform. The work described in this paper

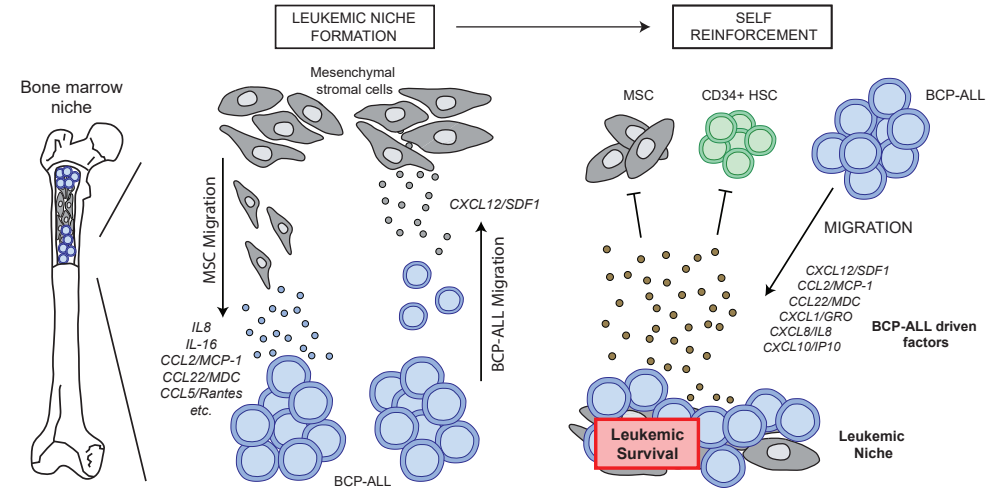

Figure 3. Model of the self-reinforcing BCP-ALL niche. Proposed model for the formation of a leukemic niche by BCP-ALL cells. BCP-ALL cells actively migrate toward MSCs in a CXCL12 dependent manner. Simultaneously, MSC migration is induced by BCP-ALL cells. When BCP-ALL cells and MSCs are in close proximity, a leukemic microenvironment is created that specifically attracts other BCP-ALL cells and inhibits the migration of MSCs and healthy CD34⁺ cells. This process is CXCR4/CXCL12 independent and is characterized by the secretion of patient-unique cytokines.

was funded by the KiKa Foundation (Stichting Kinderen Kankervrij – Kika-39), the Dutch Cancer Society (UVA 2008; 4265, EMCR 2010; 4687), the Netherlands Organization for Scientific Research (NWO – VICI M.L. den Boer) and the Pediatric Oncology Foundation Rotterdam.

AUTHOR CONTRIBUTIONS

Co-first authors B. de Rooij and R. Polak contributed equally to the study. B. de Rooij and R. Polak designed the study, performed the experiments, collected and analyzed all data, and wrote the paper. L. van den Berk performed experiments. F. Stalpers isolated MSCs and leukemic cell samples. M.L. den Boer and R. Pieters analyzed data and wrote the paper. All authors discussed the results and approved the submitted manuscript.

REFERENCES

1. Colmone A, Amorim M, Pontier AL, Wang S, Jablonski E, Sipkins DA. Leukemic cells create bone marrow niches that disrupt the behavior of normal hematopoietic progenitor cells. Science. 2008 Dec 19;322(5909):1861-5.

2. Fujisaki J, Wu J, Carlson AL, Silberstein L, Putheti P, Larocca R, et al. In vivo imaging of Treg cells providing immune privilege to the haematopoietic stem-cell niche. Nature. 2011 Jun 9;474(7350):216-9.

3. Nakasone ES, Askautrud HA, Kees T, Park JH, Plaks V, Ewald AJ, et al. Imaging tumor-stroma interactions during chemotherapy reveals contributions of the microenvironment to resistance. Cancer Cell. 2012 Apr 17;21(4):488-503.

4. Polak R, de Rooij B, Pieters R, den Boer ML. B-cell precursor acute lymphoblastic leukemia cells use tunneling nanotubes to orchestrate their microenvironment. Blood. 2015 Nov 19;126(21):2404-14.

5. Peled A, Petit I, Kollet O, Magid M, Ponomaryov T, Byk T, et al. Dependence of human stem cell engraftment and repopulation of NOD/SCID mice on CXCR4. Science. 1999 Feb 5;283(5403):845-8.

6. van den Berk LC, van der Veer A, Willemse ME, Theeuwes MJ, Luijendijk MW, Tong WH, et al. Disturbed CXCR4/CXCL12 axis in paediatric precursor B-cell acute lymphoblastic leukaemia. Br J Haematol. 2014 Jul;166(2):240-9.

7. Flomenberg N, Devine SM, Dipersio JF, Liesveld JL, McCarty JM, Rowley SD, et al. The use of AMD3100 plus G-CSF for autologous hematopoietic progenitor cell mobilization is superior to G-CSF alone. Blood. 2005 Sep 1;106(5):1867-74.

8. Burger JA, Peled A. CXCR4 antagonists: targeting the microenvironment in leukemia and other cancers. Leukemia. 2009 Jan;23(1):43-52.

9. Juarez J, Dela Pena A, Baraz R, Hewson J, Khoo M, Cisterne A, et al. CXCR4 antagonists mobilize childhood acute lymphoblastic leukemia cells into the peripheral blood and inhibit engraftment. Leukemia. 2007 Jun;21(6):1249-57.

10. Sipkins DA, Wei X, Wu JW, Runnels JM, Cote D, Means TK, et al. In vivo imaging of specialized bone marrow endothelial microdomains for tumour engraftment. Nature. 2005 Jun 16;435(7044):969-73.

11. Parameswaran R, Yu M, Lim M, Groffen J, Heisterkamp N. Combination of drug therapy in acute lymphoblastic leukemia with a CXCR4 antagonist. Leukemia. 2011 Aug;25(8):1314-23.

12. Wright DE, Bowman EP, Wagers AJ, Butcher EC, Weissman IL. Hematopoietic stem cells are uniquely selective in their migratory response to chemokines. J Exp Med. 2002 May 6;195(9):1145-54.

13. Nakagawa M, Schmitz R, Xiao W, Goldman CK, Xu W, Yang Y, et al. Gain-of-function CCR4 mutations in adult T cell leukemia/lymphoma. J Exp Med. 2014 Dec 15;211(13):2497-505.

14. Duvic M, Pinter-Brown LC, Foss FM, Sokol L, Jorgensen JL, Challagundla P, et al. Phase 1/2 study of mogamulizumab, a defucosylated anti-CCR4 antibody, in previously treated patients with cutaneous T-cell lymphoma. Blood. 2015 Mar 19;125(12):1883-9.

SUPPLEMENTARY DATA

MATERIALS AND METHODS

Cell lines and reagents

B-cell precursor ALL (BCP-ALL) cell lines, NALM6 (B-Other) and REH (TEL-AML1), were obtained from DSMZ (Braunschweig, Germany), used at low cell passages, and routinely verified by DNA fingerprinting. Cell lines were cultured in RPMI-1640 medium containing 10% fetal calf serum (FCS), 1% penicillin-streptomycin at 37 °C and 5% CO_2.

Isolation of primary BCP-ALL leukemic blasts from patients

Primary BCP-ALL leukemic blasts were isolated from patients as described earlier (Polak *et al.* Blood 2015). In short, mononuclear leukemic cells were collected from bone marrow aspirates obtained from children with newly diagnosed BCP-ALL prior to treatment. All samples used in this study contained > 95% leukemic blasts.

Isolation and characterization of primary MSCs

Primary MSCs were isolated and characterized using positive (CD44/ CD90/ CD105/ CD54/ CD73/ CD146/ CD166/ STRO-1) and negative surface markers (CD19/ CD45/ CD34)(8). In addition multilineage potential was confirmed as described earlier (Polak *et al.* Blood 2015).

Isolation of $CD34^+$ cells

$CD34^+$ cells were obtained from umbilical cord blood using the Direct CD34 Progenitor Cell Isolation kit, human (Miltenyi Biotec, Gladback, Germany). $CD34^+$ cells were positively selected by magnetic microbeads using the MACS LS column (Miltenyi Biotec) in combination with a MACS separator (Miltenyi Biotec). The purity of the isolated cells was confirmed by flow cytometry using the CD34-PE fluorescent antibody (BD Pharmingen, San Diego, USA).

Collection of bone marrow aspirates

Serum samples of bone marrow aspirates were collected from children with ALL at initial diagnosis and after completion of two courses of chemotherapy according to the ALL-10 protocol of the Dutch Childhood Oncology Group (day 79 after start of treatment) as previously described (van den Berk *et al.* Br J Haemat 2014). This study was approved by the Institutional Review Board and informed consent was obtained from parents or guardians.

Cell viability assays

Cell viability assays of primary material was performed as earlier described (Polak *et al.* Blood 2015). In short, primary patient cells (1 x 10^6 cells) were co-cultured with or

without primary stromal cells (5 x 10^4) for five days in a 24-well plate at 37 °C and 5% CO_2. Stromal cells were allowed to attach prior to the start of an experiment. Before the start of each experiment, leukemic cells were screened for CD19 positivity (Brilliant Violet 421 anti-human CD19 antibody), which was used to discriminate leukemic cells from $CD19^{neg}$ MSCs. The percentage of viable leukemic cells was determined after 5 days of culture by staining with Brilliant Violet 421 anti-human CD19 (Biolegend), FITC Annexin V (Biolegend), and Propidium Iodide (PI; Sigma), after which the percentage of $AnnexinV^{neg}/PI^{neg}/CD19^{pos}$ cells within the MSC negative fraction was determined by flow cytometry (BD Biosciences).

Multiplexed fluorescent bead-based immunoassay (Luminex)

Primary leukemic cells were co-cultured with different sources of primary MSCs for 5 days at 37°C and 5% CO_2. Supernatant was collected upon which the viability of leukemic cells was assessed as described above. The concentration of 64 known cytokines/chemokines in these supernatants was analyzed using fluorescent bead-based immunoassay (Luminex Human Cytokine/Chemokine Panel I and II; Merck Millipore) according to the manufacturer's protocol.

Serum of bone marrow aspirates of leukemia patients or healthy controls were used to determine the concentration of 64 known cytokines/chemokines using the same fluorescent bead-based immunoassay (Luminex Human Cytokine/Chemokine Panel I and II; Merck Millipore) according to the manufacturer's protocol

BCP-ALL migration assay

BCP-ALL migration experiments were performed using RPMI 10% FCS at 37°C and 5% CO_2. 5 x 10^4 primary MSCs and 2 x 10^5 BCP-ALL cells were cultured either separate or in co-culture in the lower compartment of a transwell in a volume of 750 µL for 24 hours prior to the start of the experiment. At the start of experiment, 4 x 10^5 NALM6-GFP cells in a volume of 250 µL were added to the upper compartment of a 6.5 mm diameter transwell system (Corning, NY, USA) with a pore size of 3.0 µm. Cells were allowed to migrate for 48 hours. At the end of experiment, transwells were removed and cells in the bottom compartment were harvested and stained with DAPI (Life Technologies). $DAPI^-/GFP^+$ cells were used as a measure for cell migration and quantified by flow cytometry using a MACSQuant analyzer (Miltenyi Biotec, Gladbach, Germany).

$CD34^+$ migration assay

Experiments were performed using either RPMI Dutch Modified 15%FCS or Iscove modified Dulbecco medium (Gibco) containing 10% FCS, 50µM β-mercaptoethanol, 1% penicillin-streptomycin, 2mM glutamine, stem cell factor (SCF; 50ng/mL; Peprotech) and fms-like tyrosine kinase-3 ligand (Flt3L; 50 ng/mL; Peprotech) at 37°C and 5% CO_2. Primary MSCs (5 x 10^4) and NALM6-GFP cells (2 x 10^5) were cultured either separate or in co-culture in a volume of 750 µL for 24 hours prior to start of experiment (bottom compartment). At the start of experiment, 5 x 10^5 $CD34^+$ cells in a volume of 250 µL were added to the top chamber of a 3.0 µm transwell system (Corning, NY, USA) and allowed to migrate for 48 hours at 37°C and 5% CO_2. At the end of experiment, transwell inserts were removed upon which the cells in the bottom compartment were harvested and stained with Propidium Iodide (PI; Sigma) and Brilliant Violet 421 anti-human CD45 antibody (Biolegend). $PI^-/GFP^-/CD45^+$ cells were quantified by flow cytometry using a MACSQuant analyzer (Miltenyi Biotec, Gladbach, Germany).

MSC migration assay

Experiments were performed using DMEM medium containing 5% FCS, 1% penicillin-streptomycin at 37°C and 5% CO_2. REH cells (0.1 – 1.6 x 10^6) and primary MSCs (5 x 10^4) were cultured either separate or in co-culture in a volume of 750 µL for 48 hours prior to start of experiment. At the start of experiment, 5 x 10^4 MSCs were added to the top chamber of a 8.0 µm transwell system (Corning) and allowed to migrate through the membrane overnight (12-16 hours). Non-migrated cells were removed from the upper side of the transwell insert using a cotton swab. Cells that migrated through the membrane insert were fixed using 10% Formalin (Sigma) for 10 minutes, washed with PBS and stained for 30 minutes with Crystal violet at room temperature. Images were captured using a Leica DM IL microscope mounted with a Leica DFC430C camera (Leica, Germany). Next, Crystal violet contained by MSCs was dissolved in 150 µL methanol, quantified by spectrophotometer using 540-570 nm wavelength settings (Versamax, San Francisco) and used as a measure of migration.

Statistical analysis

We used the R2 Genomics Analysis and Visualization Platform (http://r2.amc.nl) to visualize gene expression data in Figure 4 and performed one way analysis of variance (ANOVA). For other statistics, Student's t-test was used and a Student's paired t-test was used when applicable. Bar graphs represent the mean of biological replicates. Error bars show standard error of the mean (SEM).

SUPPLEMENTARY FIGURES

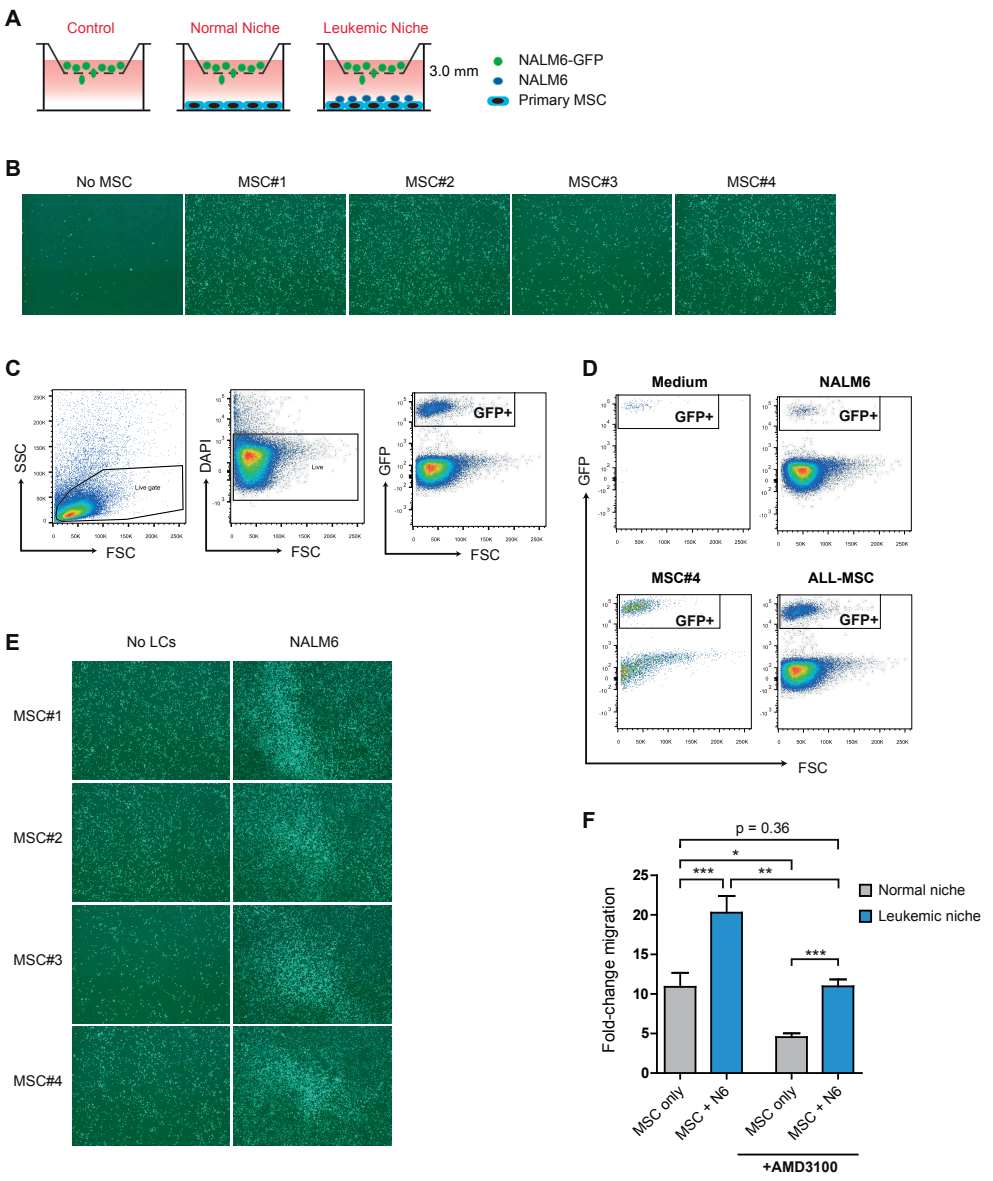

Supplementary Figure 1. ALL-MSC co-cultures induce leukemic cell migration. (**A**) Schematic overview of the experimental conditions used for experiments shown in Figure 1D-E. The migration of GFP-positive NALM6 cells is measured toward: culture medium (Control), primary MSCs (Normal Niche) or GFP-negative ALL-MSC co-cultures (Leukemic Niche). (**B**) Representative microscope images depicting migrated GFP-positive NALM6 cells after 48 hours in a 3.0 µm transwell system. GFP-positive NALM6 cells were allowed to migrate toward a bottom compartment containing either culture medium, GFP-negative NALM6 cells or primary MSCs (n = 4). (**C**) Gating strategy for quantification of migrated GFP-positive NALM6 cells. (**D**) Representative flow cytometry plots showing the migration of GFP-positive NALM6 cells toward GFP-negative NALM6 cells, MSCs and GFP-negative ALL-MSC co-cultures. (**E**) Representative microscope images showing the migration of GFP-positive NALM6 cells toward GFP-negative ALL-MSC co-cultures (right panel) or migration to a bottom compartment containing only MSCs (left panel; n = 4). No LCs = no leukemic cells in the bottom compartment. (**F**) Graph showing the effect of CXCR4 inhibition by AMD3100 (10 µM) on migration of NALM6 cells towards MSC mono-cultures (normal niche, grey bars) and ALL-MSC co-cultures (leukemic niche, blue bars). Migration towards culture medium is used to calculate the foldchange migration. CXCR4 inhibition decreases migration of NALM6 cells towards the healthy and leukemic niche in a similar manner. However, the leukemic niche still induces migration of NALM6 cells in the presence of AMD3100. Data are means ± SEM; * $p \leq 0.05$, ** $p \leq 0.01$, *** $p \leq 0.001$, N6 = NALM6. See also Figure 1.

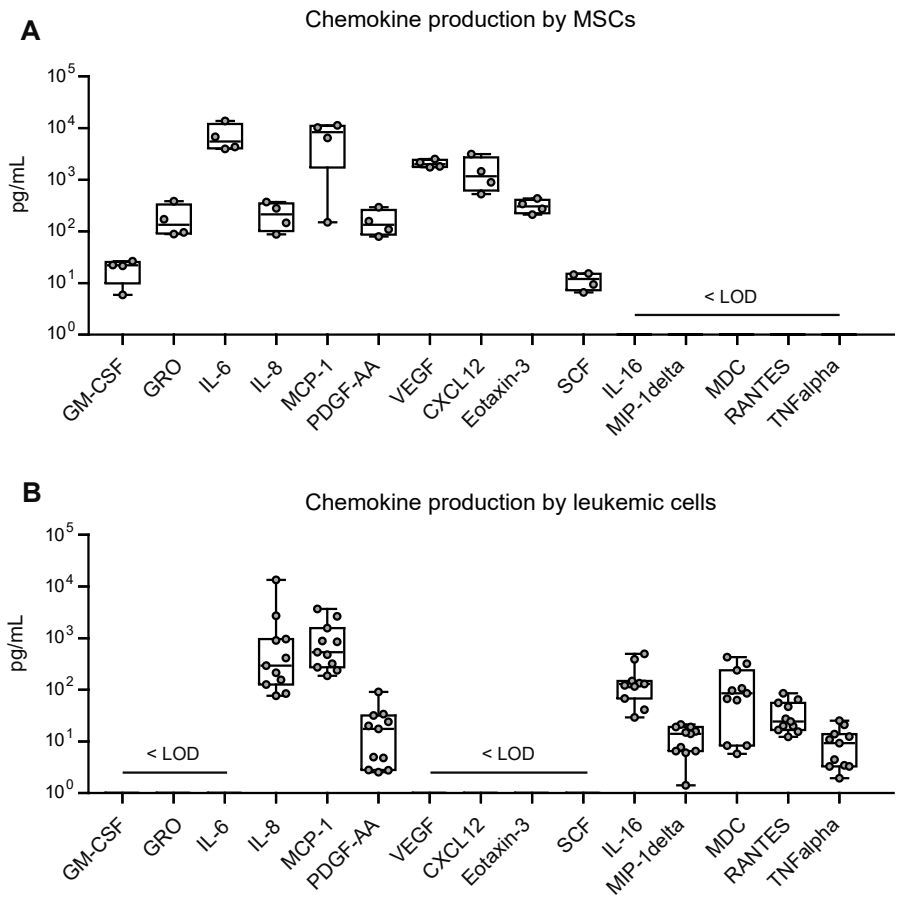

Supplementary Figure 2. Cytokine secretion of primary MSCs and BCP-ALL cells in mono-culture. (**A**) Graph showing the cytokine production of MSCs from four donors after 5 days of mono-culture. (**B**) Graph showing the cytokine production of BCP-ALL cells from 10 different donors after 5 days of mono-culture. Data was obtained using a multiplexed fluorescent bead-based immunoassay. Secreted levels of 64 cytokines/chemokines were analyzed. Cytokines/chemokines that were not detected in mesenchymal stromal cells or ALL cells were not depicted in this figure. < LOD = below limit of detection. See also Figure 2.

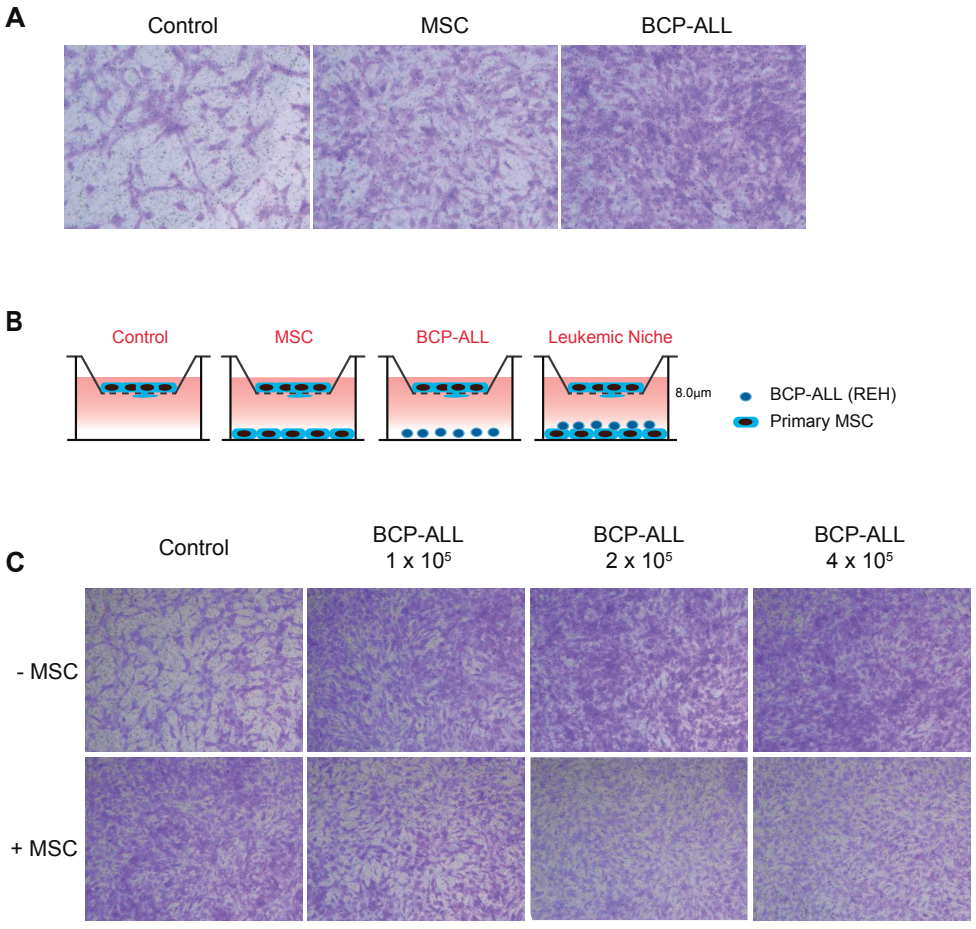

Supplementary Figure 3. BCP-ALL cells recruit MSCs and stop recruiting after the leukemic niche is established. (**A**) Images of a representative experiment showing MSCs that migrated to the other side of a 8.0 µm transwell insert for 16 hours. Cells were fixed and subsequently stained with crystal violet. Images show MSCs migrated toward a bottom compartment containing culture medium, MSCs or BCP-ALL cells (REH) (n = 4). (**B**) Schematic overview of experimental conditions used in Figure 1I and supplementary Figure 2C. (**C**) Images of a representative experiment showing that MSCs migrate to the other side of a 8.0 µm transwell insert for 16 hours toward an increasing amount of BCP-ALL cells (REH) in mono-culture (upper panels) or in co-culture with MSCs (MSC + REH; lower panels). See also Figure 1.

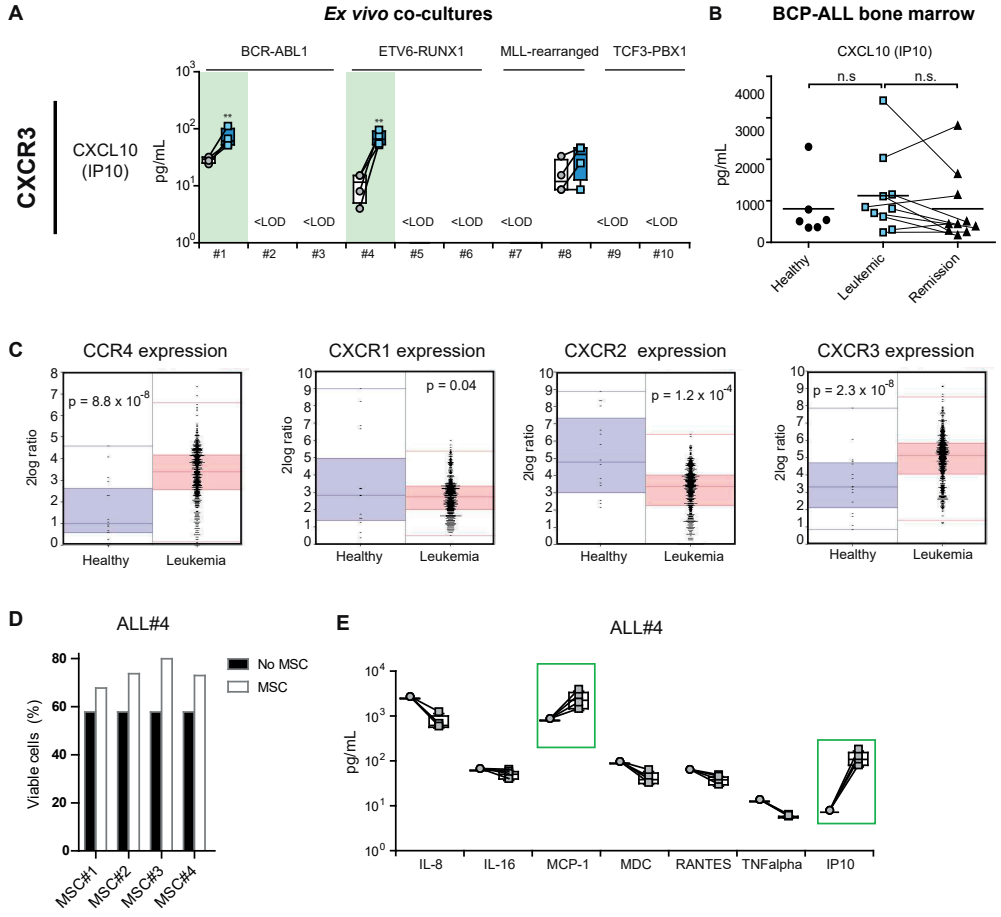

Supplementary Figure 4. Chemokines and receptors upregulated in the BCP-ALL niche. (**A**) Plots showing the secretion of CXCL10 (IP10) by primary MSCs and primary BCP-ALL cells in mono-culture (circles represent the sum of cytokine secretion in mono-culture of BCP-ALL and mono-culture of MSC) compared to ALL-MSC co-cultures (squares). Data was obtained using a multiplexed fluorescent bead-based immunoassay. Boxes represent p25-p75 intervals. Raw data was logarithmically transformed to obtain a normal distribution of the data and upregulation of cytokines was tested using a one-tailed paired t-test * $p \leq 0.05$, ** $p \leq 0.01$, *** $p \leq 0.001$. (**B**) Plot showing the serum levels of CXCL10 (IP10) in bone marrow aspirates from healthy controls (n = 7, circles), from untreated BCP-ALL patients at diagnosis (n = 10, blue squares) and from BCP-ALL patients after induction treatment (n = 10, triangles; lines indicate paired samples). Data was obtained using a multiplexed fluorescent bead-based immunoassay in which we measured the levels of 64 cytokines. Healthy (circles) and leukemic samples (blue squares) were compared using a two-tailed unpaired t-test. Leukemic samples before and after induction therapy (blue squares versus triangles) were compared using a one-tailed paired t-test * $p \leq 0.05$, ** $p \leq 0.01$, *** $p \leq 0.001$. (**C**) Gene expression levels of the CCR4, CXCR1, CXCR2 and CXCR3 receptors in healthy hematopoietic cells (Andersson et al. BMC Med Genomics. 2010) and pediatric ALL cells (Den Boer et al. Lancet Oncol. 2009). Data was visualized using R2: microarray analysis and visualization platform. (**D-E**) Graphs showing that the increase in patient-specific cytokines was not the effect of induced cellular survival in ALL-MSC co-cultures. (**D**) Graph showing the viability of leukemic cells from patient ▸

ALL#4 cultured in absence or in presence of primary MSCs. (**E**) Plots showing the secretion of cytokines by BCP-ALL cells from patient ALL#4 in mono-culture (grey circles) and the secretion of cytokines by ALL#4 cells in ALL-MSC co-culture corrected for the secretion of MSCs (grey boxes). The dashed boxes indicate significantly upregulated cytokines shown in Figure 2. See also Figure 2.

SUPPLEMENTARY TABLES

Supplementary Table 1. Cytokine and chemokine screening panel

Cytokine tested	Receptor
VEGF	VEGFR
sCD40L	C40; αIIbβ3; α5β1
EGF	EGFR
Eotaxin	CCR2; CCR3; CCR5
FGF-2	FGFR1
Flt-3 ligand	Flt-3
Fractalkine	CX3CR1
G-CSF	GCSFR
GM-CSF	GMCSFR
GRO	CXCR2
IFNα2	IFNAR
IFN-γ	IFNGR1; IFNGR2
IL-1α	IL1R
IL-1β	IL1R
IL-1ra	IL1R
IL-2	IL2R
IL-3	IL3R
IL-4	IL4R
IL-5	IL5R
IL-6	CD126 and CD130 complex
IL-7	IL7R
IL-8	CXCR1; CXCR2
IL-9	IL9R
IL-10	IL10R1-IL10R2 complex
IL-12 (p40)	IL12R
IL-12 (p70)	IL12R
IL-13	IL13R
IL-15	IL15RaR
IL17A	IL17R
IP-10	CXCR3
MCP-1	CCR2 and CCR4
MCP-3	CCR2
MDC (CCL22)	CCR4
MIP-1α	CCR1
MIP-1β	CCR1;CCR5

Supplementary Table 1. (continued)

Cytokine tested	Receptor
PDGF-AA	PDGFR
PDGF-AB/BB	PDGFR
RANTES	CCR5
TGF-α	EGFR
TNF-α	TNFR1
TNF-β	LTB
TSLP	CRLF2 and IL7-R complex
6Ckine	CCR7
BCA-1	CXCR5
CTACK	CCR10
ENA-78	CXCR2
Eotaxin-2	CCR3
Eotaxin-3	CCR3
I-309	CCR8
IL-16	CD4
IL-20	IL20R
IL-21	IL21R
IL-23	IL23R
IL-28A	IL28R
IL-33	IL1RL1
LIF	LIFR
MCP-2	CCR1; CCR2a; CCR5
MCP-4	CCR2; CCR3; CCR5
MIP-1d	CCR1; CCR3
SCF	c-Kit
CXCL12	CXCR4; CXCR7
TARC	CCR4
TPO	CD110
TRAIL	TRAILR-complex

Supplementary Table 2. Overview of cytokines upregulated in BCP-ALL/MSC co-cultures

	ID	G-CSF CSF3	GM-CSF CSF2	GRO CXCL1	IP10 CXCL10	MCP-1 CCL2	MCP-3 CCL8	MDC CCL22	ENA-78 CXCL5	I-309 CCL1	IL-6	IL-8 CXCL8
BCR-ABL1	#1	■	■	■	■	■	■	■	■	■	■	■
	#2			■		■		■			■	■
	#3							■				
ETV6-RUNX1	#4				■	■						
	#5			■		■		■			■	
	#6			■				■				
MLL	#7					■		■				
	#8					■		■				
TCF3-PBX1	#9					■	■				■	■
	#10							■			■	

Supplementary Table 3. Primary mesenchymal stromal cells used in this study

Name	Derived from	Subtype
MSC #1	Healthy BM	-
MSC #2	Healthy BM	-
MSC #3	Leukemic BM	B-Other
MSC #4	Leukemic BM	ETV6-RUNX1

Chapter 6

GENERAL DISCUSSION AND SUMMARY

CANCER IS A DISEASE OF BOTH INTRINSICALLY AND EXTRINSICALLY MODIFIED CELLS

Historically, research on cancer cells has been focused on identifying *intrinsic* alterations that separate these cells from their healthy counterparts. At the end of the 19th century, David von Hansemann discovered that cancer cells underwent aberrant cell divisions that deregulate the chromatin content[1]. He hypothesized that these alterations were responsible for the behavior of cancer cells, although the tools at that time did not allow him to investigate these mitotic anomalies in more depth. As technologies advanced, a chromosomal abnormality was identified that was consistently present in cancer cells. Researchers discovered an exchange of genetic material between chromosome 9 and chromosome 22 called the BCR-ABL1 translocation, or Philadelphia chromosome, which is often found in chronic myeloid leukemia (CML) but also in B cell precursor acute lymphoblastic leukemia (BCP-ALL) cells[2,3]. The BCR-ABL1 fusion protein displays constitutive kinase activity and drives a malignant cellular phenotype[4]. The identification of an abnormality discriminative for leukemic cells presented an opportunity to develop cancer-specific treatment. It led to the development of imatinib, a tyrosine-kinase inhibitor that releases the BCR-ABL1 fusion protein from its activated oncogenic state. Survival of CML patients has improved significantly since the FDA approval of imatinib[5]. This is an example how genetic alterations which drive the phenotype of cancer cells can be targeted by specific drugs. It represents the dominant view in oncology today that cancer cells are separate entities which are driven by *intrinsic* (epi)genetic alterations.

There is also evidence that cancer cells do not function as separate entities but are dependent on their cellular context. As early as 1889, physician Stephen Paget noticed that when cancer cells spread through the body, they have a propensity to find shelter in specific organs. He discussed this in his "seed and soil" hypothesis in which he compared the outgrowth of cancer cells to those of plant seeds. Paget stated: "When a plant goes to seed, its seeds are carried in all directions. But they can only live and grow if they fall on congenial soil[6]." Similarly, cancer cells need a specific environment to thrive in. This was supported by his observations that breast cancer metastases were more prone to grow out of the liver than other organs, even those with similar blood flow[6]. While the site of tumor growth is important, there are even observations of cancer cells that are completely 're-educated' by their microenvironment. Mouse blastocysts injected with tetracarcinoma cells developed into healthy mice without cancer[7]. Interestingly, the 'former' cancer cells were still present but now performed healthy cell functions in multiple tissues[7]. These observations show that cells do not act like independent entities, but rather function as a system that is driven by highly complicated communication mechanisms. Hence, cancer is more accurately described as a disease of both *intrinsically* and *extrinsically* altered cells. The influence of cells surrounding tumor cells, or the tumor microenvironment, is an emerging field of leukemia research. The leukemic microenvironment has been shown to play a major role in conferring chemotherapy resistance and to be critical

in leukemogenesis[8,9]. Cytokines and other soluble factors, as well as direct cell-cell interactions, are thought to be important for this process[10]. However, we lack insight into how the crosstalk between leukemic cells and their microenvironment is regulated. This is why we were intrigued by the discovery of a new signaling module in eukaryotic cells: tunneling nanotubes (TNTs)[11]. TNTs are thin membrane protrusions capable of transporting a multitude of signaling molecules between distant cells. Tumor cells might use TNTs to influence surrounding cells and concomitantly induce cell intrinsic changes. Therefore we investigated the presence and importance of TNTs in the leukemic niche.

DISCOVERY OF TNT SIGNALING BETWEEN ALL CELLS AND MSCS

A few years after Rustom and colleagues identified TNTs in eukaryotic cells for the first time[11], Sowinski *et al*. showed that T lymphocytes could connect using TNTs, presenting a route for HIV-1 tranmission[12]. At that time there were no studies investigating TNT signaling in leukemia, and therefore we tried to recapitulate these findings using malignant B lymphocytes in **chapter 2**. We observed that BCP-ALL cells connect via TNTs and actively exchange lipophilic structures. Next, we visualized TNT formation between BCP-ALL cells and mesenchymal stromal cells (MSCs). MSCs are one of the most abundant and important cells in the bone marrow, where BCP-ALL cells create a leukemic niche[13,14]. Surprisingly, the amount of TNTs formed between BCP-ALL cells and MSCs far surpassed that of TNTs between leukemic cells. Also, this signaling was mostly unidirectional: from leukemic cells toward MSCs. To assess the functional effects of TNT signaling, we used a combination of three experimental setups: 1) reducing TNT formation through actin inhibition[11], 2) mechanical disruption of TNT connections through gentle shaking of cell cultures[12,15], and 3) prevention of TNT formation by physically separating leukemic cells (cultured in a 3.0 µm pore-sized insert) and MSCs (cultured in the bottom compartment of a transwell system)[12,16]. None of these setups specifically inhibits TNTs and their effects on other cellular signaling modules are depicted in Table 1. However, by combining these experimental setups we were able to assess the effect of TNT signaling. In these experiments, we observed that BCP-ALL cells actively modulate their microenvironment using TNTs, causing the release of pro-survival cytokines and, subsequently, an increase in survival and resistance to chemotherapeutic drugs. Disruption of TNTs inhibited this cytokine release, decreased the survival benefit that MSCs provide to BCP-ALL cells, and sensitized BCP-ALL cells to the important anti-leukemic drug prednisolone. These data provide a new concept to target the leukemic niche in B-cell acute lymphoblastic leukemia.

FINDING NOVEL COMPOUNDS THAT INHIBIT TNT SIGNALING

TNT signaling between BCP-ALL cells and MSCs was discovered using *ex vivo* cultures of primary patient material. We wanted to translate these findings to *in vivo* models, but unfortunately, no agents were available that induce specific inhibition of TNTs. To identify

Table 1. Off-target effects of TNT inhibition. Table showing how actin inhibitors, mechanical disruption (shaking), or separating cells with a transwell system affect intercellular communication mechanisms other than TNTs. Blank cells represent no effect. Combining TNT inhibitory setups is crucial to assess the effect of TNT signaling.

	Actin inhibition	Shaking	Transwell
Tunneling nanotubes	inhibition	inhibition	inhibition
Soluble factors			
Extracellular vesicles	inhibition		
Integrins		stimulation	inhibition
Gap junctions			inhibition

novel TNT inhibitors, we created a system that accurately measures TNT signaling from BCP-ALL cells toward MSCs in **chapter 2**. We quantified TNT signaling by using lipophilic carbocyanine dyes which stain organelles and membrane components actively transported by TNTs[11]. It is important to note that these lipophilic dyes can also be exchanged by extracellular vesicles (ECVs). However, using a 3.0 µm pore-sized transwell system that allows the transfer of ECVs but abrogates all direct cell contact, we observed that dye transfer was inhibited by 500fold. This means that > 99.99% of the observed lipophilic dye transfer is caused by TNT signaling. Therefore, using flow cytometry to measure the lipophilic dye transfer from BCP-ALL cells toward MSCs is an accurate method to measure TNT activity. Quantifying dye transfer between cells is also performed in numerous other studies[11,12,17-20]. A different method is to count the frequency of TNTs in fixated cell cultures. This reveals information about TNTs present during fixation, but not of those that formed and disappeared prior to fixation. Counting TNTs is especially problematic when investigating compounds that induce apoptosis. In these cases, a reduction in TNTs after drug exposure might be caused by a lack of cells to form TNTs. It is impossible to exclude the possibility that TNTs were abundant and highly active prior to fixation. In contrast, flow cytometric analysis of lipophilic dye transfer quantifies the accumulation of TNT activity in time. Therefore we used this system to test the effect of compounds on TNT signaling between BCP-ALL cells and MSCs in **chapter 3**. Since TNTs are cytoskeletal structures, we investigated a large range of tubulin and actin inhibitors. Inhibition of microtubules did not negatively affect TNT signaling but rather increased lipophilic dye transfer from BCP-ALL cells toward MSCs. The finding that these drugs induce TNT signaling possible uncovers a rescue mechanism used by leukemic cells in response to tubulin treatment. In addition, it shows that inducing apoptosis is not sufficient to inhibit TNT signaling in a dye transfer based co-culture system. Next, we investigated the ability of 11 actin disrupting molecules to inhibit TNT signaling. Actin polymerization inhibitors are often used to inhibit TNT formation and we confirmed their efficacy using four different compounds[21-25]. The effect of other classes of actin disrupting molecules on TNT signaling are unknown. Disrupting the actin nucleation proteins Arp2/3 and formins[26,27], which are

responsible for providing a stable start point for actin monomers[28,29], strongly reduced TNT signaling. Interestingly, affecting the plasticity of actin polymers by cucurbitacin E[30] and jasplakinolide[31,32] also strongly interfered with TNT signaling. These observations show that TNT signaling is driven by the interplay of fundamental actin regulating processes. Moreover, combining actin disassembly and actin nucleation or polymerization inhibitors increased TNT disruption in a synergistic-like manner. These findings provide new targets for TNT inhibition and increase our knowledge on the molecular mechanisms regulating TNTs.

THE TOXICITY OF ACTIN INHIBITORS

Disrupting the cytoskeleton as anti-cancer treatment was serendipitously discovered during the study of *Vinca* alkaloids as antidiabetics[33,34]. These agents interfere with microtubules which regulate critical steps in cell division. While very effective these drugs induce significant side effects including peripheral neuropathy[35], and cardiovascular and thromboembolic events[36,37]. Nevertheless, it has been argued that tubulin inhibitors represent the most successful class of anti-cancer agents thus far, and they will likely remain important even as more selective drugs are developed[25,34,38]. Our data shows that TNT signaling is abrogated by multiple classes of actin inhibitors and the cytotoxic effects of these compounds were investigated in **chapter 3**. Healthy mononuclear cells were more resistant to actin inhibition than BCP-ALL cells, while MSCs and CD34$^+$ hematopoietic progenitor cells (HPCs) were also affected. These observations show that actin inhibitors might be an important novel class of anti-leukemic agents that act in a cytotoxic manner and disrupt TNT signaling. In addition, the potential off-target effects of actin inhibitors demonstrate that attacking the cytoskeleton should be done with great caution.

TUNNELING NANOTUBE STRUCTURE AND SIGNALING DEPEND ON THE CELL TYPE

A common hurdle for TNT research is the large diversity in TNT function and morphology across cells. For example, macrophages propagate calcium fluxes through TNTs while T cells do not[12,39]. There is a great variety in the length, width, and lifespan of TNTs, and some have been reported to contain tubulin[11,12,17,39]. Adding to the complexity, two forms of *de novo* TNT formation have been observed (Figure 1). TNTs can protrude from one cell and actively elongate towards a distant cell (Figure 1A), or appear after the dislodgement of two connecting cells (Figure 1B). Using live confocal microscopy, we observed that ALL cells form TNTs with MSCs after dislodging in **chapter 2**. Importantly, there are three TNT characteristics identical across cell types. All TNTs contain polymerized actin, connect distant cells without adhering to the culture bottom, and actively transport molecules between cells[40]. The nanotubular structures between ALL cells and MSCs display all three characteristics. In **chapter 2 and 3** we observed that TNTs in the leukemic niche actively transport lipophilic molecules. In **chapter 4** we further elucidated the identity of those molecules. To this aim, we ectopically expressed fluorescent proteins that are markers

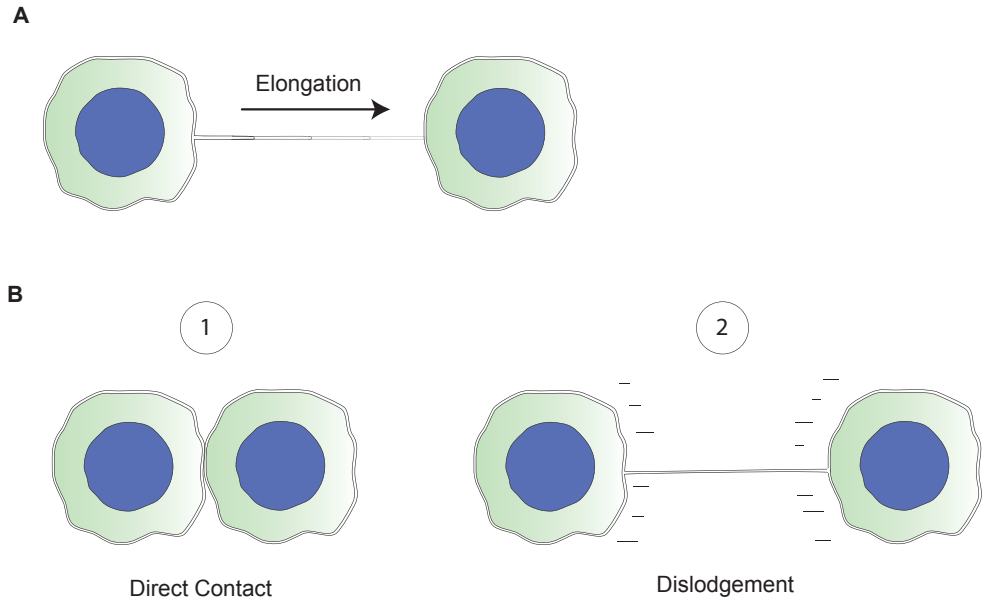

Figure 1. Two types of de novo TNT formation. Figure illustrating two types of de novo TNT formation: (A) TNTs elongate from one cell and actively anchor to another cell. (B) After cell-cell contact, dislodgement leads to TNT formation.

for specific cellular structures in ALL cells. Our results indicate that actin, endoplasmatic reticulum, adhesion molecule ICAM1, autophagosomes, mitochondria, and endosomes are contact-dependently transferred from leukemic cells toward MSCs. Transfer of mitochondria, adhesion molecule ICAM1, and autophagosomes were significantly reduced when TNT signaling was inhibited. Mitochondria and membrane-associated proteins have previously been shown to be transported via TNTs by other cell types[41-45], demonstrating the validity of our setup. Strikingly, transfer of autophagosomes was > 3.0-fold greater than the transfer of other tested proteins and was also significantly disrupted by inhibiting TNTs. To our knowledge this is the first observation that TNTs transport autophagosomes. These structures are responsible for degrading damaged intracellular proteins and organelles[46]. Autophagosomes have a distinct double layered membrane, which is shaped through the actin cytoskeleton[47]. Since, TNT formation is also dependent on actin[11,17] this co-dependence might be important for autophagosome transport through TNTs. Interestingly, starvation of cells, a potent inducer of autophagy, has been shown to increase the formation of TNTs[48]. Autophagy is a known regulator of cytokine signaling and this process is influenced by mitochondrial reactive oxygen species and/or mitochondrial DNA[49].The transfer of mitochondria and autophagosomes from leukemic cells toward MSCs might therefore explain the release of supportive factors by the tumor microenvironment. In addition, both TNTs and autophagy have been shown to

play a role in chemotherapy resistance of cancer cells[17,50] and our data implies that these processes may be connected.

LEUKEMIC CELL MIGRATION

A straightforward way to disrupt the leukemic niche is to induce clearance of leukemic cells from the bone marrow. Migration of leukemic cells is thought to be similar to that of hematopoietic stem cells (HSCs)[51,52]. HSCs migrate towards stromal cell derived factor 1 (SDF1/CXCL12) which is actively produced by MSCs in the bone marrow[51-53]. The CXCL12 receptor CXCR4 is highly expressed on both HSCs and leukemic cells[13,51-53]. Consequently, researchers have tried to disrupt the CXCR4/CXCL12 axis using small molecule inhibitors. These studies are mostly focused on acute myeloid leukemia (AML). Disruption of the CXCR4/CXCL12 axis led to mobilization of leukemic cells, increased sensitivity to therapeutic agents and prolonged survival in AML mouse models[54-62]. In ALL the effect of CXCR4/CXCL12 disruption is unclear. CXCR4 antagonists reduce engraftment of ALL cells in mouse models[63,64], but paradoxically do not decrease the leukemic cell number in the bone marrow of leukemic mice[63,65]. In addition, CXCL12 expression is downregulated in murine bone marrow regions of extensive leukemia growth[13]. Finally, CXCL12 levels in the bone marrow of BCP-ALL patients are decreased compared to that of healthy controls and patients in remission[53].

We investigated the migration of ALL cells using an *ex vivo* co-culture model with primary BCP-ALL cells and MSCs in **chapter 5**. Interestingly, we observed that ALL cells affect the migration potential of their microenvironment by inducing migration of leukemic counterparts and reducing migration of healthy HPCs and MSCs. Leukemic cells migrated 2.2fold more potently toward leukemic co-cultures (ALL-MSC) compared to MSC mono-cultures. This process is independent of the CXCR4/CXCL12 axis as CXCL12 levels were unaltered in leukemic co-cultures. Moreover, CXCR4 inhibition was unable to inhibit the increase in migration toward the leukemic niche. These observations might explain the contradictory results of CXCR4 inhibition in ALL. Engraftment studies of ALL cells use mice that do not harbor leukemic cells in their bone marrow. Consequently, migration of cells is regulated by the healthy microenvironment and sensitive to CXCR4/CXCL12 disruption[13,51-53]. In contrast, the bone marrow niche in mice suffering from ALL has been disrupted by leukemic blasts and uses alternative pathways. Our data shows for the first time that this leukemic niche is disrupted independently of CXCR4/CXCL12 signaling. Next, we tried to identify which pathways might play a role in leukemic niche formation. We used a biased approach by quantifying the secretion of 64 cytokines in ALL-MSC co-cultures known to be important in immunology/hematology. The primary leukemic cells induced patient unique secretomes after co-culture with MSCs. Changing the source of MSC had no influence on the secreted factors showing that this process is governed by the leukemic cells. Interestingly all primary BCP-ALL cells induced MCP1/CCL2 and/or MDC/CCL22 (CCR4-ligands), six out of ten induced IL-8 and/or GRO-1 (CXCR1/2-ligands), and two out of ten induced IP10/CXCL10 (CXCR3-ligands). Importantly, we validated these findings using serum derived from bone marrow aspirates from 10 ALL patients at diagnosis and compared them to samples from the same patients in remission. Furthermore, we used bone marrow aspirates of 7 healthy controls to analyze cytokine/chemokine patterns of the healthy niche. We observed an upregulation of CCR4 and CXCR1/2 ligands in the serum of leukemic bone marrow. After induction therapy, the levels of CCR4 and CXCR1/2 ligands in the bone marrow of ALL patients decreased to levels observed in healthy controls. These data point to CCR4 and CXCR1/2 as valuable future therapeutic targets to interfere with the leukemic niche in ALL.

FUTURE PERSPECTIVES

TNT research is performed mostly *in vitro*, because these structures are difficult to image and no inhibitors are available that specifically disrupt TNTs. However, imaging methods are becoming more powerful and drive the study of increasingly smaller structures *in vivo*[66,67]. Multiphoton, or two-photon, confocal microscopy is especially suited for *in vivo* imaging because of its low background noise[68,69]. Recently, Osswald and colleagues used multi-photon microscopy to visualize TNT-like structures in brain tumors[70]. Moreover, multiple groups have shown the possibility of imaging hematopoietic cells in the bone marrow niche of mice[13,71,72]. In these experiments, hematopoietic cells were marked using lipophilic tracker dyes similar to those used in our TNT studies. Interestingly, HSCs have been observed to transfer lipophilic dye during *in vivo* experiments[73]. Experiments revealing the underlying mechanism have not yet been performed. These developments show the exciting opportunities for *in vivo* imaging of TNTs in the leukemic niche.

We studied potential TNT disrupting compounds by screening inhibitors of the cytoskeleton in **chapter 3**. Other approaches for TNT disruption consist of finding novel genes that regulate TNT signaling. While limited, there have been reports on genes that regulate TNTs. Hase and colleagues investigated M-sec, also called tumor necrosis factor-α-induced protein 2, which is highly expressed in myeloid cells[39]. They showed that shRNA knockdown of M-sec in murine macrophages reduced the amount of TNT formation and decreased TNT length. In addition they provided evidence that M-sec cooperates with Ral and the exocyst complex[39]. The exocyst complex controls vesicle trafficking and the cytoskeleton[74], while Ral is a small GTPase that plays a role in the (oncogenic) activation of proteins[75]. In addition to M-sec, Schiller *et al*. implicate the importance of LST1 in TNT formation between HeLa cells, by showing interaction between MSec, the exocyst complex, and Ral proteins[18]. However, the effect of M-sec or LST1 knockdown has not yet been reproduced using different cell types. An unbiased way to identify TNT-regulatory genes is to perform a large scale RNA interference screen. Huang *et al*. have demonstrated the value of such screens by revealing the pathway responsible for resistance to MEK and BRAF inhibitors in multiple cancers[76]. Our lab is

currently using RNA interference to investigate the effect of multiple candidate genes on lipophilic dye transfer from BCP-ALL cells toward MSCs.

Identification of the molecules that are transported by TNTs is mostly performed by biased approaches. For example, we ectopically expressed a panel of fluorescent marker proteins in ALL cells and measured their transfer toward MSCs in **chapter 4**. Others have studied TNT signaling by using dyes that stain cellular compartments[42]. A non-biased approach to study TNTs is the "Trans-SILAC" system, which uses stable-isotope labeling of amino acids in cell culture (SILAC). Cells labeled with heavy isotope proteins are co-cultured with a population of "light" acceptor cells. After co-culture, the two cell populations are high-purity sorted based on a fluorescent or membrane marker. The acceptor population is analyzed using mass spectrometry based proteomics, revealing which molecules have been transported between cell populations[77]. Using this method, Rechavi *et al*. have shown that oncogenic H-Ras transfers from cancer cells toward natural killer (NK) cells and T lymphocytes[78]. The pathway of transfer was unknown, but several years later Rainy *et al*. revealed that H-Ras transfers from B to T cells via TNTs[43]. Trans-SILAC experiments with and without TNT inhibition provides a compelling method to characterize TNT signaling.

CONCLUDING REMARKS

The discovery of TNT signaling between ALL cells and MSCs may provide a novel therapeutic target for antileukemic therapy. Leukemic cells use TNTs to stimulate the secretion of pro-survival cytokines in their microenvironment, subsequently inducing leukemic cell survival and drug resistance. Currently, it is unclear how to inhibit these cytoskeletal structures in the leukemic niche. The identification of new targets is strongly dependent on research that elucidates the molecular mechanisms driving TNTs. We show that TNT signaling in the leukemic niche is dependent on the interplay of actin regulating processes and cannot be disrupted by targeting tubulin. In addition, our data point to the importance of autophagosome and mitochondria transfer in this process. An alternative way to interfere with the leukemic niche is to induce clearance of leukemic cells from the bone marrow. Our data show that ALL cells modify their niche and induce the migration of leukemic counterparts, while inhibiting migration of healthy hematopoietic cells. This process was independent of CXCR/CXCL12. Instead we found the recurrent upregulation of CCR4 and CXCR1/2 ligands. These data underline the importance of the leukemic niche and provide novel insights that may improve the future treatment of leukemia patients.

REFERENCES

1. von Hansemann D. Ueber asymmetrische Zelltheilung in epithel Krebsen und deren biologische Bedeutung. Vol. 119. Virchow's Arch. Path. Anat.; 1890.
2. Nowell PC. The minute chromosome (Phl) in chronic granulocytic leukemia. *Blut*. 1962;8:65-66.
3. Meijerink JP, den Boer ML, Pieters R. New genetic abnormalities and treatment response in acute lymphoblastic leukemia. *Semin Hematol*. 2009;46(1):16-23.
4. Salesse S, Verfaillie CM. BCR/ABL: from molecular mechanisms of leukemia induction to treatment of chronic myelogenous leukemia. *Oncogene*. 2002;21(56):8547-8559.
5. Kantarjian H, O'Brien S, Jabbour E, et al. Improved survival in chronic myeloid leukemia since the introduction of imatinib therapy: a single-institution historical experience. *Blood*. 2012;119(9):1981-1987.
6. Paget S. The distribution of secondary growths in cancer of the breasts. *Lancet*. 1889;1:571-573.
7. Mintz B, Illmensee K. Normal genetically mosaic mice produced from malignant teratocarcinoma cells. *Proc Natl Acad Sci U S A*. 1975;72(9):3585-3589.
8. Meads MB, Gatenby RA, Dalton WS. Environment-mediated drug resistance: a major contributor to minimal residual disease. *Nat Rev Cancer*. 2009;9(9):665-674.
9. Nakasone ES, Askautrud HA, Kees T, et al. Imaging tumor-stroma interactions during chemotherapy reveals contributions of the microenvironment to resistance. *Cancer Cell*. 2012;21(4):488-503.
10. Schepers K, Pietras EM, Reynaud D, et al. Myeloproliferative neoplasia remodels the endosteal bone marrow niche into a self-reinforcing leukemic niche. *Cell Stem Cell*. 2013;13(3):285-299.
11. Rustom A, Saffrich R, Markovic I, Walther P, Gerdes HH. Nanotubular highways for intercellular organelle transport. *Science*. 2004;303(5660):1007-1010.
12. Sowinski S, Jolly C, Berninghausen O, et al. Membrane nanotubes physically connect T cells over long distances presenting a novel route for HIV-1 transmission. *Nat Cell Biol*. 2008;10(2):211-219.
13. Colmone A, Amorim M, Pontier AL, Wang S, Jablonski E, Sipkins DA. Leukemic cells create bone marrow niches that disrupt the behavior of normal hematopoietic progenitor cells. *Science*. 2008;322(5909):1861-1865.
14. Morrison SJ, Scadden DT. The bone marrow niche for haematopoietic stem cells. *Nature*. 2014;505(7483):327-334.
15. Sourisseau M, Sol-Foulon N, Porrot F, Blanchet F, Schwartz O. Inefficient human immunodeficiency virus replication in mobile lymphocytes. *J Virol*. 2007;81(2):1000-1012.
16. Gyorgy B, Szabo TG, Pasztoi M, et al. Membrane vesicles, current state-of-the-art: emerging role of extracellular vesicles. *Cell Mol Life Sci*. 2011;68(16):2667-2688.
17. Polak R, de Rooij B, Pieters R, den Boer ML. B-cell precursor acute lymphoblastic leukemia cells use tunneling nanotubes to orchestrate their microenvironment. *Blood*. 2015;126(21):2404-2414.
18. Schiller C, Diakopoulos KN, Rohwedder I, et al. LST1 promotes the assembly of a molecular machinery responsible for tunneling nanotube formation. *J Cell Sci*. 2013;126(Pt 3):767-777.
19. Bukoreshtliev NV, Wang X, Hodneland E, Gurke S, Barroso JF, Gerdes HH. Selective block of tunneling nanotube (TNT) formation inhibits intercellular organelle transfer between PC12 cells. *FEBS Lett*. 2009;583(9):1481-1488.

20. Wang Y, Cui J, Sun X, Zhang Y. Tunneling-nanotube development in astrocytes depends on p53 activation. *Cell Death Differ*. 2011;18(4):732-742.

21. Bubb MR, Spector I, Bershadsky AD, Korn ED. Swinholide A is a microfilament disrupting marine toxin that stabilizes actin dimers and severs actin filaments. *J Biol Chem*. 1995;270(8):3463-3466.

22. Hori M, Saito S, Shin YZ, Ozaki H, Fusetani N, Karaki H. Mycalolide-B, a novel and specific inhibitor of actomyosin ATPase isolated from marine sponge. *FEBS Lett*. 1993;322(2):151-154.

23. Saito S, Watabe S, Ozaki H, Fusetani N, Karaki H. Mycalolide B, a novel actin depolymerizing agent. *J Biol Chem*. 1994;269(47):29710-29714.

24. Morton WM, Ayscough KR, McLaughlin PJ. Latrunculin alters the actin-monomer subunit interface to prevent polymerization. *Nat Cell Biol*. 2000;2(6):376-378.

25. Jordan MA, Wilson L. Microtubules and actin filaments: dynamic targets for cancer chemotherapy. *Curr Opin Cell Biol*. 1998;10(1):123-130.

26. Nolen BJ, Tomasevic N, Russell A, et al. Characterization of two classes of small molecule inhibitors of Arp2/3 complex. *Nature*. 2009;460(7258):1031-1034.

27. Rizvi SA, Neidt EM, Cui J, et al. Identification and characterization of a small molecule inhibitor of formin-mediated actin assembly. *Chem Biol*. 2009;16(11):1158-1168.

28. Evangelista M, Zigmond S, Boone C. Formins: signaling effectors for assembly and polarization of actin filaments. *J Cell Sci*. 2003;116(Pt 13):2603-2611.

29. Pruyne D, Evangelista M, Yang C, et al. Role of formins in actin assembly: nucleation and barbed-end association. *Science*. 2002;297(5581):612-615.

30. Sorensen PM, Iacob RE, Fritzsche M, et al. The natural product cucurbitacin E inhibits depolymerization of actin filaments. *ACS Chem Biol*. 2012;7(9):1502-1508.

31. Bubb MR, Senderowicz AM, Sausville EA, Duncan KL, Korn ED. Jasplakinolide, a cytotoxic natural product, induces actin polymerization and competitively inhibits the binding of phalloidin to F-actin. *J Biol Chem*. 1994;269(21):14869-14871.

32. Bubb MR, Spector I, Beyer BB, Fosen KM. Effects of jasplakinolide on the kinetics of actin polymerization. An explanation for certain in vivo observations. *J Biol Chem*. 2000;275(7):5163-5170.

33. Gerzon K. Anticancer Agents Based on Natural Product Models. New York; 1980.

34. Jordan MA, Wilson L. Microtubules as a target for anticancer drugs. *Nat Rev Cancer*. 2004;4(4):253-265.

35. Wienecke A, Bacher G. Indibulin, a novel microtubule inhibitor, discriminates between mature neuronal and nonneuronal tubulin. *Cancer Res*. 2009;69(1):171-177.

36. Lu Y, Chen J, Xiao M, Li W, Miller DD. An overview of tubulin inhibitors that interact with the colchicine binding site. *Pharm Res*. 2012;29(11):2943-2971.

37. Gidding CE, Kellie SJ, Kamps WA, de Graaf SS. Vincristine revisited. *Crit Rev Oncol Hematol*. 1999;29(3):267-287.

38. Giannakakou P, Sackett D, Fojo T. Tubulin/microtubules: still a promising target for new chemotherapeutic agents. *J Natl Cancer Inst*. 2000;92(3):182-183.

39. Hase K, Kimura S, Takatsu H, et al. M-Sec promotes membrane nanotube formation by interacting with Ral and the exocyst complex. *Nat Cell Biol*. 2009;11(12):1427-1432.

40. Abounit S, Zurzolo C. Wiring through tunneling nanotubes--from electrical signals to organelle transfer. *J Cell Sci*. 2012;125(Pt 5):1089-1098.

41. Wang X, Gerdes HH. Transfer of mitochondria via tunneling nanotubes rescues apoptotic PC12 cells. *Cell Death Differ*. 2015;22(7):1181-1191.

42. Pasquier J, Guerrouahen BS, Al Thawadi H, et al. Preferential transfer of mitochondria from endothelial to cancer cells through tunneling nanotubes modulates chemoresistance. *J Transl Med*. 2013;11:94.

43. Rainy N, Chetrit D, Rouger V, et al. H-Ras transfers from B to T cells via tunneling nanotubes. *Cell Death Dis*. 2013;4:e726.

44. Gurke S, Barroso JF, Gerdes HH. The art of cellular communication: tunneling nanotubes bridge the divide. *Histochem Cell Biol*. 2008;129(5):539-550.

45. Onfelt B, Nedvetzki S, Benninger RK, et al. Structurally distinct membrane nanotubes between human macrophages support long-distance vesicular traffic or surfing of bacteria. *J Immunol*. 2006;177(12):8476-8483.

46. Kaur J, Debnath J. Autophagy at the crossroads of catabolism and anabolism. *Nat Rev Mol Cell Biol*. 2015;16(8):461-472.

47. Mi N, Chen Y, Wang S, et al. CapZ regulates autophagosomal membrane shaping by promoting actin assembly inside the isolation membrane. *Nat Cell Biol*. 2015;17(9):1112-1123.

48. Lou E, Fujisawa S, Morozov A, et al. Tunneling nanotubes provide a unique conduit for intercellular transfer of cellular contents in human malignant pleural mesothelioma. *PLoS One*. 2012;7(3):e33093.

49. Harris J. Autophagy and cytokines. *Cytokine*. 2011;56(2):140-144.

50. Sui X, Chen R, Wang Z, et al. Autophagy and chemotherapy resistance: a promising therapeutic target for cancer treatment. *Cell Death Dis*. 2013;4:e838.

51. Aiuti A, Webb IJ, Bleul C, Springer T, Gutierrez-Ramos JC. The chemokine SDF-1 is a chemoattractant for human CD34+ hematopoietic progenitor cells and provides a new mechanism to explain the mobilization of CD34+ progenitors to peripheral blood. *J Exp Med*. 1997;185(1):111-120.

52. Peled A, Petit I, Kollet O, et al. Dependence of human stem cell engraftment and repopulation of NOD/SCID mice on CXCR4. *Science*. 1999;283(5403):845-848.

53. van den Berk LC, van der Veer A, Willemse ME, et al. Disturbed CXCR4/CXCL12 axis in paediatric precursor B-cell acute lymphoblastic leukaemia. *Br J Haematol*. 2014;166(2):240-249.

54. Petit I, Szyper-Kravitz M, Nagler A, et al. G-CSF induces stem cell mobilization by decreasing bone marrow SDF-1 and up-regulating CXCR4. *Nat Immunol*. 2002;3(7):687-694.

55. Becker PS. Targeting the CXCR4 Pathway: Safety, Tolerability and Clinical Activity of Ulocuplumab (BMS-936564), an Anti-CXCR4 Antibody, in Relapsed/Refractory Acute Myeloid Leukemia. *ASH Abstract 386*. 2014.

56. Fierro FA, Brenner S, Oelschlaegel U, et al. Combining SDF-1/CXCR4 antagonism and chemotherapy in relapsed acute myeloid leukemia. *Leukemia*. 2009;23(2):393-396.

57. Azab AK, Runnels JM, Pitsillides C, et al. CXCR4 inhibitor AMD3100 disrupts the interaction of multiple myeloma cells with the bone marrow microenvironment and enhances their sensitivity to therapy. *Blood*. 2009;113(18):4341-4351.

58. Burger JA, Peled A. CXCR4 antagonists: targeting the microenvironment in leukemia and other cancers. *Leukemia*. 2009;23(1):43-52.

59. Burger M, Hartmann T, Krome M, et al. Small peptide inhibitors of the CXCR4 chemokine receptor (CD184) antagonize the activation, migration, and antiapoptotic responses of CXCL12 in chronic lymphocytic leukemia B cells. *Blood*. 2005;106(5):1824-1830.

60. Heuser M, Kuchenbauer F, Argiropoulos B, et al. Priming reloaded? *Blood*. 2009;114(4):925-926; author reply 926-927.

61. Tavor S, Petit I, Porozov S, et al. CXCR4 regulates migration and development of human acute myelogenous leukemia stem cells in transplanted NOD/SCID mice. *Cancer Res*. 2004;64(8):2817-2824.

62. Tavor S, Eisenbach M, Jacob-Hirsch J, et al. The CXCR4 antagonist AMD3100 impairs survival of human AML cells and induces their differentiation. *Leukemia*. 2008;22(12):2151-5158.

63. Juarez J, Dela Pena A, Baraz R, et al. CXCR4 antagonists mobilize childhood acute lymphoblastic leukemia cells into the peripheral blood and inhibit engraftment. *Leukemia*. 2007;21(6):1249-1257.

64. Sipkins DA, Wei X, Wu JW, et al. In vivo imaging of specialized bone marrow endothelial microdomains for tumour engraftment. *Nature*. 2005;435(7044):969-973.

65. Parameswaran R, Yu M, Lim M, Groffen J, Heisterkamp N. Combination of drug therapy in acute lymphoblastic leukemia with a CXCR4 antagonist. *Leukemia*. 2011;25(8):1314-1323.

66. Zomer A, Maynard C, Verweij FJ, et al. In Vivo imaging reveals extracellular vesicle-mediated phenocopying of metastatic behavior. *Cell*. 2015;161(5):1046-1057.

67. Sewald X, Gonzalez DG, Haberman AM, Mothes W. In vivo imaging of virological synapses. *Nat Commun*. 2012;3:1320.

68. Denk W, Delaney KR, Gelperin A, et al. Anatomical and functional imaging of neurons using 2-photon laser scanning microscopy. *J Neurosci Methods*. 1994;54(2):151-162.

69. Denk W, Strickler JH, Webb WW. Two-photon laser scanning fluorescence microscopy. *Science*. 1990;248(4951):73-76.

70. Osswald M, Jung E, Sahm F, et al. Brain tumour cells interconnect to a functional and resistant network. *Nature*. 2015;528(7580):93-98.

71. Barrett O, Sottocornola R, Lo Celso C. In vivo imaging of hematopoietic stem cells in the bone marrow niche. *Methods Mol Biol*. 2012;916:231-242.

72. Rashidi NM, Scott MK, Scherf N, et al. In vivo time-lapse imaging shows diverse niche engagement by quiescent and naturally activated hematopoietic stem cells. *Blood*. 2014;124(1):79-83.

73. Progatzky F, Dallman MJ, Lo Celso C. From seeing to believing: labelling strategies for in vivo cell-tracking experiments. *Interface Focus*. 2013;3(3):20130001.

74. Heider MR, Munson M. Exorcising the exocyst complex. *Traffic*. 2012;13(7):898-907.

75. Yan C, Liu D, Li L, et al. Discovery and characterization of small molecules that target the GTPase Ral. *Nature*. 2014;515(7527):443-447.

76. Huang S, Holzel M, Knijnenburg T, et al. MED12 controls the response to multiple cancer drugs through regulation of TGF-beta receptor signaling. *Cell*. 2012;151(5):937-950.

77. Cox J, Mann M. MaxQuant enables high peptide identification rates, individualized p.p.b.-range mass accuracies and proteome-wide protein quantification. *Nat Biotechnol*. 2008;26(12):1367-1372.

78. Rechavi O, Goldstein I, Vernitsky H, Rotblat B, Kloog Y. Intercellular transfer of oncogenic H-Ras at the immunological synapse. *PLoS One*. 2007;2(11):e1204.

Chapter 7

NEDERLANDSE SAMENVATTING VOOR NIET INGEWIJDEN

KANKER

Het leven op aarde stamt af van een gemeenschappelijke voorouder die zich ongeveer 3,5 miljard jaar geleden ontwikkelde. De samenwerking tussen simpele ééncellige levensvormen legde de basis voor de ontwikkeling van complexe meercellige organismen. Dit proces wordt elegant gevisualiseerd door het kweken van de bacterie *Pseudomonas Fluorescens*. Het DNA van individuele bacteriën muteert spontaan, waardoor ze een speciale lijm uitscheiden. Dit helpt in het vormen van zogenaamde "bacteriematten", waar bacteriën samenwerken om meer zuurstof uit de lucht te halen. Op een zelfde manier, werken de 40,000 miljard cellen in ons lichaam samen om onze gezondheid te waarborgen. Soms wordt de samenwerking tussen cellen verstoord. In het voorbeeld van de bacterie *Pseudomonas Fluorescens*, ontstaan bacteriën die "valspelen" en gebruik maken van de bacteriematten zonder lijm te produceren. Dit leidt uiteindelijk tot het uiteenvallen van de matten en de dood van alle betrokken bacteriën. Cellen in het menselijke lichaam kunnen ook eigenschappen ontwikkelen die hen laat gedijen ten koste van het gehele organisme. Als deze cellen zich gedragen volgens verschillende kenmerken dan noemen we dit kankercellen. Kankercellen induceren groeisignalen, ontwijken groeionderdrukking, weerstaan celdood, delen oncontroleerbaar, induceren bloedvatvorming en dringen gezonde weefsels binnen. Kanker kan ontstaan uit elk weefsel in het menselijk lichaam en is één van de leidende oorzaken van sterfte wereldwijd. Het aantal mensen dat lijdt aan kanker stijgt naar verwachting met 70% in de komende decennia.

HET BLOEDSTELSEL EN BEENMERG

Alle cellen in het menselijk lichaam zijn verbonden aan het bloedvatenstelsel: een dynamisch netwerk van aders en slagaders die twee type bloedcellen transporteren. Rode bloedcellen transporteren zuurstof en koolstofdioxide, terwijl witte bloedcellen beschermen tegen infectieziekten. Bloedcellen stammen af van één celtype, de hematopoëtische stamcel (HSC), die wordt beschermd en gereguleerd door het beenmerg. HSCs creëren voorlopercellen die op hun beurt volwassen bloedcellen produceren. Myeloïde voorlopers produceren afweercellen die men al bij geboorte bezit, en lymfoïde voorlopers maken B- en T cellen die pas na blootstelling aan infecties ontwikkelen. Normale bloedcellen hebben een beperkte levensduur. Daarentegen kunnen HSCs zichzelf vernieuwen en nieuwe HSCs produceren. Deze bijzondere eigenschappen worden gedreven door chemische en fysieke signalen vanuit het beenmerg waarin HSCs zich bevinden. Het beenmerg micromilieu is rijk aan voedingsstoffen zoals "stromal cell-derived factor 1", ook wel CXCL12 genoemd. Daarnaast bevat het een scala aan cellen, waaronder mesenchymale stromale cellen (MSCs), die cruciale cel-cel interacties bieden die HSCs onderhouden. Samen bepalen deze signalen de hiërarchie tussen HSCs en alle andere bloedcellen. HSCs zorgen dat het bloedstelsel continu wordt aangevuld, terwijl andere bloedcellen hun taak vervullen en daarna in apoptose (celdood) gaan.

LEUKEMIE

Leukemie is een type kanker dat ontstaat in het beenmerg en de balans verstoord tussen bloedcellen. Het wordt veroorzaakt door witte bloedcellen die ongecontroleerd delen. Als leukemie niet wordt behandeld is het een dodelijke ziekte. Leukemie wordt geclassificeerd op basis van het gedrag van de kankercellen. Acute leukemie wordt veroorzaakt door een snelle toename van onrijpe witte bloedcellen, terwijl chronische leukemie jaren kan duren om te ontstaan. Dit proefschrift richt zich op acute lymfatische leukemie (ALL), de meest voorkomende doodsoorzaak van kanker bij kinderen. Meer specifiek kijken we naar B cel precursor ALL (BCP-ALL), de meest voorkomende vorm van ALL. BCP-ALL cellen zijn genetisch verschillend vergeleken met normale B cellen, door veranderingen in het DNA.

BEHANDELING VAN LEUKEMIE

Het classificeren van leukemie op basis van genetische afwijkingen voorspelt de overlevingskans van de patiënt en de slagingskans van chemotherapie. Deze kennis is gebruikt voor het optimaliseren van de behandeling en hierdoor is de overleving gestegen van 10% in de jaren zestig tot 90% in de 21ste eeuw. Andere vormen van kinderkanker volgen deze trend en de gemiddelde overleving is rond de 80%. Deze progressie heeft ervoor gezorgd dat 1 op de 1000 twintigjarigen een overlever is van kinderkanker. Door een gebrek aan specifieke medicijnen hebben twee-derde van de overlevenden last van een chronische aandoening en in 28% zijn deze bijwerkingen zelfs levensbedreigend. Hartschade, longschade, littekens in de darmen, leverontsteking en levercirrose, nier- en blaasschade, botschade en krimping van de spieren, schildklierafwijkingen, obesitas, dwerggroei, onvruchtbaarheid, schade aan het centrale zenuwstelsel, oogschade, gehoorverlies, tand- en tandvleesschade; allen zijn bijwerkingen van chemo- en radiotherapie. Daarnaast hebben overlevenden van kinderkanker een 19-voud verhoogde kans op het ontwikkelen van een andere kanker. Dit onderstreept het belang van het ontwikkelen van nieuwe medicijnen die specifiek en effectief leukemiecellen doden.

KANKER IS EEN ZIEKTE VAN CELLEN DIE INTRINSIEK EN EXTRINSIEK AANGETAST ZIJN

Historisch gezien is kankeronderzoek gericht op het ontdekken van de *intrinsieke* veranderingen die kankercellen onderscheiden van gezonde cellen. Aan het einde van de 19de eeuw ontdekte David von Hansemann dat kankercellen zich op een afwijkende manier vermenigvuldigen en hierdoor hun DNA beschadigen[1]. Hij dacht dat deze beschadigingen verantwoordelijk waren voor het agressieve gedrag van kankercellen, maar de technologie was toen niet ver genoeg om dit te bewijzen. Naarmate de technologie verbeterde, bevestigden onderzoekers dat kankercellen worden getypeerd door schade aan het DNA. Ze ontdekten een verschuiving van DNA tussen twee chromosomen genaamd de BCR-ABL1 translocatie, of het Philadelphia chromosoom, die vaak voorkomt in leukemie. Doordat het DNA op een onjuiste manier vastzit, wordt een fusieeiwit gemaakt dat niet in gezonde cellen voorkomt. Dit BCR-ABL1 eiwit zorgt ervoor dat cellen hyperactief worden en ongecontroleerd groeien. De ontdekking van een fusieeiwit dat het gedrag van kankercellen stuurt, maakte het mogelijk om specifieke medicijnen tegen kankercellen te ontwikkelen. Het leidde tot de ontwikkeling van imatinib, een remmer van het BCR-ABL1 eiwit. De overleving van leukemiepatiënten is aanzienlijk gestegen sinds het gebruik van dit medicijn. Dit is een voorbeeld van hoe schade aan het DNA het gedrag van kankercellen aanstuurt en dat dit doelwitten kunnen zijn voor specifieke medicatie.

Behalve afwijkingen aan het DNA is ook bewijs aanwezig dat kankercellen niet onafhankelijk functioneren, maar gedreven worden door hun omgeving. Al in 1889 viel het Stephen Paget op dat als kankercellen zich verspreiden in het lichaam, ze een voorkeur hebben voor specifieke organen. Hij besprak dit in zijn "zaai en oogst" hypothese, waarin hij het uitgroeien van kankercellen vergeleek met dat van plantenzaad. Paget zei: "Een plant verspreid zijn zaden in alle richtingen. Maar de zaden zullen alleen overleven en uitgroeien als ze op vruchtbare grond vallen." In een soortgelijke manier hebben kankercellen ook een specifieke omgeving nodig om in te groeien. Dit werd ondersteund door zijn observaties dat borstkanker vaker uitzaaide in de lever dan in andere organen. Daarnaast zijn observaties gedaan waar kankercellen in bedwang werden gehouden door hun omgeving. Muis embryo's werden geïnjecteerd met kiemceltumorcellen, maar groeiden uit tot gezonde muizen zonder kanker. De tumorcellen waren nog steeds aanwezig maar werden door de omringende cellen aangezet om gezonde taken uit te voeren. Deze observaties laten zien dat cellen zich niet gedragen als onafhankelijke entiteiten, maar als een systeem dat wordt gedreven door complexe communicatiemechanismen. Kanker kan dus beter beschreven worden als een ziekte van zowel *intrinsiek* als *extrinsiek* aangetaste cellen. De invloed van cellen rondom de tumor, ofwel het tumor micromilieu, is een opkomend veld binnen leukemieonderzoek. Het leukemische micromilieu induceert chemotherapie resistentie en is cruciaal voor het ontstaan van leukemie. Groeifactoren en celcel interacties zijn belangrijk in dit proces. Onze huidige kennis schiet echter tekort in het verklaren hoe het leukemische micromilieu wordt gereguleerd en gecontroleerd. Dit is waarom we geïntrigeerd waren door de ontdekking van een nieuw communicatiemechanisme tussen cellen: tunneling nanotubes (TNTs). TNTs zijn dunne buizen die cellen verbinden en een grote variatie aan signaalmoleculen kunnen overbrengen. Kankercellen zouden TNTs kunnen gebruiken om de cellen in hun omgeving aan te tasten en tegelijkertijd zichzelf te beschermen. De aanwezigheid en het belang van TNTs waren onbekend en zijn onderwerp van het onderzoek beschreven in dit proefschrift.

ONTDEKKING VAN TNT SIGNALERING TUSSEN LEUKEMIECELLEN EN BEENMERGCELLEN

Al snel na de ontdekking van TNTs observeerden onderzoekers dat witte bloedcellen ook TNTs maken. Toentertijd waren geen studies die TNTs in leukemie hadden onderzocht en daarom onderzochten we dit in **Hoofdstuk 2**. We ontdekten dat leukemiecellen onderling TNTs maken en hiermee actief signalen uitwisselen. Daarna bekeken we de TNT signalering tussen leukemiecellen en MSCs, een belangrijke cel uit het beenmerg. Verbazingwekkend vormden leukemiecellen veel meer TNTs naar MSCs dan naar andere leukemiecellen. Deze communicatie via TNTs zorgde voor de uitscheiding van overlevingsfactoren en een verhoogde resistentie tegen prednisolone, één van de belangrijkste medicijnen tegen leukemie. Het verbreken van TNTs leidde tot celdood van leukemische cellen en een verhoogde gevoeligheid voor prednisolone. Deze bevindingen laten zien dat TNTs een rol spelen in de communicatie van leukemiecellen met hun omgeving.

HET VINDEN VAN NIEUWE TNT REMMERS

De ontdekking van TNT signalering in de leukemische niche was gedaan met zogenaamde *ex vivo* proeven (ex vivo = buiten het lichaam). Tijdens *ex vivo* proeven worden TNTs geremd door het schudden van cellen (mechanische disruptie) of het verbreken van direct cel contact door het gebruik van speciale filters. Helaas zijn deze technieken niet toe te passen op diermodellen of mensen. Daardoor is een grote vraag naar specifieke TNT remmers. Om nieuwe TNT remmers te identificeren hebben we een systeem opgezet dat nauwkeurig TNT signalering kan meten in **Hoofdstuk 2**. We gebruikten hiervoor een speciale kleurstof die moleculen aankleurt die door TNTs worden overgebracht tussen cellen. Gekleurde leukemiecellen werden gekweekt met ongekleurde MSCs en de verplaatsing van kleur werd gebruikt als een maat van signalering. TNTs zijn structuren die worden gemaakt door het cytoskelet van cellen. Dit cytoskelet is opgebouwd uit eiwitten die zorgen voor stevigheid en beweeglijkheid. We hebben een grote hoeveelheid remmers getest die een effect hebben op de cytoskeletale eiwitten actine en tubuline. Het remmen van tubuline leidde niet tot verminderde TNT signalering. In tegendeel, tubuline remmers induceerden TNT signalering meer dan tweevoud. Daarentegen resulteerde het remmen van actine in een sterke vermindering van TNT signalering (meer dan 20-voud). Deze bevindingen laten zien dat actine cruciaal is in het proces van TNT signalering tussen leukemiecellen en MSCs.

TOXICITEIT VAN ACTINE REMMERS

Het verstoren van het cytoskelet wordt al langer gebruikt als kankertherapie. Het gaat hier om tubuline remmers die de celdeling van kankercellen remmen. Deze medicijnen zijn erg effectief, maar veroorzaken heftige bijeffecten, zoals schade aan zenuwen, het hart en een vergrote kans op bloedproppen. Desalniettemin, worden tubuline remmers gezien als één van de meest succesvolle kankermedicijnen. Wij hebben de invloed van actine remmers getest op de overleving van leukemiecellen en verschillende soorten gezonde bloedcellen. We observeerden dat een aantal gezonde bloedcellen de actine remmers beter verdragen dan leukemiecellen. Actine remmers zouden in de toekomst een nieuw type leukemie medicijn kunnen worden die zowel de leukemiecel doden als de communicatie tussen leukemiecellen en hun micromilieu kunnen verbreken.

TNT STRUCTUUR EN SIGNALERING ZIJN AFHANKELIJK VAN HET CELTYPE

In **Hoofdstuk 2 en 3** hebben we gezien dat TNTs in de leukemische niche structuren overbrengen tussen cellen. In **Hoofdstuk 4** probeerden we te identificeren welke moleculen getransporteerd worden van leukemiecellen naar MSCs via TNTs. Hiervoor gebruiken we fluorescent gelabelde moleculen die we tot expressie brachten in leukemiecellen. Deze moleculen markeren specifieke structuren in de cel. De gelabelde leukemiecellen werden vervolgens gekweekt met ongelabelde MSCs en de overgang van deze gekleurde structuren werd gemeten. Wij observeerden dat adhesiemoleculen, mitochondriën en autophagosomen werden getransporteerd via TNTs. De overdracht van adhesiemoleculen zou de TNT-verbinding tussen cellen kunnen versterken. Mitochondriën zijn structuren die de cel voorzien van energie, terwijl autophagosomen eiwitten en voedingsstoffen recyclen. Beide zijn bekend een rol te spelen in de uitscheiding van overlevingsfactoren. Het zou kunnen dat leukemiecellen mitochondriën en autophagosomen transporteren naar cellen in hun omgeving om hen aan te zetten tot het produceren van overlevingsfactoren. Dit zou een mogelijk mechanisme kunnen zijn dat de overleving en resistentie van leukemiecellen tegen medicijnen verhoogd.

LEUKEMISCHE CEL MIGRATIE

Het ontcijferen van moleculaire mechanismen die het ontstaan van een leukemische niche stimuleren zou kunnen leiden tot nieuwe therapeutische strategieën. Een vanzelfsprekende manier om de leukemische niche te verstoren is om de leukemiecellen te verdrijven uit het beenmerg. De migratie van leukemiecellen wordt gedacht hetzelfde te zijn als die van HSCs. HSCs migreren naar CXCL12 toe, een stof die actief wordt geproduceerd door MSCs in het beenmerg. HSCs en leukemiecellen hebben beiden een hoge expressie van CXCR4, de receptor die CXCL12 opvangt. Onderzoekers hebben geprobeerd om de interactie tussen CXCR4 en CXCL12 te verstoren door middel van specifieke remmers. Op deze manier lukte het om de migratie van leukemiecellen naar een gezond beenmerg te remmen. Als het beenmerg echter al vol zat met leukemiecellen, werden deze cellen niet meer verstoord door CXCR4/CXCL12 remming en bleven ze in het beenmerg zitten. Daarnaast is de uitscheiding van CXCL12 in het beenmerg verminderd in gebieden van veel leukemiecellen. Deze bevindingen duiden op het belang van andere mechanismen dan CXCR4/CXCL12 in de leukemische niche.

Wij onderzochten de migratie van ALL cellen met behulp van *ex vivo* culturen van BCP-ALL cellen en MSCs in **Hoofdstuk 5**. We toonden aan dat leukemiecellen het beenmerg veranderen en hierdoor MSCs aanzetten om nog meer leukemiecellen aan te trekken en gezonde bloedcellen te weren. Dit proces was onafhankelijk van CXCR4 en CXCL12. Wanneer leukemiecellen in contact kwamen met MSCs induceerden ze de stoffen MCP-1/CCL2 en/of MDC/CCL22. Deze moleculen binden aan de CCR4 receptor, die hoger tot expressie komt in ALL cellen in vergelijking met gezonde bloedcellen. Ook kwamen in sommige gevallen liganden vrij voor CXCR1, CXCR2 en CXCR3 receptoren. Deze bevindingen laten zien dat CXCR4/CXCL12 inhibitie niet succesvolle is in het verstoren van het leukemische micromilieu en ze onthullen nieuwe mogelijke doelwitten voor therapie.

SLOTBESCHOUWING

De ontdekking van TNTs tussen ALL cellen en MSCs zou kunnen leiden tot een nieuw therapeutisch doelwit voor leukemie. Leukemische cellen gebruiken TNTs om de secretie van overlevingsfactoren te stimuleren die overleving en drugsresistentie induceren. Helaas zijn op dit moment TNT remmers niet specifiek genoeg om te gebruiken in de kliniek. De ontdekking van nieuwe remmers is sterk afhankelijk van onderzoek dat de moleculaire mechanismen ontrafelt die TNTs aansturen. Wij laten zien dat TNT signalering in de leukemische niche afhankelijk is van actine en niet verstoord kan worden door het remmen van tubuline. Daarnaast hebben we aanwijzingen dat autophagosomen en mitochondriën een belangrijke rol spelen in dit proces. Een alternatieve manier om de leukemische niche te verstoren is om leukemiecellen te verdrijven uit het beenmerg. Onze experimenten tonen aan dat leukemiecellen hun micromilieu veranderen en hierdoor de migratie stimuleren van andere leukemiecellen en de migratie van gezonde bloedcellen remmen. Dir proces was onafhankelijk van CXCR4/CXCL12. In plaats daarvan zagen we de secretie van liganden van CXCR1/2 en CCR4 receptoren. Deze data onderstrepen het belang van de leukemische niche en geven nieuwe inzichten die de therapie van leukemiepatiënten in de toekomst zou kunnen verbeteren.

Chapter 8

ABOUT THE AUTHOR
LIST OF PUBLICATIONS
PHD PORTFOLIO
DANKWOORD

ABOUT THE AUTHOR

Bob de Rooij was born in Woerden on the 2nd of September 1987. At age 10 he became the youth chess champion of Woerden. Bob finished his pre-university education (Atheneum) at the "Woerden Minkema College" in 2005. His passion for science led him to the University of Leiden where he studied Biomedical Sciences and received a Master of Science degree in 2011. In January 2012, he started his scientific research as a PhD student in the department of Pediatric Oncology in the Erasmus Medical Center. During this period, he detected the presence of tunneling nanotubes between leukemic cells and bone marrow cells, together with his colleague Roel Polak. This discovery became the focus of his research which was supervised by professor Monique L. den Boer. It led to a collaboration with GlaxoSmithKline who are currently testing novel anti-cancer agents with assays developed during Bob his research. In 2016, Bob finished his work on the tumor microenvironment in leukemia which is described in this thesis.

LIST OF PUBLICATIONS

J.T. Buijs, G. van der Horst, C. van den Hoogen, H. Cheung, ***B. de Rooij****, J. Kroon, M. Petersen, P.G. van Overveld, R.C. Pelger and G. van der Pluijm*
The BMP2/7 heterodimer inhibits the human breast cancer stem cell subpopulation and bone metastases formation; Oncogene 2012

R. Polak,* ***B. de Rooij*****, R. Pieters and M.L. den Boer*
B-cell precursor acute lymphoblastic leukemia cells use tunneling nanotubes to orchestrate their microenvironment; Blood 2015
*: shared first-authorship

B. de Rooij, *R. Polak, R. Pieters and M.L. den Boer*
Autophagosome transfer in the leukemic niche through tunneling nanotubes; Accepted in Leukemia

B. de Rooij**, R. Polak*, L.C.J. van den Berk, F. Stalpers, R. Pieters and M.L. den Boer*
B-cell precursor acute lymphoblastic leukemia cells create a leukemic niche without affecting the CXCR4/CXCL12 axis; Submitted
* shared first-authorship

B. de Rooij*, R. Polak, F. Stalpers, R. Pieters and M.L. den Boer*
Disrupting tunneling nanotube signaling in the leukemic niche using actin inhibitors; Submitted

R. Polak, M. Bierings, R. van den Dungen, ***B. de Rooij****, R. Pieters, M. Buitenhuis and M.L. den Boer*
Small molecule inhibition of LARG/RhoA signaling blocks migration of ETV6-RUNX1 positive B-cell Precursor Acute Lymphoblastic Leukemia; Manuscript submitted

E.M.P. Steeghs, R. Polak, ***B. de Rooij****, L.C.J. van den Berk, J.M. Boer, C. van de Ven, F. Stalpers, M. Bakker, R. Pieters and M.L. den Boer*
Upregulation of pro-inflammatory gene expression in mesenchymal stromal cells coincides with increased survival of primary leukemic cells; Manuscript submitted

PHD PORTFOLIO

Name PhD candidate	Bob de Rooij
Erasmus MC department	Pediatric Oncology
Research school	MolMed
PhD period	January 2012 – January 2016
Promotor	Prof.dr. M.L. den Boer
Supervisor	Dr. J.M. Boer

		ECTS
Courses		
Molecular aspects of hematological disorders	(2014/2015)	2.0
Annual molecular medicine day	(2012/2013/2014)	1.0
Visualising the invisible: from single molecule Super-resolution to patient	(2013)	1.0
OIC LEICA confocal course	(2015)	1.0
Symposia		
Daniel den Hoed symposium	(2013/2015)	2.0
Stichting Kinderoncologie Nederland (SKION) Research Retraite	(2014/2015/2016)	1.4
56th annual ASH meeting, San Francisco, USA	(2014)	1.0
57th annual ASH meeting, Orlando, USA	(2015)	1.0
Tunneling Nanotubes: Cell-to-Cell Social Networking In Disease, Pennsylvania, USA	(2016)	1.0
Peer-review		
Pediatric Blood and Cancer (2x)	(2015)	2.0
Blood	(2015)	1.0
Presentations		
56th annual ASH meeting, San Francisco, USA; oral presentation	(2014)	2.0
57th annual ASH meeting, Orlando, USA; poster presentation	(2015)	1.6
International conference on the tumour microenvironment In the haematological malignancies and its therapeutic targeting; oral presentation	(2015)	2.0
Grand Round Sophia Children Hospital; oral presentation	(2015)	2.0
12 oral presentations at weekly Pediatric Oncology Research Meeting and Pediatric Oncology meeting	(2012-2016)	8.0
Journal Club at B-cell acute lymphoblastic leukemia Research Group meeting	(2012-2016)	3.0
Daniel den Hoed symposium; oral presentation	(2015)	2.0
Stichting Kinderoncologie Nederland (SKION) Research Retraite; oral presentation	(2015)	2.0

PhD Portfolio (continued)

		ECTS
Training and supervising		
Supervising Evelien Vinke, HLO student for 6 months	(2014)	10
Supervising Iris van Baarsen, PhD student for 6 months	(2015/2016)	10
Total		57

DANKWOORD

Dit proefschrift is tot stand gekomen door de inzet van een groot aantal mensen. Ten eerste wil ik Rob en Monique bedanken voor de kans die jullie mij hebben gegeven. Door middel van jullie begeleiding heb ik mij maximaal kunnen ontwikkelen. Ik wil Judith bedanken voor haar inzet voor dit proefschrift. Ook ben ik dankbaar voor het werk van alle commissieleden en opponenten. Veel dank voor lab specieel en het SKION voor het verzorgen van patiëntenmateriaal. Daarnaast wil ik iedereen van de ALL groep bedanken. João, ik heb nog nooit een buurman met zo een mooie baard gehad. Isabel die statistisch heeft laten zien dat ze moeite heeft met een appel in de vuilnisbak gooien. Lieneke die slechts één keer iets naar mijn hoofd gegooid heeft. Alex, een koning in het bouwen van pc's. Farhad die een record aantal MSCs heeft gekweekt. Arian, een geduchte tegenstander met zaalvoetbal. Lieke, die de MSC dienst heeft opgezet. Ingrid, voor het laten zien dat het mogelijk is om tijdig te promoveren. Aurélie, met wie ik een -80 vriezer getrotseerd heb. Rosanna, voor het draaien van de beste ABBA hits in de ML-II. Cesca, voor je advies over MSCs. Femke, voor het in elkaar zetten van een fantastische paper.

Daarnaast alle leden van de kinderoncologie. Mark die een ongelooflijk repertoire aan stemmen en typetjes heeft (Sean Connery zou trots op je zijn). Priscilla die me heeft laten vastketenen in de kelder van een psychopathische clown. Rui, de voetballende Portugees die ik nog nooit boos heb gezien. Patricia, die 6 talen vloeiender spreekt dan ik. Eric voor zijn droge humor. Jessica, de 'echte' baas van het suspensielab. Dirk, die als enige een stoel zonder wielen had en letterlijk door de grond is heen geschuurd. Marcel, die de ontelbare bestellingen van mij in goede banen leidde. Pauline, voor het in stand houden van alle labs.

Daar daarnaast wil ik iedereen van de 15de verdieping bedanken. Sylvia voor de strenge controle op toxische stoffen. Theo voor alle goede raad en verhalen. Wilco, de enige echte dungeonmaster van het lab. Linda voor het tappen van liters bloed. Lisette de baas van de Canto. Léa voor een leuke treinrit. Yvette, Kirsten, Rolien, Sandra, Lonneke, Yunlei, Dicky, Ytje, Sharon, Wendy, Susan, Noorjahan, Patty en Janneke voor alle gezellige lunches. Ad, voetballend niet te passeren op het strand. Ruben, voor zijn slagzin als ik een superheld zou zijn. Maarten, Ronald en Jules voor hun kritische vragen.

Zelfs buiten de afdeling ben ik 'en passant' geholpen in mijn onderzoek. Een kopje koffie en een wandeling door het park kunnen wonderen doen. Dank je wel Hugo.

Dan zijn we bij Roel gekomen. Onze samenwerking heeft mijn ontwikkeling in een stroomversnelling gebracht en is sindsdien niet meer gestopt. Ik heb ongelooflijk veel van je geleerd en je tomeloze energie was een drijvende kracht achter ons onderzoek. Ongetwijfeld zullen we in de toekomst hier een vervolg aan geven.

Ik wil mijn familie bedanken. Mijn ouders voor het mogelijk maken om te leren, studeren en promoveren. Mijn broer en zussen voor het leren discussiëren.

En ten slotte wil ik Renée bedanken. Jij maakte hard werken makkelijk. Jouw goede zorgen hebben dit proefschrift tot leven gebracht. Dank je wel.